Durham E-Theses

The oxidation of porus carbon: the development of porosity of a cellulose carbon by reaction with oxygen

Weedon, C. J.

How to cite:

Use policy

THE UNIVERSITY OF DURHAM

THE OXIDATION OF POROUS CARBON –

THE DEVELOPMENT OF POROSITY OF A CELLULOSE CARBON

BY REACTION WITH OXYGEN

A THESIS SUBMITTED FOR THE DEGREE OF

MASTER OF SCIENCE

BY

CHRISTOPHER JOHN WEEDON

B.Sc. Dunelm., Dip.Ed. Oxon.

MARCH, 1968.

For Angela and My Parents

ACKNOWLEDGEMENTS

I am indepted to Dr. B. McEnaney formerly Senior Lecturer in Physical Chemistry in the Department of Chemistry, Sunderland Technical College for supervising this work and for his invaluable suggestions and encouragement throughout.

I would also like to express my sincere thanks to:-

Dr. G. Kohnstam for acting as my University Supervisor;

The Teaching and Technical staff of Sunderland Technical College for their advice and assistance at various stages of the work;

Messrs. G. Dovaston and S. M. Rowan for their stimulating discussion and valuable assistance;

Sunderland Education Authority for a grant which enabled me to carry out the research project.

Finally I wish to thank my wife for typing the thesis and for her constant encouragement and support which helped me to complete the work.

ABSTRACT

The work reported in the thesis is an examination of the influence of temperature of activation on the development of microporosity in a polymer carbon. It involves the investigation of the rate of reaction with oxygen over the temperature range 400° - $726^{\circ}C$ and the measurement of the porosity produced by adsorptive methods.

It was concluded from experimental activation energies obtained for the reaction that the temperature ranges 400° - $460^{\circ}C$ and 480° - $726^{\circ}C$ were in Zones II and III respectively of the classification of Hedden and Wicke*. These conclusions were supported by investigation of the influence of partial pressure of oxygen, sample weight and crucible geometry on the rate of reaction.

Analysis of adsorption isotherms shows that the development of porosity depends on the temperature of activation. In Zone III where reaction is on the external surface of the carbon there is little or no development of porosity whereas in Zone II where the reaction occurs within the pores of the carbon, substantial development of porosity occurs.

A method for the determination of the thermodynamic criterion, $\Delta S < 0$, for the applicability of the Dubinin Theory to the adsorption isotherms was developed. Application of the Dubinin Equation to the regions of the isotherms where the

thermodynamic criterion was shown to apply gave lines that
were not generally straight as originally postulated. However
analysis of the results in terms of the Dubinin Equation in
general confirmed the effects of temperature of activation on
the development of porosity.

Comparison of oxygen and carbon dioxide as activating
gases was made by reference to Rowan's[I] work and showed that
under comparable conditions of activation carbon dioxide is
a more efficient activating gas.

[*] Hedden and Wicke, 'Proceedings of the Third Conference on
Carbon'., Pergamon Press, New York, 1959, P.249.

[I] Rowan, M.Sc. Thesis, Durham University, 1966.

CONTENTS

CHAPTER 1

CHAPTER 2

The Oxidation of Carbon

CHAPTER 5

Results and Discussion of Adsorption Measurements

CHAPTER 6

Summary and Conclusions

APPENDIX I

Preparation of Cellulose Carbon

APPENDIX II

Activation

APPENDIX III

Measurement of Adsorption Isotherms

APPENDIX IV

APPENDIX V

CHAPTER 1

1.1. Introduction

The properties of many forms of carbon such as lampblack, charcoal and diamond have been utilised for several thousand years. One of these, charcoal, was used as a fuel and as a constituent of gunpowder long before de Saussure (1) made the first systematic investigation of its remarkable adsorptive properties in the late eighteenth century. Since then many new and varied applications have been found for adsorptive chars including use in gas and liquid purification.

For several decades chemists have pursued two broad fields of study, (i) the reactions of carbons with oxidising gases and (ii) measurement of the adsorptive properties of activated carbons produced by such reactions. However the detailed work done in each field has rarely been related to the other.

One reason for this appears to have been lack of reproducibility when working with natural materials such as coconut-shell and wood charcoals. This was undoubtedly due in part to both variation in the chemical nature of the material and in the amount of inorganic impurities. Each of these factors has been shown to affect both rates of activation (2,3) and development of porosity (4,5). In recent years the pyrolysis of well characterised polymeric materials e.g. polyvinylidene chloride, divinylbenzene polymers and cellulose, has yielded

far more reproducible carbons relatively free of inorganic matter. Also carbons prepared from polymers have a wider range of graphitic character than those prepared from traditional starting materials.

For these reasons a number of polymer carbons were chosen for a recent study (6) of the relation between the development of porosity in carbons by activation with carbon dioxide and the kinetics of the activation process. A somewhat surprising conclusion was that the development of porosity did not vary significantly within a range of temperatures used for activation.

The work reported in this thesis is a more detailed examination of the influence of temperature of activation on the development of porosity in a polymer carbon. It involves the investigation of the rate of activation of a cellulose carbon by reaction with oxygen over the temperature range $400^{\circ}-700^{\circ}C$ and the measurement of the porosity produced by adsorptive methods.

There follows a description of the preparation, general structure and activation of carbons before the detailed aims of the present work are given.

1.2. Carbonisation

Carbonisation has been defined as 'the gradual process of organic compounds towards carbon under the influence of heat' (7).

This process is complex and varies with the nature of the material and the conditions to which the material is subjected. However the process can be divided into three temperature dependant stages. (i) Below 300°C the major reactions to occur are dehydration and decarboxylation in the case of coal and other cellulosic materials (8-10) and the loss of side chain constituents in the case of some vinyl polymers (4). (ii) Between 300° and 550°C the major breakdown of the material occurs resulting in simultaneous evolution of gaseous and liquid products, and condensation to give a carbon residue (7, 8, 11). (iii) Above 550°C the evolution of gases such as hydrogen and methane increases sharply while the evolution of liquids ceases (8). More specifically Tang and Bacon (9) have proposed the following outline mechanism for the thermal decomposition of cellulose to carbon. (a) Physical desorption of water (25°-150°C). (b) Dehydration from the cellulose unit (150°-240°C). (c) Thermal cleavage of the glycosidic links and scission of other carbon-oxygen bonds and some carbon-carbon bonds via a free radical reaction (240°-400°C). (d) Aromatisation (400°C and above).

The processes which occur in the range 300°-550°C have the most influence on the structure of the resulting carbon. Two broad classes of carbon can be identified from whether or not fusion accompanies carbonisation in this region (12,13).

A coke results when fusion takes place and a char when it does not. The carbonisation of cellulose is a charring process as has been shown (13,14) by examination of the resulting carbon.

Whether coking or charring takes place on carbonisation appears to depend on a number of factors including the following. (i) The degree of cross linking either in the original material or as produced by the carbonisation process, e.g. highly cross-linked material such as a phenol-formaldehyde resin produces a char (4). (ii) The presence of oxygen during the early stages of carbonisation has an indirect effect in that it influences the amount of cross linking (12,13). Thus a process which produces a coke in an inert atmosphere may in air produce a char, e.g. the carbonisation of polyvinyl chloride (4,15). (iii) The rate of heating may also affect the course of the decomposition (4, 9, 15). For cellulose it has been shown that a slow rate of heating increases the amount of cross linking and also the carbon yield (13).

1.3. Crystallographic Structure and Physical Properties of Carbons

As a result of X-ray examination many substances formerly considered amorphous have been shown to possess structural characteristics typical of the crystalline state. Debye and Scherrer (16) concluded that amorphous carbons were merely graphite in various states of very fine subdivision. This view

however, is oversimplified and it is clear that there are regions of disordered material within the carbon (17) and that small quantities of other elements such as oxygen, hydrogen, nitrogen and sulphur can be incorporated. The crystalline regions contain carbon atoms in parallel layers as in graphite. However the stacked layers have been shown by Biscoe and Warren (18) to be randomly oriented ie. no 'stacking sequence' is present. This structure is termed turbostratic. A consequence of the random stacking is that the interlayer distance (3.4 - 3.7Å) (19) is greater than in macrocrystalline graphite (3.35Å). The size of the crystallites in an amorphous carbon can be extremely small. The c-dimension of some small crystallites indicates that they can be built of as few as three or four layer planes while the size of the layer planes (20Å across) is approximately the same as that of large polynuclear aromatic molecules.

Franklin (20, 21) has classified carbons into (i) graphitic carbons which contain a high degree of graphitic structure, (ii) graphitising carbons, which develop this structure on heating and (iii) non-graphitising carbons which do not.

Graphitising carbons consist of crystallites which show a tendency to near parallel orientation of layer planes. Non-graphitising carbons consist of crystallites which although increasing in size and number on heating at the expense of

disordered matter, stay randomly orientated e.g. a poly-
vinylidene carbon (22).

More recent work (23, 24) has shown that Franklin's
classification cannot be considered rigid and that some
carbons graphitise to an amount intermediate between the
classification types.

Graphitisation and fusion during carbonisation are inter-
related and Kipling et al. (25, 26) have shown for a large
number of carbons which they examined that a graphitising
carbon is not obtained unless fusion occurs. However they
point out that not all cokes are graphitisable. Brooks and
Taylor (27) have used polarised light microscopy to help
explain the formation of graphitised carbon from the liquid
phase which arises on carbonisation. They observed the
formation of anisotropic spheroidal particles which had grown
from an isotropic liquid matrix. These spheroids consisted
of polynuclear aromatic compounds in nearly lamellar orienta-
tion which coalesced on heating to form the nuclei from which
the graphite microcrystals were able to grow.

The final temperature of carbonisation influences several
physical properties of carbons. Paramagnetic Susceptibility
(28) and Electron Spin Resonance (29, 30) both reach a maxi-
mum in the region $500^{\circ} - 700^{\circ}C$ indicating the presence of
large numbers of unpaired electrons. From $500^{\circ}C$ upwards the

electrical conductivity (31, 32) increases up to a maximum in the region of $1100^{\circ}C$. It is in this region that the evolution of gases is complete. The conductivity then remains nearly constant up to a heat treatment temperature of $2000^{\circ}C$ (33). These observations and X-ray evidence from the carbonisation of coals (34) indicate that the crystallite thickness and mean aromatic layer diameter increase rapidly with heating in the $500^{\circ} - 700^{\circ}C$ region and then increase more slowly on heating to higher temperatures.

Information on the nature of the disordered material in an amorphous carbon cannot be obtained by X-ray diffraction techniques and its nature has been the subject of speculation by Gibson et al. (35). They proposed a structure consisting of a repetition of o-tetra phenylene residues or discrete benzenoid hexagons connected by valency bonds in a three dimensional network.

1.4.   Pore Structure of Carbons

Everett (36) has shown that the model of Gibson et al. (35) based on the o-tetra phenylene unit could give rise to a large open system of micropores resembling a zeolite structure. Pore structures of this type give carbons their adsorptive properties. The pore structure varies with the nature of the original starting material and the method of manufacture.

The size ranges of the pores in carbons have been the subject of much investigation notably by Dubinin (37 - 39). It is convenient to arbitrarily divide all pores into three types dependent on the pore size.

Macropores are mostly large enough to be seen and measured by means of the optical microscope although more detailed information concerning their size distribution can be found from measurement of the volume of mercury forced into the pores under various pressures i.e. by use of mercury porisimetry. A lower limit for the diameter of macropores is conveniently set at about 1000 - 2000Å; there is no upper limit.

Transitional or intermediate pores can be directly observed using an electron microscope and measured using mercury porisimetry. Another method for their study is based on analysis of the characteristic hysteresis loops found on the measurement of sorption isotherms. The diameter of transitional pores is conveniently set at between 1000 - 2000Å and about 30Å.

The smallest pores are called micropores. As yet these have not been directly observed although such observations may just be possible using an electron microscope. The linear dimensions of these pores are comparable with those of molecules normally used as adsorbates. Their diameter is set

at less than about 30Å.

A carbon generally contains pores of all three types although the contribution of each type to the total adsorption may greatly differ. For a carbon micropores normally make the largest contribution. Dubinin (37, 38) has shown for various carbons that there is a distinct tridisperse size distribution i.e. the carbons contain pores lying within three relatively narrow ranges of dimension one within each pore classification.

1.5. Activation

The activity of a solid is not a quantity which can be exactly defined. It is a term indicating the physico-chemical reactivity of the solid. Activation and de-activation can be characterised by changes in the X-ray structure, surface area, density, pore volume, pore distribution and in the heat of adsorption of adsorbates.

With microporous materials such as a carbon a meaningful surface area is difficult to obtain and a measure of the porosity gives a more useful indication of its activity.

Activation of carbons can be effected in two ways. (i) The addition of oxidising or dehydrating agents e.g. anhydrous zinc chloride to the parent material before carbonisation. (ii) Reaction of carbon with a gas such as steam, carbon dioxide or oxygen at high temperatures removing part of the

carbon and thus increasing its porosity; this method is employed in the present work.

As already stated the structure of a particular unactivated carbon depends on the parent material and the carbonisation process. For most carbons the pore volume varies from 0.05 to 0.5 $cm.^3g.^{-1}$ carbon. Activation can increase this pore volume by about a further 1 $cm.^3g.^{-1}$ for the highly porous carbons and by correspondingly less for the carbons of lower porosity.

1.6. Aims of Present Investigation

In any study of the reactions of a gas with a porous solid account must be taken of the influence of diffusion of reactants and products both within the pores and on the exterior surface. Hedden and Wicke (40) have proposed that the temperature dependence of the reactions of porous solids, notably carbons, with gases can be broadly divided into three zones. It will be useful to consider this classification before discussing the aims of the present work.

In the low temperature Zone I, the rate of gasification i.e. the observed rate of reaction depends on the rates of chemical reactions taking place on the carbon surface. In this range the whole of the internal surface of the solid takes part in the reaction and the rate of reaction is not affected by mass transfer processes as the concentrations of

reactant and product gases are evenly distributed within the carbon. Hence the experimentally observed activation energy is described as the 'true' activation energy for the reaction of the gas with the carbon surface.

At higher temperatures in Zone II the overall rate of reaction is increasingly dependent on the rate of diffusion of reactant and product gases through pores of the carbon. The observed activation energy falls to approximately half the 'true' activation energy.

At even higher temperatures in Zone III the mass transfer of gaseous products and reactants through a boundary gas layer around the external surface of the carbon determines the overall rate of reaction. Thus the activation energy for the reaction falls to very low values.

Rowan's work (6) on the activation of polymer carbons by carbon dioxide was carried out under conditions which indicated that the reaction was occuring in Zone II and on the borders of Zones I and II of the above classification. He concluded that within this range the temperature of activation had little effect on the development of the porosity of the carbons investigated.

In the present work the reaction of cellulose carbon with oxygen was carried out in the temperature range $400^{\circ} - 700^{\circ}C$ which under the conditions present was expected to cover Zones

II and III. It was expected, that carbons activated in Zone III would have little development of pore structure as the activating gas does not penetrate far into the carbon. Oxygen was chosen in preference to carbon dioxide as an activating gas for this study principally because the temperatures involved in the reaction were considerably lower (400° - $700^\circ C$ for oxygen and 850° - $1250^\circ C$ for carbon dioxide).

The main aims of the work may therefore be summarised as follows:-

(i) To investigate the rate of reaction of a porous cellulose carbon with oxygen over a temperature range extending over Zones II and III of the Hedden and Wicke (40) classification.

(ii) To attempt to relate the development of porosity to the rate and extent of the activation process; in particular to investigate the influence of diffusion control of reaction rate on the development of porosity.

(iii) To compare the properties of oxygen and carbon dioxide as activating gases by comparison with Rowan's work (6).

This work involved four main stages:-

(i) The preparation of a reproducible carbon by carbonisation of cellulose to 1000° in nitrogen.

(ii) The investigation of the rate of reaction

of the carbon with oxygen over the temperature

range 400° - 700°C.

(iii) The preparation of activated series of

carbons at several temperatures between 400° and

700°C.

(iv) The measurement of the porosity of the carbon

samples by adsorption of carbon dioxide at 195°K.

1.7. Outline of Thesis

The thesis consists of six chapters. The next two

chapters complete an introduction to the various aspects of

the work and the final three chapters constitute an account

of the work undertaken.

Chapter 2 contains a review of the carbon-oxygen reaction

and a discussion of some of the many factors influencing its

overall features. In Chapter 3 the methods available for the

measurement of the porosity in carbons and the Dubinin

Theory for adsorption in micropores are discussed. The effect

of surface oxide on adsorption and the development of porosity

which occurs on activation are also considered.

In Chapter 4 the results of the reactivity studies are

presented and discussed. Chapter 5 consists of the results of

the adsorption measurements and discussion of them both

qualitatively and in terms of the Dubinin Theory. Chapter 6

ends the thesis with a summary of the conclusions made and a number of suggestions for extension of the work.

CHAPTER 2

The Oxidation of Carbon

2.1. Introduction

Any development of a fundamental understanding of the mechanism of the reaction of amorphous carbons with oxygen has been greatly hindered by the complex structure of carbons and their resultant surface heterogeneity, and often by the changing extent and nature of the carbon surface during the course of the reaction. The product, or products of the reaction have not been clearly determined let alone the individual reaction steps. In fact the understanding of the carbon-oxygen reaction is poor compared with that of other gas-carbon reactions.

The traditional method of investigating the reactions of carbons with gases involves the measurement of the weight change of a carbon sample and/or the collection, identification and measurement of the gaseous products. This work has been carried out over a wide range of gas pressures and temperatures giving thermodynamic and kinetic parameters of the reaction (41). Recently much information has been gained from investigation of the reaction of oxygen with natural graphite using microscopic techniques (42).

Many factors have been shown to affect the carbon-oxygen reaction. Gaseous diffusion processes have been shown (41) to

influence the overall features of the reaction and will be
discussed in Section 2.4. The reactivity of the carbon
also depends on its crystallinity, heat-treatment tempera-
ture and the presence of impurities (See Section 2.5.).
The chemical nature of the surface complexes by which the
reaction is believed to proceed will be discussed in Section
2.6.

2.2.   Thermodynamic Features of the Reaction

The heats of reaction at $18^{o}C$ and 1 atm. for the
reactions to be considered in the combustion of carbon in
oxygen are given below. These have been determined (44) for
β-Graphite. Amorphous carbons have been reported (45) to
have positive heats of formation ranging from 1.7 to 2.6 k.cal.
$mole^{-1}$ on the basis of β-graphite having zero heat of forma-
tion.

[1] C   + O_2 =: CO_2 ΔH = -94.03 k.cal.$mole^{-1}$

[2] C   + $\frac{1}{2}O_2$ =: CO ΔH = -26.62 k.cal.$mole^{-1}$

[3] CO   + $\frac{1}{2}O_2$ = CO_2 ΔH = -67.41 k.cal.$mole^{-1}$

[4] CO_2 +   C   = $2CO$ ΔH = +40.79 k.cal.$mole^{-1}$
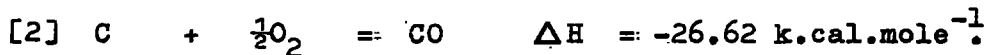
Equilibrium constants for the above reactions have been
tabulated (44). They show that equilibrium considerations do
not restrict the oxidation to carbon monoxide and carbon dioxide
up to $4000^{o}K$. However many investigations have been made to
decide the relative extent to which these reactions contribute

to the overall combustion reaction at different temperatures and under different conditions (41). In particular, experimental evidence has been sought to decide whether the final mixture of carbon dioxide and carbon monoxide obtained by the combustion, arises from reaction [1] and reaction [2] occuring simultaneously or whether the first formed gas(es) subsequently undergo the secondary reactions [3] and [4]. Because of the various chemical and physical conditions that inevitably prevail in combustion investigations, the conclusions of different workers on the primary products of the carbon-oxygen reaction have often been conflicting.

The problem has been approached in many ways but all methods have the same object in view; to eliminate or severely reduce the complications which the secondary reactions [3] and [4] introduce. This has been done by four main methods:- (i) use of low pressures (46 - 51), (ii) use of high gas flow over the carbon (52 - 55), (iii) addition of substances known to inhibit reaction [3] (56 - 61) and (iv) conducting the carbon-oxygen reaction at sufficiently low temperatures to be able to assume that the rates of reactions [3] and [4] were negligible (62, 63).

Near total agreement has been reached that both carbon monoxide and carbon dioxide are the primary products. However the relative proportion of the two gases obtained

would appear to depend on the temperature and conditions of the oxidation reaction. Arthur (59) and Rossberg (62) have determined that the temperature dependence of the ratio of carbon monoxide to carbon dioxide on gasification of a variety of different carbons over temperature ranges of $460^{o} - 900^{o}C$ (59) and $520^{o} - 1420^{o}C$ (62) is given by the equation $CO/CO_2 = ae^{-b/RT}$ where a is of the order of $10^{3.4}$ and b is approximately 12.4 k.cal.mole^{-1}. Arthur claimed that the results of several low pressure experiments (58 - 60) over the range $900^{o} - 2000^{o}C$ were consistent with this equation. Lewis et al. (63) in agreement with Arthur found that the CO/CO_2 ratio is constant below $520^{o}C$ at ca. 0.3, Arthur having found a value of 0.9.

Both Rossberg and Arthur felt that reaction [4] was not a factor affecting the CO/CO_2 ratio even at the higher temperatures. More recently Frey (64) investigated the extent of secondary reactions on the oxidation of charcoal by addition of CO and CO_2 labelled with ^{14}C to the reaction. He found that reaction [4] did not occur below $600^{o}C$. Reaction [3] occured to some extent below $550^{o}C$ but did not account for all the carbon dioxide formed; above this temperature the secondary oxidation occured more readily.

Using high gas flow-rates to study the carbon-oxygen reaction, Day (54, 55) found the CO/CO_2 ratio to be independent

of the rate of gas flow over the temperature range
1300° - $1900^{\circ}C$ and concluded that carbon dioxide is a primary
product. At lower flow-rates the gas phase oxidation of
carbon monoxide occured. At variance with Arthur (59) and
Rossberg (62) he found that the CO/CO_2 ratio varied with the
type of carbon. He found a similar temperature dependence of
the CO/CO_2 ratio to these workers but the ratio was much lower.

The use of gas phase inhibitors of reaction [3] such as
CCl_4, Cl_2, HCl and $POCl_3$ (56 - 61) produces substantial
increases in the CO/CO_2 ratio. However this increase could
also be ascribed to the fact that halogen acids can be incorp-
orated into the carbon structure (64), thus affecting the
reaction at the carbon surface.

A summary of available evidence would seem to suggest
that carbon dioxide and carbon monoxide are both primary
products below $600^{\circ}C$ but above that temperature as Blyholder
and Eyring (65, 66) have claimed for the reaction of a
graphitic carbon with a low pressure of oxygen, carbon monoxide
may be the only reaction product. In any case the amount of
carbon dioxide produced above $600^{\circ}C$ is very small. The
CO/CO_2 ratio is probably dependent on the carbon surface and is
a function of the temperature of reaction. Lack of agreement
in much of the work in this field may therefore be caused by
actual differences in the CO/CO_2 ratio for different surfaces

or by the inability to prevent secondary reactions.

2.3. Kinetic Features of the Reaction

2.3.1. The Reaction Mechanism

In kinetic studies of the oxidation of carbon many attempts have been made to produce a detailed mechanism of the process from consideration of reaction order, activation energy and the pre-exponential factor. However these results have often been misinterpreted owing to the fact that mass transport of gaseous reactants and products has controlled the course of the reaction. The effect of mass transport control on the reaction will be discussed in Section 2.4., while the chemical reaction itself will be discussed under this heading.

A mechanism for the carbon-oxygen reaction which accounted for the wide variation of experimentally observed data would probably be very complicated. This discussion will be limited to consideration of an outline reaction scheme (41) which nevertheless can account for the general features of the reaction kinetics, although it may not account for all details.

Step [1] Transport of oxygen to surface reaction site.

Step [2] Adsorption of oxygen to form a surface complex.

$$C + O_2 \xrightarrow{k_2} C(O_2)$$
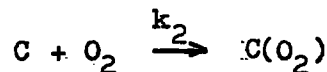
Step [3] Rearrangement of the surface complex to give a desorbable product.

$$C(O_2) \xrightarrow{k_3} C(O_2)'$$
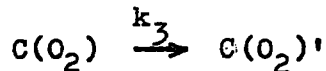
Step [4] Desorption to yield the reaction products

CO and/or CO_2.

$$C(O_2)' \xrightarrow{k_4} \text{Products}$$
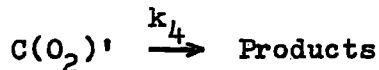
Step [5] Transport of reaction products away from the surface.

It would appear reasonable (41, 60) to assume in the absence of transport control (See Section 2.4) that the rate controlling step is either step [3], or step [4] since step [2] occurs readily at temperatures above ca. $100^{\circ}C$ (67). The discussion will assume that step [3] is rate controlling but a similar argument would result if step [4] were rate controlling.

Thus the rate of reaction will depend on the fraction (Θ) of surface available for reaction covered by surface complex and, k_3, the rate constant for rearrangement of the complex to a desorbable product. Hence at a fixed temperature the order of reaction depends on the variation of Θ with respect to oxygen pressure. At high pressures if $\Theta \longrightarrow 1$, near zero order dependence would be expected, whereas at low pressures if $\Theta \longrightarrow 0$ near first order dependence would be expected; at intermediate pressures the order would be expected to vary from $0 \longrightarrow 1$. Attempts have been made (68 - 70) to quantitatively express the rate of reaction of a carbon black

with oxygen at low pressures (ca. 4×10^{-3} cm.Hg) and in the temperature range $575^\circ - 675^\circ C$ by

$$-dP_{O_2}/dt = k_{O_2} (P_{O_2}) (ASA) (1 - \theta)$$

where P_{O_2} is the oxygen pressure, (ASA) is the active surface area of the sample at the temperature in question, $(1 - \theta)$ is the fraction of (ASA) unoccupied by surface complex and k_{O_2} is the rate constant. It can be seen that the order of reaction predicted by this equation is determined by θ in the manner discussed above. However another complication is introduced by the fact that the active surface area may vary during the early stages of the reaction (60). Thus the value of θ and hence the order of the reaction may also be influenced by the extent of the reaction.

Activation energies for the overall reaction have been much studied. The activation energy for the overall reaction is a complex composite of the activation energies for the individual steps of the reaction. It will be related to the rate controlling step and if this were to vary with temperature one would expect the overall activation energy to vary as well as the reaction order. Rossberg (62) has attempted to relate the activation energy for several gas-carbon reactions to the dissociation energy required to remove an oxygen atom from the reactant gas. The dissociation energy for $\tfrac{1}{2}O_2 \longrightarrow O$ is 59 k.cal.mole^{-1}. But as Walker (41) points out unless oxygen

chemisorbs in the form of a peroxide structure this is not a valid comparison with the activation energy.

Although, the above mechanism accounts for some of the features of the carbon-oxygen reaction, it is clearly only an outline mechanism. There may for instance be several varieties of surface complex (71) taking part in the reaction and a more detailed mechanism would need to account for the formation of more than one reaction product. A more detailed reaction scheme has been proposed by Ong (72) to account for a wide range of data but, as he admits, it may not be correct in all details.

2.3.2. Experimental Parameters of the Reaction

2.3.2.1. Reaction Order

A large number of workers (48 - 50, 54, 62, 63, 73 - 75) have found that under a wide range of conditions the reaction follows first order kinetics. These results must be carefully scrutinised before the observed order is seen to be a function of the chemical reaction and not influenced by mass transfer. For example, Day et al. (54) found a first order dependence on the oxygen pressure but were clearly working under diffusion-controlled conditions. Lewis et al. (63) studying the reaction of a coke with air flowing over the sample found the order to be one; this result may also have been influenced by diffusion. In addition, as Duval (51) notes, several workers determine or

assume a reaction order on the basis of apparently incomplete data.

A number of workers (47, 48, 50, 74) have found a first order dependence of the reaction rate on the oxygen pressure at temperatures less than $1500^{\circ}C$ and at pressures of less than ca. 0.5cm.Hg. when the influence of mass transfer may be presumed to be minimised. The two investigations claiming the presence of zero order kinetics must be carefully assessed. Blyholder and Eyring's (65) work using thin graphite coatings on ceramic substrates indicated a zero order reaction at $600^{\circ} - 800^{\circ}C$. However their work was carried out over a limited pressure range ($10^{-5} - 10^{-3}$cm.Hg) and the data presented could be interpreted within the experimental error as indicating fractional order kinetics (51); there is also the possibility of catalytic effects associated with the ceramic base. Gulbransen and Andrew (77) report the reaction rate [R] of spectroscopically pure graphite between 425° and $575^{\circ}C$ over oxygen pressures [P] of 0.5 - 9.8cm.Hg. in the form R = A + BP, where A and B are constants. They claimed the order to be near zero below 1.5cm.Hg. and to be one above 9.8cm.Hg. However Blyholder and Eyring (65) consider the evidence to be inconclusive and that the order of reaction could equally well be fractional. It is interesting to note that Gulbransen and Andrew's (77) suggestion is not consistent with the reaction

scheme discussed in Section 2.3.1.

2.3.3.2. <u>Activation Energy and Pre-exponential factor</u>

A wide variation in values of the activation energy have also been reported in the literature. Activation energies of about 80 k.cal.mole^{-1} have been found for reactions with pressures of oxygen of less than ca. 10^{-3}cm.Hg. (48, 65). Rossberg (62) and Wicke (60) working with porous carbons and an oxygen-nitrogen mixture at atmospheric pressure found activation energies of 50 - 58 k.cal.mole^{-1} and 58 ($\pm$ 4) k.cal. mole^{-1} respectively. From their results it is apparent that they were working in the region of chemical control. Gulbransen and Andrew (77) report an activation energy of 36.7 k.cal.mole^{-1} for the initial rate of reaction between thin graphite plates and oxygen at a pressure of 7.6cm.Hg. and at temperatures of 425° to 575°C; mass transport was apparently not affecting their results. Many other workers (63, 75, 78 - 88) have reported widely varying activation energies ranging from 17 k.cal.mole^{-1} (63) to 100 ($\pm$ 30) k.cal.mole^{-1} (78); some of these values are obviously affected by mass transport and the catalytic effects of impurities.

Serpinet (85) has reported an activation energy, for the reaction between spectroscopically pure graphite and air which apparently varies with temperature within the region of chemical control. Under atmospheric pressure he found activation energies

ranging from 40 k.cal.mole^{-1} at·500°C to 75 k.cal.mole^{-1} at 720°C. A similar variation has been observed by Bonnetain (85) working with the same graphite and oxygen pressures of the order of 10^{-3}cm.Hg. Heuchamps (87) also working with the same graphite found·that the activation energy varies as a function of the amount of burn-off. Values of the activation energy ranged from 62 k.cal.mole^{-1} at 17% burn-off to 37 k.cal.mole^{-1} at 98% burn-off. This could possibly·be accounted for by an increase in the concentration of impurities as the amount of burn-off increases.

When the variation of reaction rate with temperature is expressed by means of the Arrhenius equation Rate·= A$e^{-E_a/RT}$ the value of the pre-exponential or frequency factor A can be useful in giving information about the reaction. However values of this factor have rarely been reported for gas-carbon reactions. This is possibly due to the difficulty in expressing the parameter in units which allow useful comparison between different investigations. Rates·of reaction and hence pre-exponential factors are commonly expressed in terms of a unit area of carbon surface or a unit of carbon weight. Thus unless specific surface areas are known with some certainty comparisons are difficult.

Wicke (60) reported values of the pre-exponential factor for both the C – O_2 and the C – CO_2 reactions expressed in

cm^3(NTP) gas. cm^{-2}.surface. sec^{-1}. He found the factors for the two reactions were very similar (ca. 3×10^9) and deduced from this that the rate controlling step was in each case the rearrangement of the surface oxide to form a desorbable product. Gregg and Tyson (88) report a pre-exponential factor of ca. 2×10^{-8} $g.sec^{-1}.g.$ for the reaction of oxygen at $490°$ - $550°C$ with a petroleum pitch carbon prepared at $1000°C$. They express their rates in this way because of the uncertainty attached to values of surface area for fine-pored solids. For carbons prepared at higher heat-treatment temperatures the frequency factor varies in parallel to the activation energy (See Section 2.5.).

2.4. Influence of Mass Transport on the Reaction

It has already been said in Chapter 1 that mass transport of reactants and products can have a great influence on the overall features of the reaction between a porous solid and a gas. Tu et al. (89) were the first to develop a theory which indicated the conditions under which the diffusion of reactant and product gases to and from the surface could be expected to control the reaction. Their approach has been substantially developed and improved by others (90 - 92, 60, 40, 41).

When considering the reactions of gases with porous solids, the transport of reactant and product gases across a relatively stagnant layer of gases between the exterior solid surface and

the main gas stream, and through the porous body of the material must be considered. Hedden and Wicke (40) have discussed the temperature dependence of rates of reaction of a porous solid with gases in terms of the three temperature zones discussed in Section 1.6. However Walker et al. (41) have proposed situations under which the ideas of Hedden and Wicke (40) may not represent the true situation. For example it is possible that when the reaction takes place within the pores in Zone II that product retardation may have an influence on the overall chemical reactions and thus alter the activation energy in that zone.

A more detailed explanation of the features of the reaction in Zones II and III is now necessary.

In Zone II where diffusion within the pores controls the overall reaction rate, Wheeler (91) has shown that the rate of reaction $\frac{dw}{dt}$ is given by

$$\frac{dw}{dt} = C_R^{\frac{m+1}{2}} \cdot \sqrt{k_v D_{eff.}}$$

where C_R is the reactant gas concentration at the exterior surface of the solid, k_v is the specific rate constant per unit volume of carbon, m is the order of reaction with respect to reactant gas pressure, and D_{eff} is the effective diffusion coefficient of the gases through the pores of the material. In determining this equation Wheeler (91) assumed that the gas concentration at any depth of penetration into the specimen is constant and that all the surface area at any given penetration is available

for reaction with the gas present at that depth. Implicitly, the derivation assumed that the penetration of gas occurs along a series of pores of varying size and dimensions, interconnected at short intervals. If it is assumed that the effective diffusion coefficient of the gases throughout the pores is constant throughout the solid and that the surface area available for reaction does not vary with burn-off, the above equation will represent the reaction in Zone II. Evidence that the surface area available for reaction does not vary after the early stages of burn-off has been presented by Wicke (60) and Walker et al. (41). Using Wheeler's (91) equation it is possible to show that the activation energy in Zone II is half that in Zone I. Also, certain experimental criteria can be evaluated for reaction in Zone II, although at present these have only been tested with specimens of known geometry (41).

Walker et al. (41) have shown that at temperatures high enough to give appreciable rates of reaction at the external surface, $\frac{dw}{dt} = \frac{C_g \, D_{free}}{\delta}$ where C_g is the reactant gas concentration of the free gas and D_{free} is the diffusion coefficient of reactant gases through the external layer of product gases of thickness δ. Thus the reaction in Zone III is clearly seen to be first order with respect to the reactant gas concentration. Day (54, 55) has confirmed this for the

carbon-oxygen reaction and has shown that the activation energy was less than 8 k.cal.mole^{-1}. under the conditions employed. This is in agreement with a small variation of diffusion coefficient with temperature. The equation indicates that in Zone III the rate of reaction is independent of the type of carbon and Day (54, 55) has shown this to be approximately true.

2.5. <u>The Influence of Other Factors on the Reaction</u>

The influence of mass transport has already been discussed in the previous section (2.4). It is useful to consider now those features of the carbon itself which are known to influence reactivity. The effects of crystallite orientation and size, heat-treatment temperature and presence of impurities will therefore be considered under this heading.

Carbons are substances containing various amounts of crystalline material and the degree of surface heterogeneity depends to some extent on the size and orientation of the crystallites. The two extremes in which the crystallites can orientate are (i) with the basal {0001} planes parallel to the surface and (ii) with basal planes perpendicular to the surface.

Much work (93 - 95) has been directed to obtain the ratio of the oxidation rates parallel and perpendicular to the basal plane. The ratio appears to differ with the sample of carbon used but the rate parallel to the basal plane is much the

greater. From this work one would expect a graphitic carbon containing crystallites with basal planes mainly parallel to the carbon surface to be less reactive than a non graphitised carbon where the crystallites are more randomly orientated. Smith and Polley (95) interpreted their results for the reactivity of a non-graphitised and a graphitised carbon in these terms. Walker et al. (41) also suggested a similar explanation to account for their results of markedly different rates of reaction of carbon dioxide with cokes and graphitised carbon blacks.

Heat treatment will affect the graphitisation of some carbons and hence the reactivity. Gregg and Tyson (88) studied the oxidation of a series of carbons prepared from a petroleum pitch - coke mixture by heat treatment to temperatures between 1000° and $3000^{\circ}C$. They measured the oxidation rates for these carbons in the temperature range 490° - $550^{\circ}C$ and at 7.6cm.Hg. pressure of oxygen and also determined activation energies. The activation energy varied with the temperature of preparation from 44 k.cal.mole^{-1}. for the $1000^{\circ}C$ carbon to a maximum of 67 k.cal.mole^{-1}. for a $1580^{\circ}C$ carbon falling to 44 k.cal.mole^{-1}. for the $3000^{\circ}C$ carbon. They considered that by increasing the temperature of preparation the graphitic character of the carbon increased, thus tending to increase the activation energy. However this effect was masked by a decrease in porosity of the

carbons with increasing temperature of heat treatment. They
proposed that the oxidation occured in Zone I of the Hedden
and Wicke classification. for carbons of high porosity, i.e.
those prepared below ca. 1500°C, and in Zone II for those
of lower porosity.

The widely varying range of activation energies reported
by many workers for the carbon-oxygen reaction can be
ascribed in some cases to varying amounts of impurities in
the carbons. Although a number of workers (2,3, 42, 77, 81,
94, 95, 97) have investigated the catalytic effect of certain
inorganic impurities on the rate of reaction of carbons with
oxidising gases, the reasons for the catalytic behaviour are
not well understood. The ash normally present in carbon as
an impurity may have a considerable catalytic effect. Long
and Sykes (2) de-ashed a carbon by leaching with hydrofluoric
acid and found a much reduced rate of oxidation, yet the same
quantity of chemisorbed oxygen. However Frey (64) has
suggested that this may be due to halogen atoms being incor-
porated in the carbon structure and thus reducing the rate of
reaction.

Gallagher and Harker (3) showed that addition of small
quantities of iron, cobalt and nickel compounds decreased the
ignition temperature of a cellulose char by up to 70°C, show-
ing that the rate of reaction was increased by the addition of

the impurity. They also showed that the addition of impurity had little effect on the thermal stability of the surface-oxide at 400°C (See Section 2.6.). In agreement with Gulbransen and Andrew (77) they found the CO/CO_2 ratio of the evolved products increased with addition of impurity.

2.6. The Nature of Surface Oxides

The formation of solid surface oxygen complexes on charcoal is intimately bound with the reaction to form gaseous products. The fact that there is evidence that some reactions (52, 98, 99) proceed via a surface complex to gaseous products indicates that a knowledge of their structure may be important in determining the reaction mechanism. The chemisorption of oxygen by carbons has been much studied, however a structural theory is far from being found. The nature and amount of complexes on any sample varies with the surface area, porosity, particle size, degree of carbonisation and graphitisation, and impurities present.

Temperature is the most important factor determining the nature and formation of surface complexes by reaction with oxidising gases. Below 195°K oxygen has been shown (100) to be predominantly physically adsorbed on carbon surfaces. At higher temperatures substantial chemisorption occurs, the amount increasing with temperature.

Lowry and Hulett (101) found that charcoal exposed to

air at room temperature contained up to 3 - 4% oxygen. Weller and Young (104) and Snow et al. (82) have shown that this amount increases with temperature up to 400° - $500^{\circ}C$ where carbons containing up to 20% oxygen may be prepared. At higher temperatures the amount of surface oxide formation decreases and the formation of gaseous products increases. At $1000^{\circ}C$ there is no evidence for the formation of solid surface complexes. Whatever the nature of the carbons the optimum temperature for oxygen fixation appears to be 400° - $500^{\circ}C$ (43).

Chemisorbed oxygen can be completely removed from the carbon surface by heating to a temperature in the region of 1000° - $1200^{\circ}C$. It is removed as carbon monoxide and carbon dioxide (52, 103). Puri and Bansal (103) showed that carbon dioxide was evolved from ca. 200° - $300^{\circ}C$ to ca. 500° - $700^{\circ}C$ while carbon monoxide was evolved from ca. 500° - $700^{\circ}C$ to ca. 1000° - $1200^{\circ}C$. They found that the ratio of CO/CO_2 evolved on heating varied with the nature of the carbon.

The principal functional groups which have been shown (104, 105) by chemical analysis to be present in surface complexes are carbonyl, phenolic hydroxyl, and carboxylic acids. The presence of oxygen in the form of ether linkages is also postulated. Infra-red spectroscopy has in general confirmed the presence of these groups (43) and detected aromatic rings

and carbon-hydrogen bonds. However as carbons containing more than 94% elemental carbon are opaque to infra-red radiation, the technique has its limitations.

Dependent on the condition of the surface and the temperature of oxidation, the surface oxide can either be acidic or basic in character. From studies on the adsorption of acids and bases from dilute aqueous solution, workers (71, 106 - 108) have suggested that different oxides form at different temperatures.

The acidic functional groups are carboxyl and phenolic hydroxyl. These undergo normal organic reactions (109). Although the presence of basic oxides has been known for much longer, nothing is definitely known about their constitution. Garten and Weiss (110, 111) suggested they are chromene-like or semi-quinone structures but this has not been confirmed.

It has been shown that oxygen is almost entirely chemisorbed on the prism faces of graphite crystals (94). Single crystals were oxidised with molecular oxygen at $700^\circ C$ and the gaseous products were determined mass spectrometically. The experiment was repeated with the crystals cleaved five times parallel to the layer planes, i.e. with the area of the prism faces the same and the area of the basal faces increased sixfold. The amount of gas evolved was unchanged. Highly graphitised carbon blacks have a very homogeneous surface (112) which

consists almost entirely of basal graphite planes (24) and hence these blacks form very little surface oxide (113).

CHAPTER 3

The Porosity of Activated Carbons

3.1.   The Determination of Porosity in Carbons

3.1.1. Introduction

A wide variety of methods are available for the measure-
ment of porosity in carbons. In this work the analysis of
adsorption isotherms by the method of Dubinin has been used.
This method will be discussed in Section 3.2.2. while other
methods are briefly reviewed under this heading.

3.1.2. Apparent Density Methods

Information about the porosity of carbons can be obtained
from the measurement of the apparent density of a sample in
a variety of gases and liquids.

A 'true' density of the carbon may be obtained from
measurement of its displacement in a liquid or gas whose mole-
cular dimensions are such that all pores are penetrated.
Densities determined in helium at room temperature (4, 114,
115) have been widely used in this way. However, it has been
shown (116) that for certain carbons physical adsorption of
helium may occur at room temperature yielding anomalously high
densities and hence measurements must be carried out at 300°C.
At any temperature helium cannot reach closed pores and a low
value for the density will be obtained if such pores are
present. It has recently been shown (117) that in some carbons

pores which are inaccessible to helium at room temperature become accessible at 300°C.

If the density of a carbon in mercury (ρ_{Hg}) is compared with that in helium (ρ_{He}) the total pore volume can be determined. Mercury does not wet carbon and therefore pressure is required to force it into the pores. The relation between the radius of the pore entrance r, and the minimum pressure required to fill the pores P, is given by a form of the Kelvin equation (118):-

$$r = \frac{-2\,\sigma\cos\theta}{P} \qquad \text{Equation 3.1.}$$

where σ is the surface tension of mercury and θ is the angle of contact. From this equation it follows that at atmospheric pressure mercury cannot enter pores whose entrances are less than ca. 7 x 10^{4}Å diameter i.e. very large macropores. Hence the reciprocal of the mercury density of a carbon determined at atmospheric pressure effectively defines the specific volume of the carbon and pores. Thus if a reliable helium density can be obtained the total volume of pores of diameter up to 7 x 10^{4}Å is given by:-

$$\text{Total Pore Volume} = \frac{1}{\rho_{Hg}} - \frac{1}{\rho_{He}} \qquad \text{Equation 3.2.}$$

Densities can also be determined in gases and liquids of larger molecular size than helium (4, 114, 115, 119, 120).

In these cases penetrating molecules will be excluded from pores whose entrances are narrower than the molecular diameter. However densities obtained in this way are not always reliable as the density of the dilatometric fluid in the pores may not be the same as in the bulk fluid (115), particularly if adsorption occurs, and hence densities so determined may be incorrectly high. Another cause of anomalous apparent densities is the slow or incomplete penetration of accessible pores by the molecules of the dilatometric fluid (115), leading to incorrectly low values for densities in this case.

Size distributions of macro-pores and transitional pores can be obtained (121 - 123) by measuring the volume of mercury which can be forced into pores under various pressures and applying Equation 3.1; this technique is called mercury porisimetry. However the determination of micropore size distribution is not possible because of the very high pressures involved (greater than 7000 atms.).

3.1.3. Adsorptive Methods

The measurement of adsorption of gases and vapours by a porous solid can yield information about its pore structure. Several methods of interpreting isotherms have been suggested each with its advantages and limitations. As already mentioned, in the present work the Dubinin Theory of Micropore Filling, a modification of the Potential Theory has been used. This will

be discussed in Section 3.2. A brief review of some of the
other methods follows.

Values of the pore volume can be obtained by use of
the Gurvitsch Rule (124) provided that a definite amount w_s
is adsorbed at saturation. Assuming that all pores are filled
with liquid having its bulk density ρ, the pore volume
$V_s = \dfrac{w_s}{\rho}$. The amount adsorbed at saturation w_s is only readily
identifiable for Type I and some Type IV isotherms of the
Brunauer classification (125). It has also been shown (4,
117) that in some cases the pores may not be completely filled
at saturation.

The determination of surface areas by application of the
Brunauer, Emmett and Teller (BET) equation (126) to isotherms
on microporous carbons can be criticised for several reasons.
Firstly the BET theory assumes that in the monolayer localised
adsorption takes place on energetically homogeneous sites,
whereas the surface of a carbon is likely to be very hetero-
geneous in nature and, except at very low temperature, adsorp-
tion is likely to be non-localised (127). In the form of the
BET theory usually applied to porous adsorbents (128) it is
also assumed that the adsorption forces of opposite walls of
the pores do not interact and that the number of adsorbed
layers 'n' is determined by pore width alone. These two
assumptions are unlikely to be justified in the case of micro-

porous materials as the pore walls are extremely close; also 'n' has been shown (4) to decrease with increasing activation of carbons whereas all other evidence indicates that pore widths increase on activation. It has been calculated (129) that the theoretical maximum for the surface area of graphite is 2680 m^2g^{-1} assuming adsorption of a monolayer on both sides of a single layer graphite plane. However a number of workers (129 - 131) have determined surface areas in excess of this figure, and as high as 4,560 m^2g^{-1} (131). These areas must be regarded as unrealistic. It is worthwhile to note that some workers (132, 133) now consider that the concept of surface area has no physical meaning when applied to microporous materials. An advantage of the Dubinin Equation is that the concept of surface area in micropores does not arise.

The size distribution of transitional pores can be investigated by an analysis of hysteresis loops which occur in the adsorption - desorption isotherms of various adsorbates by application of the theory of capillary condensation. For an adsorbent containing non-intersecting cylindrical pores the relative pressure p/p_o at which desorption occurs is related to the radius of the pore entrance 'r', by a form of the Kelvin equation:-

$$\ln p/p_o \ = \ \frac{-2\sigma V^* \cos\theta}{rRT} \qquad\qquad \text{Equation 3.3.}$$

where V^* = molar volume of the adsorbate, σ = surface tension and θ = angle of contact. Using this method pore size distributions in the range 25 - 300Å have been found (122, 134, 140) for a variety of adsorbent-adsorbate systems. Some of these distributions have been shown to agree with those obtained by mercury porosimetry (122) and electron microscopy (137). However the Kelvin equation is not normally applied to pores of less than ca. 25Å diameter as it is doubtful whether concepts such as surface tension and angle of contact have any physical meaning in such small pores.

3.1.4. Other Methods

When a solid is immersed in a fluid, heat is evolved due to adsorption of the fluid on the surface of the solid. In the case of non-porous solids the amount of heat evolved is directly proportional to the total surface area and hence heats of immersion can be used to determine specific surface areas (141). However the method has the inherent difficulty that the conversion factor must first be obtained by finding the heat of immersion of a standard solid whose surface has been independently determined. For the determination of surface areas of porous carbon, carbon blacks are used as standards since their surface areas can be determined by electron microscopy and vapour adsorption. The surface area

---

* denotes the adsorbed state.

of a standard carbon black used by Bond and Spencer (119) was found to be ca. $230m^2.g^{-1}$ by electron microscopy and vapour adsorption. The heat of immersion in methanol was 21.5 cal.g^{-1} and hence the conversion factor used in their work was ca. $10.7m^2.cal^{-1}$. However carbon blacks have more homogeneous surfaces than porous carbons and this throws some doubt on the value of the conversion factor when applied to heats of wetting of porous carbons. Errors may also arise from the relative inaccessibility of some pores to the liquid resulting in slow liberation of the heat of immersion. This method also requires the assumption of surface area which, as previously discussed, is of doubtful validity when applied to micropores.

From the intensity distribution of the low angle scattering of X-rays by a thin layer of carbon, particle size, pore volume and surface area can be obtained as well as the crystalline/non-crystalline ratio. (142, 143). However to obtain values of the surface area and pore volume a number of assumptions are required, not least a model for the pore structure. In order to facilitate interpretation of the intensity distributions, these models are usually simple and since the pore structure of carbons is known to be complex, the results are of limited value.

Optical microscopy can be used to study macropores, which

can be clearly seen in sections of polished surfaces (37).

Using an electron microscope pores of ca. 200Å have been

observed (37). By statistical evaluation the average numbers

and dimensions of pores can be obtained using both techniques

(137). As yet micropores have not been observed using the

electron microscope although this may be possible with

improved resolution.

3.2.   **Theories of Adsorption in Micropores**

3.2.1. **Polanyi Potential Theory**

Polanyi who introduced (144, 145) the concept of adsorp-

tion potential proposed that the forces of attraction between

a surface and adsorbed molecules decreased with the distance

from the surface. He defined the adsorption potential at any

point as the work required to bring a molecule from the gas

phase to that point. According to the Polanyi Theory the

adsorption space may be considered to consist of series of

surfaces of equipotential, ε_i, enclosing volumes V_i, the

adsorption potential varying from a maximum at the adsorbent

surface to zero at the outermost layer, which encloses the

total adsorption volume V_o. Thus the variation of adsorption

potential with the distance from the adsorbent surface can

be represented by an equation of the form $\varepsilon = f(V)$ called

the characteristic curve. Polanyi proposed that the forces

of adsorption were similar to van der Waals forces in gases and

on this basis further postulated. that the characteristic curve is independent of temperature.

Polanyi suggested that when the temperature is much below the critical temperature of the adsorbate, the adsorption potential ε_V enclosing the adsorption space V is given by the work done in compressing one mole of vapour from its equilibrium pressure p to its saturated vapour p_o

i.e. $\varepsilon_V = RT \ln (p_o/p)$ Equation 3.4.

The adsorption space $V = w/\rho_T^*$, where w = weight of adsorbed film and ρ_T^* is the density of the adsorbate at temperature T.

Berenyi (146) was the first to illustrate the temperature independence of the characteristic curve. Using Titoff's (147) results for the adsorption of carbon dioxide on a charcoal at $273^\circ K$ he successfully predicted isotherms at other temperatures.

Polanyi (148) and Berenyi (146, 149) also investigated the relationship between the characteristic curves of different gases on the same adsorbent. They found empirically that the adsorption of any two gases on charcoal was related by:-

$(\varepsilon_1/\varepsilon_2)_{V = 0} = (a_1/a_2)^{1/2}$ Equation 3.5.

where a_1, a_2 are the van der Waal's constants of the two gases. Assuming this to be valid at all values of V they claim that:-

$$\ln (p/p_o)_1 = (a_1/a_2)^{1/2} \ln (p/p_o)_2 \qquad \text{Equation 3.6.}$$

This expression has been experimentally verified (150, 151).

It was the problem of predicting adsorption isotherms for any gas on a solid from the isotherm of a single gas on that material that led to the development of the Potential Theory by Dubinin and co-workers (37, 38, 133, 152-6).

3.2.2. The Dubinin Theory

Although the Dubinin Theory for adsorption in micro-pores is developed from the Polanyi Potential Theory, in its more recent formulations the term adsorption potential is not used to describe the function ϵ, as this would imply that an equipotential surface exists within the adsorbent pores on which the adsorbate pressure is equal to p_o, the saturated vapour pressure. Dubinin defines the function ΔG as the change in free energy during reversible isothermal transfer of one mole of the adsorbate from the bulk liquid to an infinitely large amount of adsorbent i.e. $\Delta G = \overline{G}^* - G_L'$ where $\overline{G}^*$ is the chemical potential of the adsorbate in the adsorbed state and G_L' is the molar free energy of the bulk liquid at unit pressure. Since adsorption is a spontaneous process ΔG must be negative. Hence as $p < p_o$, $\Delta G = + RT \ln (p/p_o)$. Thus the terms ϵ and $-\Delta G$ are interchangeable.

Dubinin retains the postulate that the characteristic curve $-\Delta G = f(V)$, i.e. a plot of $RT \ln p/p_0$ against $w \cdot V^*$ where w is the amount adsorbed of adsorbate of molar volume V^*, is temperature independent; this can be expressed as:-

$$\left(\frac{\partial \Delta G}{\partial T}\right)_{w \cdot V^*} = 0 \qquad \text{Equation 3.7.}$$

This criterion cannot be fulfilled over the whole range of adsorption from $w = 0$ to saturation and it can be shown in principle, that the molar entropy change on adsorption, $\Delta S = \overline{S}^* - S_L^{!}$, where $\overline{S}^*$ is the partial molar entropy of the adsorbate and $S_L^{!}$ is the molar entropy of the bulk liquid at unit pressure, i.e.

$$\Delta S = - \left(\frac{\partial \Delta G}{\partial T}\right)_w \qquad \text{Equation 3.8.}$$

must be negative for the criterion to be satisfied.

It it is assumed that $w = f_1(\Delta G, T)$ and $w \cdot V^* = f_2(\Delta G, T)$ then it can be shown that $\left(\frac{\partial \Delta G}{\partial T}\right)_{w \cdot V^*}$ and $\left(\frac{\partial \Delta G}{\partial T}\right)_w$ are related by:-

$$\left(\frac{\partial \Delta G}{\partial T}\right)_w = \left(\frac{\partial \Delta G}{\partial T}\right)_{w \cdot V^*} + \left(\frac{\partial \ln V^*}{\partial T}\right)_{\Delta G} \left(\frac{\partial \Delta G}{\ln w}\right)_T$$

$$\text{Equation 3.9.}$$

if the assumption $\left(\frac{\partial V^*}{\partial w}\right)_T = 0$ is made i.e. if the molar volume of the adsorbate is assumed to be independent of the amount

adsorbed at constant temperature. The function $\left(\dfrac{\partial \ln V^*}{\partial T}\right)_{\Delta G}$

can be regarded as the coefficient of thermal expansion (α^*) of the adsorbed substance at constant ΔG and this will normally be positive i.e. $\left(\dfrac{\partial \ln V^*}{\partial T}\right)_{\Delta G} = \alpha^* > 0$. Hence

$$-\Delta S = \left(\frac{\partial \Delta G}{\partial T}\right)_w = \left(\frac{\partial \Delta G}{\partial T}\right)_{w.V^*} + \alpha^*\left(\frac{\partial \Delta G}{\partial \ln w}\right)_T$$

<div align="right">Equation 3.10</div>

It is found from characteristic curves that ΔG is always an increasing function of w ; thus $\left(\dfrac{\partial \Delta G}{\partial \ln w}\right)_T$ is positive and when $\left(\dfrac{\partial \Delta G}{\partial T}\right)_{w.V^*} = 0$, $\Delta S = -\alpha^*\left(\dfrac{\partial \Delta G}{\partial \ln w}\right)_T < 0$.

Therefore the differential entropy change on adsorption must be negative if the characteristic curve is to be temperature independent. This is regarded as a necessary but not sufficient criterion for the applicability of the Dubinin theory to micro-porous solids. It merely defines a thermodynamic criterion for the upper limit of ΔG above which the existence of a temperature invariant region of the characteristic curve is impossible in principle. Bering and Serpinskii (157) have used this criterion to determine the region of applicability of the Dubinin Equation to experimental data; their method will be considered in Chapter 5.

In addition to Polanyi's postulate that the characteristic curve is independent of temperature, Dubinin and co-workers

introduce a further postulate based on experimental evidence

$$\left(\frac{\Delta G}{\Delta G_o}\right)_{w.V*} = \beta \qquad \text{Equation 3.11.}$$

i.e. for the same filling of the adsorption space the ratio
of the free energy change on adsorption of a given vapour
(ΔG) and that of a standard vapour (ΔG_o) is given by β the
relative free energy change or the affinity coefficient.
Hence Dubinin regards $\Delta G = \beta.f(V)$ as the equation of the
characteristic curve of all gases on a given adsorbent where
β is determined relative to a standard adsorbate. It was
found experimentally that the relative free energy change β,
can be approximately represented by the ratio of the molar
volumes (158) or, more accurately, by the parachors of the
bulk liquid phases of the adsorbates (159). On the basis of
extensive experimental data (153) Dubinin proposed that the
equation:-

$$V = V_o.e^{-k(-\Delta G)^2/\beta^2} \qquad \text{Equation 3.12.}$$

represents the characteristic curve for adsorption in many
microporous carbon adsorbents. A theoretical justification
for this equation was subsequently proposed by Radushkevich
(154). The total volume of adsorption space V_o, can be
equated to the micropore volume and k reflects the size
distribution of pore volumes. This equation only applies when

the pores are of molecular dimensions and the overlap of adsorption forces of opposite walls of the pores is substantial. For adsorbents with very large pores where no overlap of adsorption forces occurs and for non-porous adsorbents the equation of the characteristic curve becomes:-

$$V = V_o'.e^{-k'(-\Delta G)/\beta} \qquad \text{Equation 3.13.}$$

In this case the total volume of adsorption space V_o' has no particular significance and k' depends on the energetic non-uniformity of the surface.

In linear form Equation 3.12. becomes:-

$$\log_{10}V = \log_{10}V_o - 0.434 \ k \ (-\Delta G)^2/\beta^2$$

$$\text{Equation 3.14.}$$

If then $-\Delta G = 2.303 \ RT \ \log_{10}(p_o/p)$ and $w_o = \rho^*.V_o$;

$$\log_{10}w = \log_{10}V_o.\rho^* -D \log_{10}^2 (p_o/p)$$

$$\text{Equation 3.15.}$$

where $D = 2.303 \ k \ (RT)^2/\beta^2$ Equation 3.16.

gives an indication of the micropore size distribution. Thus by plotting experimental isotherms for microporous materials in the form $\log_{10}w$ against $\log_{10}^2(p_o/p)$ values of D and $V_o.\rho^*$ the limiting adsorption are obtained from the slope and intercept. If ρ^* the density of the adsorbate is known the micropore volume V_o can be determined. Nikolaev and Dubinin

(160) have applied this equation to the adsorption of nitrogen, krypton, xenon, tetrafluoroethylene and hexafluoropropylene on a microporous carbon at temperatures from -195° to $50^{\circ}C$ in the range of (V/V_o) from 0.06 to 0.94; straight lines were obtained whose intercepts on the ordinate axis gave constant values for the micro-pore volume, V_o, over the temperature range studied.

When the temperature at which adsorption is measured is very much less than the critical temperature of the adsorbate, its density may be approximated to that of the bulk liquid (133, 161). Two methods have been used to calculate the density (or molar volume) of the adsorbate in the temperature range from the boiling point to the critical point. Nikolaev and Dubinin (160) used a method which interpolated the adsorbate density from the density of the bulk liquid at its boiling point and its density at the critical point. Bering et al. (162) based their method on a consideration of the linearity of adsorption isosteres.

Radushkevich (154) made an attempt to substantiate theoretically the equation for adsorption in microporous substances (Equation 3.20). He concluded that the equation was the result of a Maxwellian distribution of adsorption potentials within the micropores. It is clear that while the Dubinin equation gives a useful semi-empirical account of

adsorption in micropores with some general thermodynamic validity, the theoretical aspects of the Dubinin Theory need more attention before it will meet with a wider acceptance.

3.3.   The Effect of Surface Oxide on Adsorption

Adsorption of gases and vapours on the surface of carbons may be influenced by the presence of chemisorbed oxygen on the surface (See Section 2.6.). If the surface has a polar nature polar adsorbate molecules will clearly be influenced by the polarity of the surface whereas non-polar molecules will be less affected (43, 163). The adsorption of polar gases on carbon is usually altered by the presence of surface oxygen complexes. It has been observed that the adsorption of water (164 - 165), methyl alcohol (167, 168), ammonia. (164, 169), methylamine (164, 170), sulphur dioxide (169, 171), carbon dioxide (166, 172) and hydrogen chloride (102, 173) is greatly increased; the enhanced adsorption of water and ammonia has been ascribed to the formation of hydrogen bonds with surface oxides (166, 170). The presence of surface complexes has in some cases caused misinterpretation of the adsorption of non-polar gases; e.g. carbon tetrachloride, chlorobenzene and hydrogen chloride have displaced the surface oxide on charcoals (165, 174, 175).

In order to correlate the adsorptive characteristics of carbons with the chemical composition of the surface, adsorp-

tion studies have been made with carbon blacks and porous carbons modified by heat treatment in the absence of air (164, 165, 175), by oxidation with oxygen (170, 171, 176, 179), reduction with hydrogen (180) and reaction with steam (164, 177).

Puri (176) measured the heat of immersion in water of activated charcoals which had been heat treated at various temperatures in the range $450^{\circ} - 1200^{\circ}C$. The measured surface area of the charcoals varied very little with temperature. The heat of immersion went down with heat treatment up to $750^{\circ}C$ and then remained steady. This temperature Puri correlated with the almost complete elimination of oxygen from the charcoal as carbon dioxide. He observed a linear relationship between the heat of immersion per unit surface area and the weight of oxygen removed from the charcoal as carbon dioxide. Anderson and Emmett (164) determined the adsorption of nitrogen, water and ammonia on a variety of carbon blacks before and after heat treatment at $1000^{\circ} - 1200^{\circ}C$. Although the surface areas determined from the nitrogen isotherms did not vary significantly, the adsorption of water and ammonia was reduced by heat treatment. A similar explanation has been proposed to account for the reduced adsorptive capacity of Spheron 1000 for ammonia (170) and sulphur dioxide (171).

As discussed in Chapter 2 the exposure of the surface of

carbons to gaseous reactants results in oxidation, the
amount of chemisorbed oxygen on the surface increases and
the adsorption of polar adsorbates is enhanced. A number
of workers (171, 178, 179) have observed increased adsorp-
tion of water and ammonia at lower relative pressures after
charcoals have been oxidised at $400^{\circ}C$ in air. It has been
claimed (179, 181) that the surface area of porous carbons
is not markedly increased by oxidation at this temperature
and the increased adsorption is ascribed to the presence of
chemisorbed oxygen on the porous carbon surface.

The influence of surface oxides on the adsorption of
carbon dioxide on carbons has been studied by a number of
workers (5, 167, 172, 182). This is of particular interest
in the present work since this adsorbate has been used to
obtain adsorption isotherms. Anderson et al. (167) measured
carbon dioxide isotherms at $195^{\circ}K$ and nitrogen isotherms at
$77^{\circ}K$ on a variety of carbon blacks and a charcoal. On the
carbon blacks they found that the amount of carbon dioxide
adsorbed relative to the amount of nitrogen adsorbed increased
with the increasing oxygen content per unit surface area of
the black, the surface areas being determined from the adsorp-
tion of the nitrogen. They suggested that the enhanced
adsorption was due to interaction between the carbon dioxide
and the surface oxygen. On the charcoal they found that

surfaces areas obtained by both methods were in agreement
if the saturated vapour pressure of carbon dioxide at 195°K
was calculated by extrapolating the liquid vapour pressure
curve and if the cross sectional area of the adsorbed carbon
dioxide molecule was based on the extrapolated liquid density.

Deitz et al. (182) studied the adsorption of carbon
dioxide and nitrogen on a number of carbon adsorbents and
found that both the amount of carbon dioxide adsorbed per
unit surface area (determined from the nitrogen isotherms) and
the heat of adsorption of carbon dioxide increased with the
fraction of the carbon surface covered by hydroxyl groups.
They suggested that there were three principal interactions:
(i) purely physical adsorption (ii) an adsorption complex
having a 'bicarbonate structure' and (iii) an adsorption
complex having a 'carbonate structure'.

Anderson et al. (167) have considered the possibility of
activated diffusion of nitrogen at 77°K into micropores
leading to differences in the surface areas obtained. Deitz
et al. (182) do not appear to have considered this point.
However, as the effect is well known for the adsorption of
nitrogen in micro-porous materials at liquid nitrogen
temperatures (129) it might account for the different surface
areas obtained from the adsorption of carbon dioxide and
nitrogen.

Lamond and Marsh (129) have studied the adsorption of carbon dioxide on many porous carbons with a view to surface area and pore volume determinations. They observed that the effect of removing all surface oxide by outgassing carbon blacks at $1000^{o}C$ prior to adsorption had little effect on surface areas determined by the adsorption of carbon dioxide. They found that preliminary outgassing at $340^{o}C$ when no surface oxide was removed was adequate (See Chapter 2). Their conclusion was that carbon dioxide could be used as an adsorbate as the effect of chemisorbed oxygen enhancing adsorption was very slight. The choice of carbon dioxide as the adsorbate in the present work largely follows from the recommendations of Lamond and Marsh.

3.4.   The Development of Porosity by Activation

The process of activation increases the adsorptive capacity of a carbon by removing small amounts of material and developing the porous structure. Much effort has been directed (4, 5,114, 120, 130, 131, 142, 143, 163) to find whether activation widens existing pores, creates new open pores or proceeds by a combination of both mechanisms.

Arnell and Barss (142) compared the surface areas calculated from X-ray diffraction data with those obtained by nitrogen adsorption for a series of activated coconut-shell carbons. They suggested that the activation process involved

the removal of disordered carbon from between the crystal-lites. Also from X-ray diffraction data and adsorption measurements Dubinin et al. (143) concluded that both the micropore and transitional pore volumes of a sucrose carbon increased on activation in carbon dioxide. They considered that this occured in two stages, (i) the removal of the more reactive disordered material and (ii) the combustion of the crystallites with the formation of micro-pores.

Holmes and Emmett (5) studied the influence of activation by steam, hydrogen and oxygen on the pore size distribution of various charcoals by looking at the changes of shape of nitrogen isotherms. They concluded that activation by steam increased the pore diameters over a wide size range whereas activation by oxygen merely developed the micropores. Culver and Heath (130) investigated the porosity of a series of activated carbons prepared from Saran (a copolymer of vinylidene chloride with a small amount of vinyl chloride) and found that the total pore volume increased with activation reaching a maximum at ca. 85% burn-off. On the assumption that the carbon contained a system of non-intersecting, cylindrical capillaries they concluded that about 50% of the weight loss involved the creation of new pores.

Bond and Spencer (120) investigated the development of pore structure of a carbonised coal by activation with steam

using apparent density and heats of wetting techniques. Both
methods showed that micro-pore volume and surface area increased
with activation and that the micropore size distribution became
wider. When studying a number of highly active carbons Lamond
and Marsh (131) found that with progressive activation the
shapes of adsorption isotherms changed from Type 1 in the BET
classification (125) with well defined 'knees' to almost linear
isotherms. From this and from the slopes of Dubinin plots
derived from these isotherms they deduced that the micropore
structure was being developed by the widening of existing pores.
Kipling and McEnaney (114) studied the pore volumes of three
series of activated carbons using apparent density and vapour
adsorption techniques. By analysis of the rates of attack on
external and internal surfaces and the shapes of adsorption
isotherms they found that the pore structure developed varied
according to the nature of the starting material. They concluded
that in the cases of cellulose and coco-nut shell carbons the
initial effect of activation was to remove blockages at the
entrance of pores of about 8Å in diameter. Subsequently,
widening of existing pores was the major process in activation.

CHAPTER 4

Results and Discussion of Reactivity Studies

4.1.   Carbonisation and Activation

4.1.1.   Introduction

Reproducible cellulose carbons were prepared by heating

cellulose pellets to $940^\circ C$ in a controlled atmosphere of

nitrogen at a reproducible linear rate of heating (4, 6).

Experimental details of the preparation of the cellulose

carbon and the apparatus used in this investigation are given

in Appendix I.

Activation was carried out between 401° and $726^\circ C$ with

varying conditions of partial pressure of oxygen, sample

weight and crucible geometry. The rates of reaction were

followed gravimetrically using a modification (6, 183) of the

Stanton Thermobalance, Model TR-01. Details of the procedure

adopted for activation are given in Appendix II.

4.1.2.   The Influence of Temperature on the Reaction Rate

To study the influence of temperature on the rate of reaction

a series of experiments were performed between 401° and $726^\circ C$.

Since diffusion was known to play an important part in the

reaction at these temperatures, the same starting weight of

carbon (0.4 g.), the same partial pressure of oxygen (0.1) and

the same crucible size (tall) were used at each temperature in

order to standardise the conditions as far as possible; the

weight loss curves found are shown in Fig. 4.1.

The weight loss curves were examined and it was found that from ca. 10% to ca. 50% of the reaction (10 - 50% burn-off) the variation of the weight loss (w) with time (t) at a given temperature was quite closely represented by w = a + kt, where 'a' and 'k' are constants. The constant 'k' was taken as the rate constant for the reaction and 'a' as a constant due to the build-up of surface oxide. Their values are listed in Table 4.1; 'k' is expressed in units of $g.sec^{-1}$. per gram of unactivated carbon i.e. $g.sec^{-1}.g^{-1}$. and 'a' in g. surface oxide per g. of unactivated carbon i.e. $g.g^{-1}$. The values of 'k' were measured within an experimental error of less than ca. 5% but the difficulties of extrapolation gave less accurate values for 'a' (up to $\pm$ 20%).

At temperatures greater than ca. $600^{o}C$ the rate of weight loss is constant. However at temperatures less than ca. $460^{o}C$ an initial increase in weight is observed before the rate of weight loss slowly tends to an approximately constant value. The initial increase in weight found at low temperatures was ascribed to the formation of surface oxide, an essential feature of the combustion process. Plots of rate of weight loss against time were made and at temperatures less than ca. $600^{o}C$ in general follow the form of Fig. 4.2. which is for the reaction at $456^{o}C$.

4.1.3. <u>The Influence of Partial Pressure of Oxygen on the Reaction Rate</u>

The influence of partial pressure of oxygen on the reaction was studied in order to assist in defining in which of the zones of the classification of Hedden and Wicke (40) the reaction was occuring. The reaction rate was measured at 420° and $726^{\circ}C$ using a fixed starting weight of carbon and the same crucible size. Each investigation was carried out on a single sample. The partial pressure of oxygen was set at O.1. and the linear reaction rate was measured (i.e. after ca. 10% burn-off). The partial pressure was then progressively raised to about 0.25 and the measurement repeated to give a series of reaction rates. Finally as a check the original partial pressure was reimposed to ensure the rates were consistent. The results are shown in Fig. 4.3. and Table 4.2.

4.1.4. <u>The Influence of Sample Weight on the Reaction Rate</u>

Rowan (6) has shown for the carbon-carbon dioxide reaction that variation in the starting weight can affect both the rate of reaction and the activation energy. The influence of sample weight on the reaction rate was therefore investigated in the present work at two temperatures 420° and $726^{\circ}C$ using a partial pressure of oxygen of O.1 and the same crucible size. The results are shown in Table 4.3.

4.1.5. <u>The Influence of Crucible Geometry on the Reaction Rate</u>

Since mass transport is known to be important in this

reaction especially at high temperatures, the influence of crucible geometry on the rate of reaction was investigated (See Table 4.4.). The dimensions of the three crucibles chosen are shown in Fig. 4.4.

TABLE 4.1.

The Influence of Temperature on Reaction Rate

Starting Weight = 0.4g   Tall Crucible $P_{O_2} = 0.1$

Temperature (°C)	Rate Constant k $(g.sec^{-1}. g^{-1})$ $\times 10^6$	'a' $(g.g^{-1})$ $\times 10^2$
401	2.0 (± 0.1)	-2.0 (± 0.1)
417	3.1 (± 0.1)	-1.8 (± 0.1)
420	3.5 (± 0.2)	-2.5 (± 0.1)
436	5.0 (± 0.2)	-2.8 (± 0.3)
456	8.50 (± 0.15)	-3.8 (± 0.1)
465	10.0 (± 0.1)	-5.5 (± 0.2)
485	13.0 (± 0.5)	-7.5 (± 0.5)
518	13.5 (± 0.5)	-3.6 (± 0.2)
572	15 (± 1)	-2.2 (± 0.2)
620	16.0 (± 0.5)	-1.4 (± 0.2)
726	16.4 (± 0.2)	-0.2 (± 0.1)

TABLE 4.2.

The Influence of Partial Pressure of Oxygen on Reaction Rate

Temperature = 726°C   Medium Crucible

Sample Weight (g)	P_{O_2}	Measured Rate (g.sec^{-1}.) $\times 10^6$	Rate Constant (g.sec^{-1}.g^{-1}.) $\times 10^6$
0.4	0.1	8.9 ($\pm$ 0.2)	22.0 ($\pm$ 0.4)
	0.15	13.8 ($\pm$ 0.1)	34.0 ($\pm$ 0.3)
	0.2	17.5 ($\pm$ 0.2)	43.0 ($\pm$ 0.4)
	0.25	22.2 ($\pm$ 0.2)	54.7 ($\pm$ 1.0)
	0.1	8,8 ($\pm$ 0.2)	21.8 ($\pm$ 0.4)
0.6	0.1	9.3 ($\pm$ 0.2)	16.3 ($\pm$ 0.4)
	0.15	13.5 ($\pm$ 0.2)	22.7 ($\pm$ 0.4)
	0.2	17.6 ($\pm$ 0.2)	29.6 ($\pm$ 0.4)
	0.25	22.0 ($\pm$ 0.2)	37.0 ($\pm$ 0.4)
	0.1	9.4 ($\pm$ 0.2)	16.5 ($\pm$ 0.4)

Temperature = 420°C   Tall Crucible

Sample Weight (g)	P_{O_2}	Measured Rate (g.sec^{-1}.) $\times 10^6$	Rate Constant (g.sec^{-1}.g^{-1}.) $\times 10^6$
0.4	0.1	1.6 ($\pm$ 0.1)	3.6 ($\pm$ 0.2)
	0.15	2.05 ($\pm$ 0.1)	5.1 ($\pm$ 0.2)
	0.2	2.5 ($\pm$ 0.1)	6.2 ($\pm$ 0.2)
	0.1	1.7 ($\pm$ 0.2)	3.8 ($\pm$ 0.4)

TABLE 4.3.

The Influence of Sample Weight on Reaction Rate

Temperature = $726^{\circ}C$ Medium Crucible P_{O_2} = 0.1

Sample Weight (g)	Measured Rate $(g.sec^{-1}.)$ x 10^6	Rate Constant $(g.sec^{-1}. g^{-1}.)$ x 10^6
0.4	8.9 ($\pm$ 0.2)	22.0 ($\pm$ 0.4)
0.6	9.3 ($\pm$ 0.2)	16.3 ($\pm$ 0.4)

Temperature = $420^{\circ}C$ Tall Crucible P_{O_2} = 0.1

Sample Weight (g)	Measured Rate $(g.sec^{-1}.)$ x 10^6	Rate Constant $(g.sec^{-1}. g^{-1}.)$ x 10^6
0.4	1.6 ($\pm$ 0.1)	3.6 ($\pm$ 0.2)
0.6	2.1 ($\pm$ 0.1)	3.7 ($\pm$ 0.2)

TABLE 4.4.

The Influence of Crucible Geometry on Reaction Rate

Temperature = 726°C P_{O_2} = 0.1   Sample Weight = 0.4g.

Crucible*	Rate Constant $(g.sec^{-1}. g^{-1}.)$ x 10^6
Tall	16.4 ($\pm$ 0.2)
Medium	22.0 ($\pm$ 0.4)
Short	27.3 ($\pm$ 0.5)

*   Dimensions of the crucibles are given in Fig. 4.4.

WEIGHT LOST (g.g⁻¹.)

Activation of Carbon at Temperatures from 401° – 726°C

P_{O_2} = 0.1.
Sample Weight = 0.4 g.
Tall Crucible.

726°C
620°C
572°C
518°C
485°C
456°C
436°C
420°C
401°C

0.15

0.10

0.05

1   2   3   TIME
                          (HOURS)
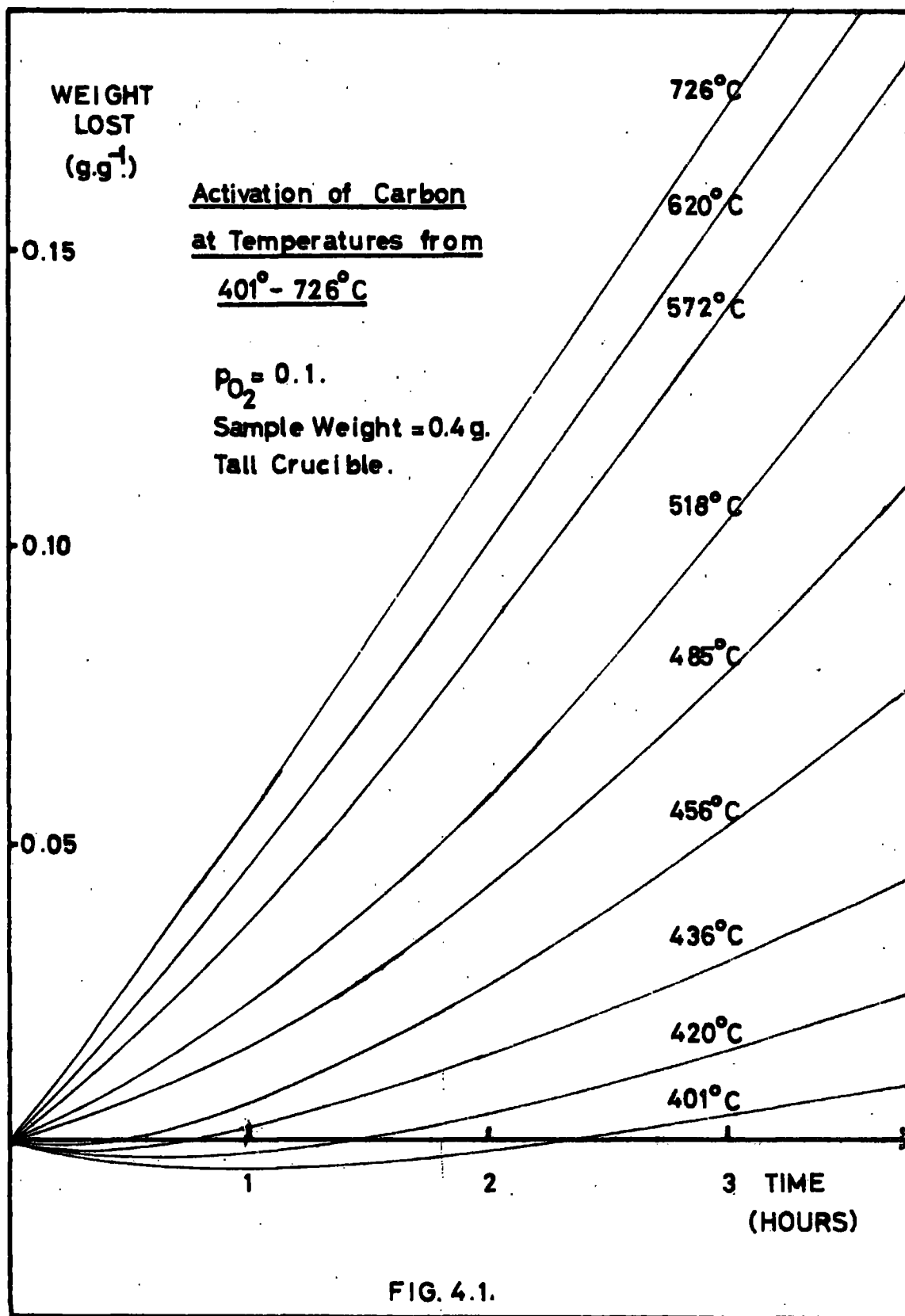
FIG. 4.1.

RATE
($g.sec^{-1}.g^{-1}.$)
($\times 10^6$)

Variation of Rate of Reaction
with Time at 456°C.

$P_{O_2}=0.1$
Sample Weight = 0.4 g.
Tall Crucible.

10%
burn-off

50%
burn-off.

TIME
(HOURS)

FIG. 4.2.

FIG. 4.3(i)

FIG. 4.3(ii)

Short

4 mm.²

<22mm. >

<22mm. >

12mm.

Medium

<22 m m>

35mm.

Tall
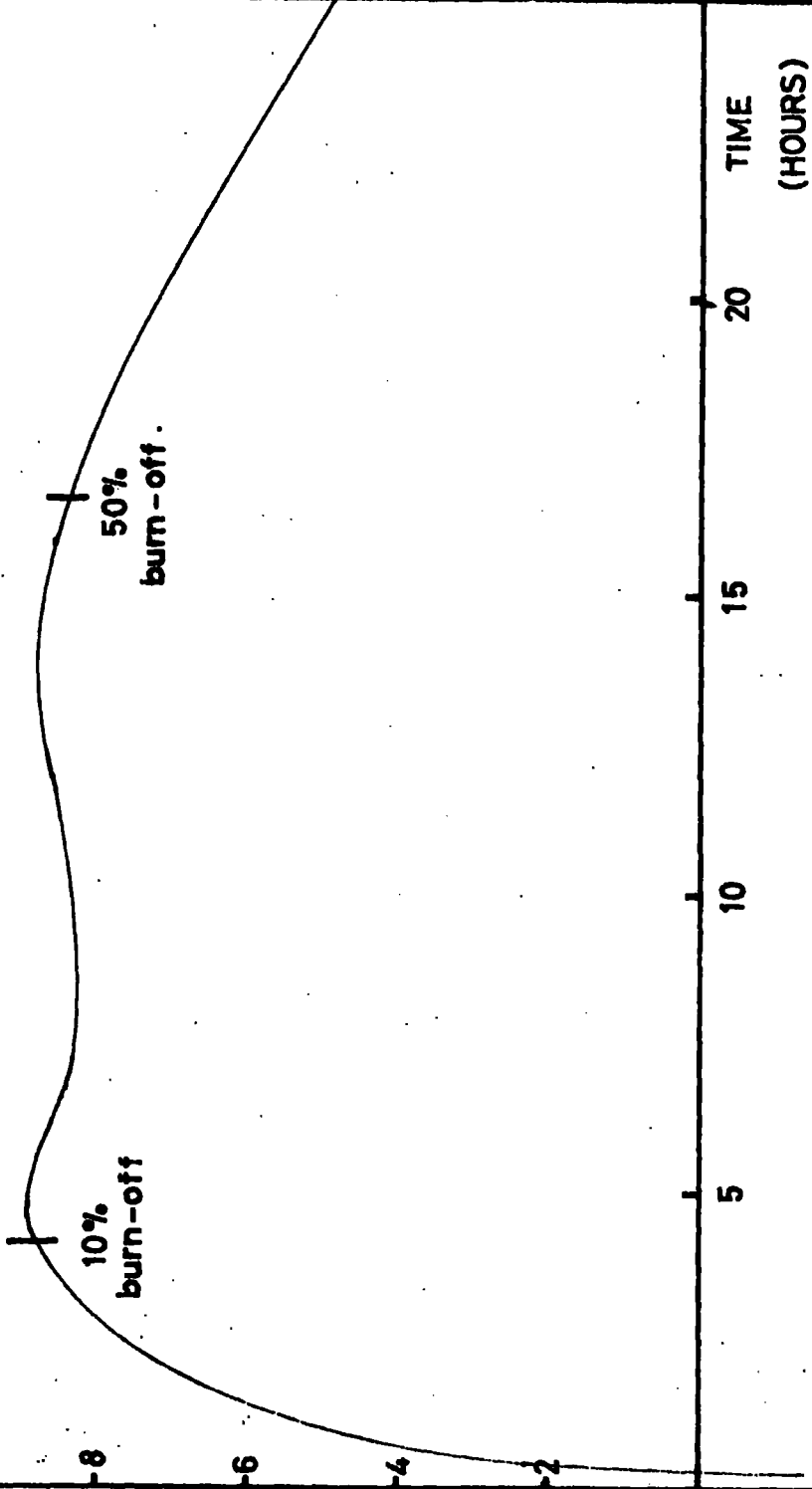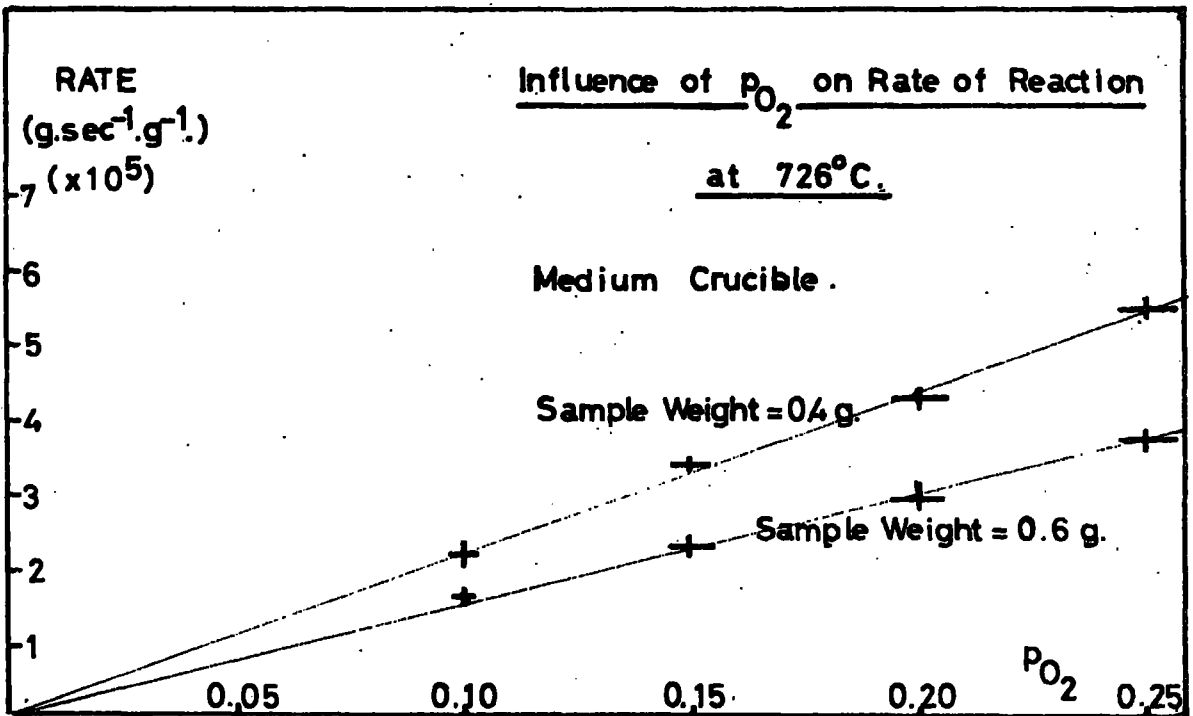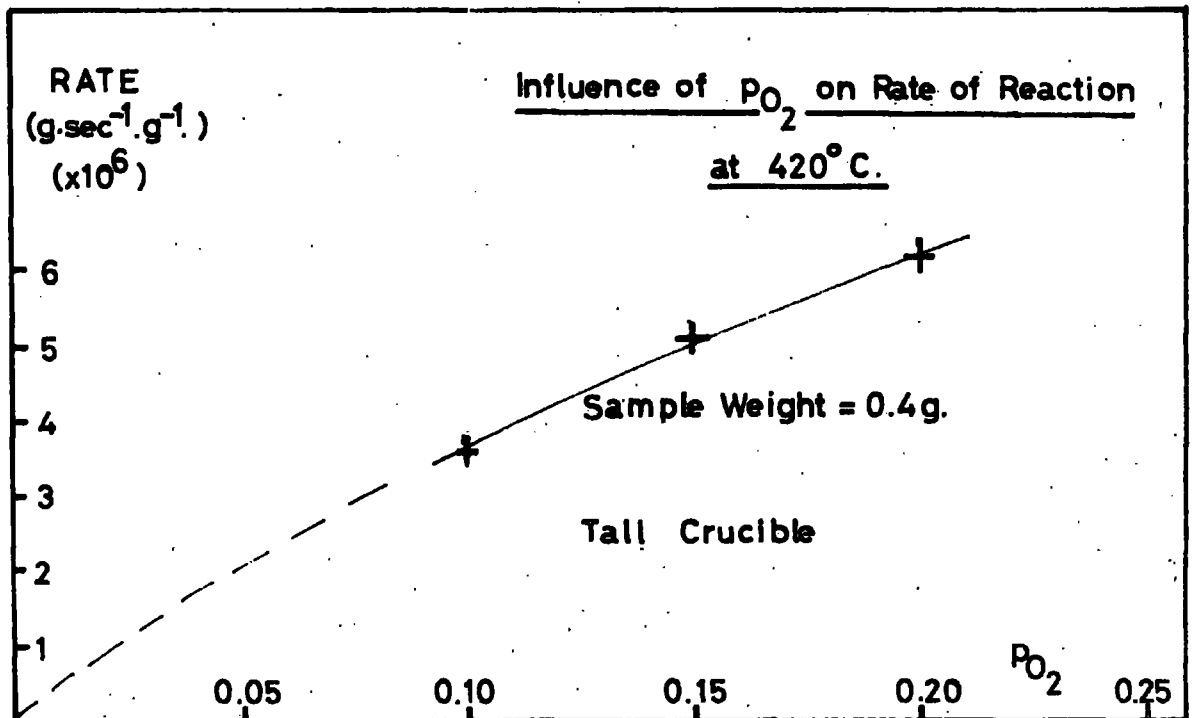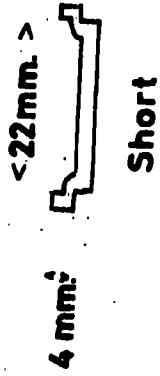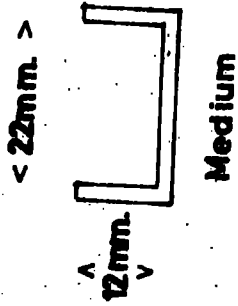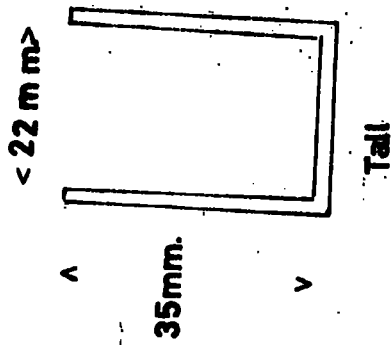
Internal Dimensions of Crucibles

FIG. 4.4.

4.2. <u>Discussion of Activation Studies</u>

4.2.1. <u>The Kinetic Parameters</u>

If the rate constants (k) for the reaction are plotted according to the Arrhenius Equation, $k = A.e^{-E_a/RT}$, the plot obtained (Fig. 4.5.) is a curve which tends to straight lines at temperatures greater than ca. 480°C and less than ca. 460°C. Although the activation parameters were only found for the reaction under one set of conditions of sample weight (0.4g.), partial pressure (0.1) and crucible size (tall) it is reasonable to assume that they will refer in general to the reaction under conditions similar to those used here but differing in detail. In the lower temperature range an experimental activation energy (E_a) of 25.2 ($\pm$ 2.5) k.cal.mole^{-1} is found. In the upper temperature range the activation energy is 2.0 ($\pm$ 0.5) k.cal.mole^{-1}.

The value of the activation energy found in the temperature range 400° - 460°C can be compared with values found by other workers using similar experimental conditions and listed in the Table 4.5.

The value of the activation energy obtained in the present investigation is seen to be similar to the values found by Wicke (60), Snow et al. (82) and Barradas et al. (83). However it is clearly different to that found by Gregg and Tyson (88) and Gulbransen and Andrew (77). This may be due to the fact

that the latter workers used a pressure of 7.6cm.Hg. of pure oxygen and did not dilute the gas with nitrogen, thus reducing the influence of diffusion.

TABLE 4.5.

Activation Energies for the Carbon - Oxygen Reaction

Workers (Ref)	Carbon	Pressure of Oxygen	Temperature Range ^{o}C	E_a k.cal.mole^{-1}.
Snow et al. (82)	Carbon Blacks		240 - 350	25 - 30
Gulbransen and Andrew (77)	Spectrographic purity Graphite	7.6 cm.Hg.	425 - 575	36.7
Gregg and Tyson (88)	1000° Petroleum Pitch Carbon	7.6 cm.Hg.	580 - 600	43.7 ($\pm$ 3.9)
Barradas et al. (83)	Saran Carbons	Partial Pressure of 0.05 - 0.20 in Nitrogen at 1 atm.	500 - 720	20 - 25
Wicke (60)	Electrode Carbon	Air at 1 atm.	600 - 700	29 ($\pm$ 1) with diffusion 58 ($\pm$ 4) in absence diffusion
Rossberg (62)	Electrode Carbon	Air at 1 atm.	600 - 700	50 ($\pm$ 4) in absence diffusion
Present Investigation	1000° Cellulose Carbon	Partial Pressure of 0.1 in Nitrogen at 1 atm.	400 - 460	25.2 ($\pm$ 2.5)

The pre-exponential factor 'A' was determined by extrapolation of the linear part of the Arrhenius plot in the temperature range 400° - 460°C and found to be ca. 3.5×10^{2} g.sec^{-1}.g^{-1}. This is much lower than the value of ca. 2×10^{8} g.sec^{-1}.g^{-1} found by Gregg and Tyson (88). It is however of the same order as the value of ca. 2.1×10^{2} g.sec^{-1}.g^{-1} calculated from the results of Wicke (60) for the reaction of an electrode carbon with air in the temperature range 600° - 700°C. This factor will be further discussed in Section 4.2.3. when a comparison with the carbon-carbon dioxide reaction will be made.

The value of the activation energy found for the temperature range 400° - 460°C, 25.2 ($\pm$ 2.5) k.cal.mole^{-1}, is approximately half the 'true' activation energy obtained by Rossberg (62) and Wicke (60) for the carbon-oxygen reaction under similar conditions of temperature and pressure (See Section 2.3.3.2.). From this fact it is reasonable to conclude that in the temperature range 400° - 460°C the reaction occurs in Zone II of the Hedden and Wicke (40) classification. This indicates that the rate of reaction is controlled by diffusion of the reactants and products through the pores of the carbon.

The activation energy of 2.5 ($\pm$ 0.5) k.cal.mole^{-1} found in the temperature range 485° - 726°C compares with the low value predicted by Walker et al. (41), for reactions in Zone III

due to the temperature dependence of the diffusion coefficients of gaseous reactants and products and with the value of 8 k.cal.mole^{-1}. found by Day (54, 55) under conditions of high temperature and flow rates. It may be concluded therefore that in the temperature range 480° - 726°C the reaction occurs in Zone III.

The influence of partial pressure of oxygen, sample weight and crucible geometry on the rate of reaction in general confirm these conclusions. The rate of reaction at 726°C can be seen from Table 4.2. and Fig. 4.3.(i) to be directly proportional to the partial pressure of oxygen i.e. the reaction is first order with respect to the partial pressure of oxygen. This agrees with the order of reaction postulated by Walker et al. (41) for reaction in Zone III, see Section 2.4, and that found by Day (54,55) for the reaction of a number of carbons with oxygen in the temperature range 1200° to 2000°C at high flow rates. At 420°C the rate of reaction can be seen from Table 4.2. and Fig. 4.3. (ii) to be dependent on the partial pressure of oxygen. However the experimental data do not permit a definite order to be deduced at this temperature; although probably fractional, it clearly approaches one.

Rowan (6) has shown that the rate of the carbon-carbon dioxide reaction (measured in g.sec^{-1}.g^{-1}.) under Zone II conditions decreases with increasing starting weight of carbon

up to ca. 0.3g. and then becomes almost independent of starting weight above ca. 0.3g. From Table 4.3. it can be seen that in the present investigation for samples of 0.4g. and 0.6g. at 420°C the reaction rate (g.sec^{-1}.g^{-1}.) is independent of starting weight. This result is thus in broad agreement with Rowan's findings for the carbon-carbon dioxide reaction when starting weights greater than ca. 0.3 g. were used. This suggests that under conditions of the present work, in Zone II, the influence of variation in starting weight on the activation energy and pre-exponential factor may be neglected.

However for the reaction at 726°C it can be seen (Table 4.3.) that it is the measured rate of reaction (g.sec^{-1}.) that is almost independent of the starting weight and therefore the rate constant (g.sec^{-1}.g^{-1}.) decreases with increasing starting weight. This however is consistent with reaction in Zone III since it has been shown (41) (See Section 2.4.), that under these conditions the reaction rate is determined by the thickness δ of the external layer of product gases through which the reactant must diffuse. Thus the measured rate (g.sec^{-1}.) will be independent of the starting weight if variation in the latter does not influence δ. This may be the case under the conditions of the present work where the size of this layer is likely to be determined predominantly by crucible geometry rather than the size of the carbon sample. This view is supported by the effect of variation of crucible geometry on

the rate of reaction at 726°C (Table 4.4). It will be seen

that the reaction rate increases as the crucible height

decreases. This can be ascribed to a decrease in δ with

decreasing crucible height.

Thus the evidence of variation of rate of reaction with

partial pressure of oxygen; sample weight and crucible geo-

metry add contributory evidence to the conclusion that over

the temperature ranges 400° - 460°C and 485° - 726°C the

carbon-oxygen reaction occurs in Zones II and III respectively

of the Hedden and Wicke classification (40).

4.2.2. The Formation of Surface Oxide

The initial weight increase observed in the reaction

below 456°C was ascribed to the formation of surface oxide

(See Section 2.6.). This phenomenon has been recorded by other

workers being first noticed by Langmuir (46).

The weight loss curves observed (Fig. 4.1.) are presumably

the net result of both weight loss due to loss of gaseous

products and weight gain due to surface oxide formation. If

therefore the rate of reaction obtained in the linear section

of each curve is assumed to represent the rate of weight loss

of gaseous products only and, if it is further assumed that

this reaction commences from the introduction of reacting

gas, then the difference between the measured rate and the

calculated rate due to loss of gaseous reaction products

represents the formation of surface oxide. The curves so obtained for the formation of surface oxide are given in Fig. 4.6., Fig. 4.7. is a plot of the amount of surface oxide formed at equilibrium as a function of reaction temperature and shows that the carbon forms most surface oxide between temperatures of 450° and $500^{\circ}C$. This agrees with the findings of Snow et al. (82) and Weller and Young (102) who found the oxygen content of their carbons was greatest after activation had been carried out at 400° - $500^{\circ}C$ (See Section 2.6.). The total surface oxide formed at $485^{\circ}C$ is equivalent to 7.5% of oxygen present in the carbon. It should be emphasised that this almost certainly does not represent all the surface oxide present in the carbon. This is because the preliminary heating at $1000^{\circ}C$ in nitrogen for 30 minutes prior to activation does not remove all the original surface oxide present (77). Indeed the thermogravimetric traces show that weight is still being lost at $1000^{\circ}C$ after 30 minutes heating in nitrogen.

The curves for surface oxide formation (Fig. 4.6) were analysed in an attempt to determine kinetic parameters since this might prove useful in elucidating the general reaction mechanism and may also help in determining the role of surface oxide, if any, in determining the development of porosity in activated carbons. It was found that for the majority of these curves plots of log (surface oxide formed) against time

were linear over a considerable range. However, first order

rate constants obtained from the slopes of these curves did

not increase regularly with temperature. This can be seen

from Table 4.6. where half-life times, $t_{\frac{1}{2}}$, found by inspection

of the curves in Fig. 4.6. are tabulated.

TABLE 4.6.

Half Life times for formation of surface oxide

T (°C)	401	420	436	456	485	518	572	620
$t_{\frac{1}{2}}$ (mins)	52	54	50	43	78	45	40	33

A number of possible reasons can be put forward for this

behaviour:- (i) The curves of Fig. 4.6. are found by an indirect

method which gives considerable leeway for error in their shape;

the values for the surface oxide formed may be subject to errors

of ± 10 - 20%. (ii) As mentioned above, pre-heating to 1000°C

in a flow of nitrogen does not completely remove the surface

oxide present and therefore may not have removed exactly the

same amount of surface oxide in each case. (iii) The influence

of diffusion control on the formation of surface oxide has not

been considered. Nevertheless Fig. 4.7. remains an indication

of the variation of surface oxide formed with temperature which

can be used to assess possible effects on the development of

porosity in the activated carbons.

4.2.3. <u>Comparison of Rates of Carbon-Oxygen and Carbon-Carbon Dioxide</u>

     <u>Reactions</u>

     Few comparisons between the rates of the carbon-oxygen reaction and other gasification reactions have been made (41). However a comparison between the rates of the carbon-oxygen reaction found in the present investigation and the rates of the carbon-carbon dioxide reaction found by Rowan (6) is desirable in order to assist in the comparison of the development of porosity by the two reactions to be discussed in Chapter 5.

     Comparisons of carbon gasification reactions in general, are made difficult for two main reasons. Firstly the experimental conditions of the work being compared may not be the same in each case. In comparing the present work with that of Rowan (6) this difficulty is reduced since the same apparatus and starting material were used. Secondly, carbon gasification reactions are rarely in the same zone of rate control over the same temperature range; this is the case in the present comparison.

     If comparisons are to be made between reactions in different temperatures ranges, it is necessary to ensure the reactions are in the same zone of rate control. Formal comparisons are then possible, but are somewhat artificial since they must be referred to a single temperature. They

therefore require, in at least one case, extrapolation of experimental data out of the temperature range for which they have been obtained.

Relevant data for a comparison of the present work with that of Rowan (6) in Zone II are shown in Table 4.7. A direct comparison of rates can be made, neglecting the difference in partial pressures, using the equation:-

$$\text{Ratio} = k_{C-O_2}/k_{C-CO_2} = A_{C-O_2}/A_{C-CO_2} \quad \text{exp.} - \left[(E_{a_{C-O_2}} - E_{a_{C-CO_2}})/RT \right]$$

TABLE 4.7.

Experimental Parameters for Carbon-Oxygen and

Carbon-Carbon Dioxide Reactions

	Carbon-Carbon Dioxide	Carbon-Oxygen
Starting Weight (g.)	0.5	0.4
Partial Pressure of Reacting Gas	1	0.1
Temperature Range of Zone II (°C)	925-950	400-460
Pre-exponential factor (g.sec^{-1}g^{-1})	16	350
Activation Energy (k.cals.mole^{-1})	31 ($\pm$ 3)	25 ($\pm$ 2.5)

If 800°C is taken as reference temperature, as has been done

by a number of workers, we obtain, neglecting errors in A,

$$\text{Ratio} = 3.4 \ (\pm \ 3.1) \times 10^2.$$

If it is assumed k_{C-O_2} is directly proportional to p_{O_2} then, correcting for the differences in partial pressure

$$\text{Ratio} = 3.4 \ (\pm \ 3.1) \times 10^3.$$

This ratio can be compared with the values of $10^4 - 10^6$ found by other workers at this temperature (60, 77, 84, 184). However, most of these comparisons were made under Zone I conditions, where activation energies and pre-exponential factors are different from those found in the present work. Table 4.8. gives a comparison of the rates of the two reactions referred to $800^{\circ}C$ and 0.1. atm.

TABLE 4.8.

Comparison of the Rates of the Carbon-Oxygen and

Carbon-Carbon Dioxide reactions referred

to $800^{\circ}C$ and 0.1 atm. Pressure

Worker	Carbon	Ratio of Reaction Rates. k_{O_2}/k_{CO_2}	Ref.
Gulbransen and Andrew	Spectrographic Purity Graphite	6×10^4	77
Wicke	Electrode Carbon	6×10^5	60
Armington	Graphite Wear Dust	4×10^4	184
Armington	Graphitised Carbon Black	2×10^5	184
Maryasin and Tesner	Graphitised Carbon Black	10^5	84
Present Work	Cellulose Carbon	$3.4 \ (\pm \ 3.1) \times 10^3$	-

Rate Constants Plotted
According to Arrhenius Equation
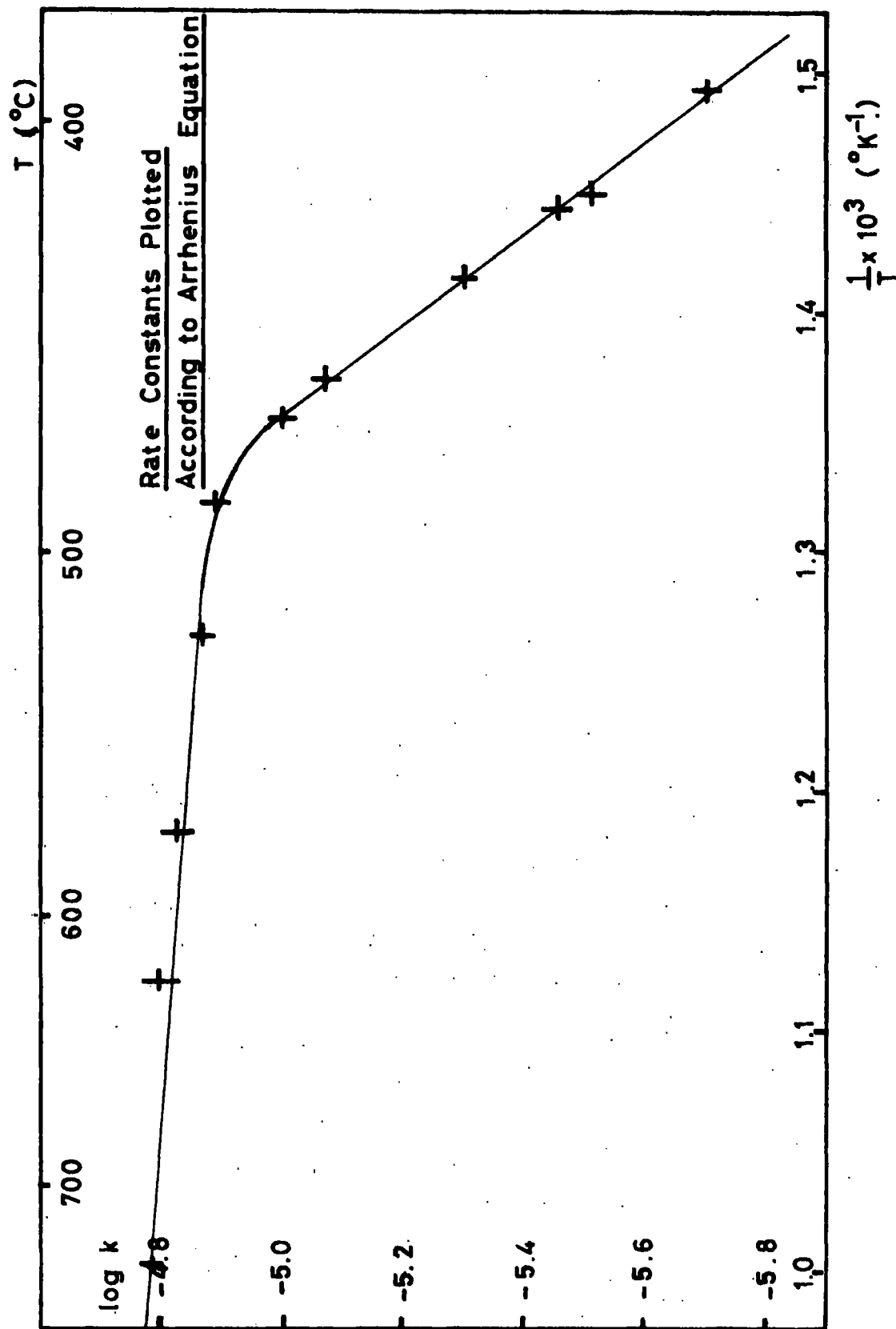
FIG.4.5.
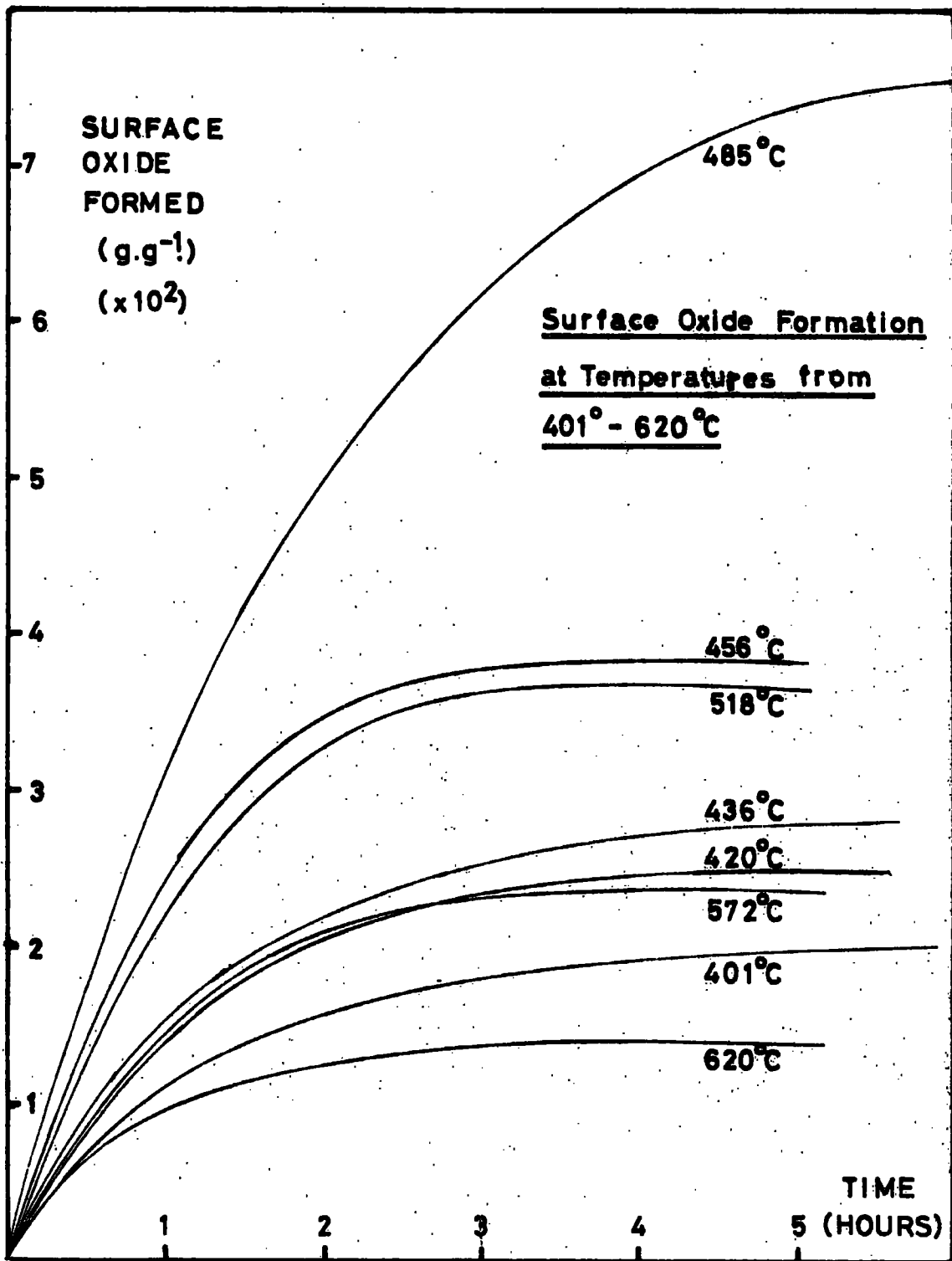
FIG. 4.6.

SURFACE
OXIDE
FORMED
$(g.g^{-1})$
$(x10^2)$

Amount Surface Oxide Formed as
a Function of Temperature.

TEMPERATURE °C
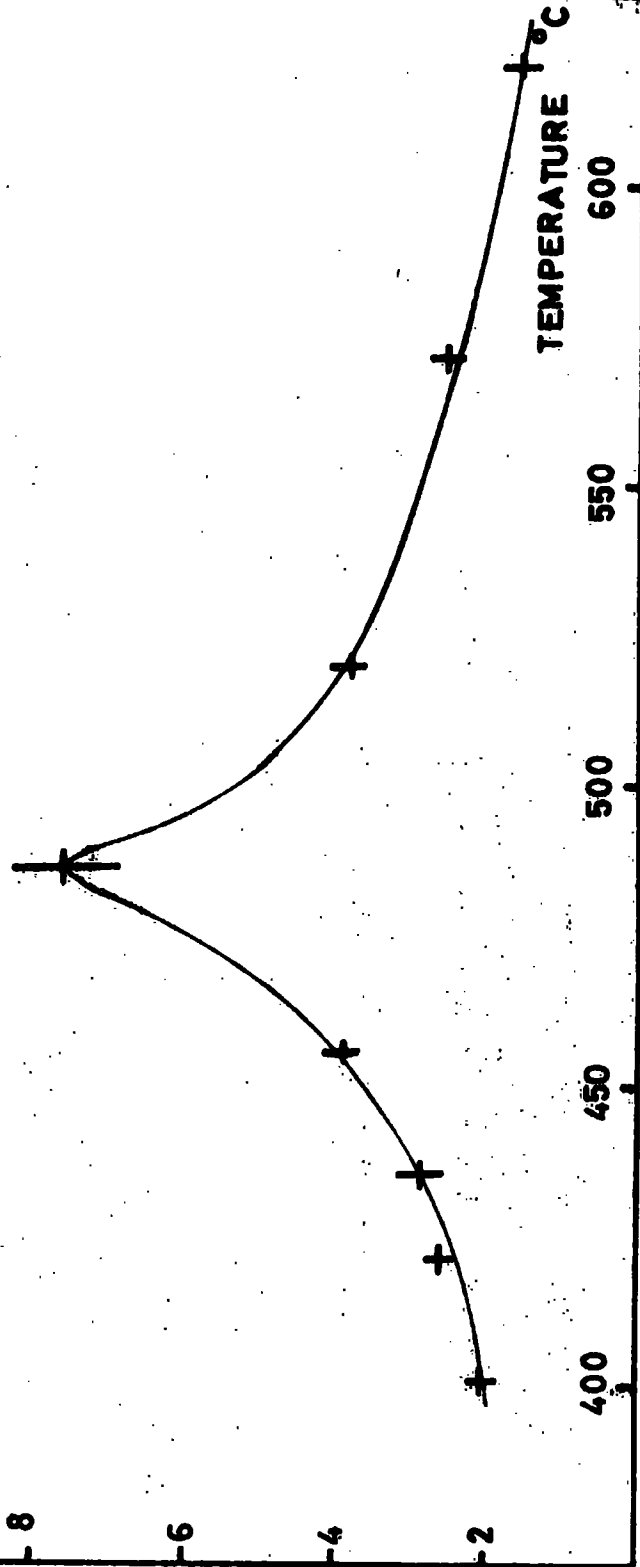
FIG.4.7.

CHAPTER 5

Results and Discussion of Adsorption Measurements

5.1.   Results of Experimental Work

Adsorption of carbon dioxide on the carbons was measured gravimetrically at $195^{\circ}K$, $273^{\circ}K$ and $298^{\circ}K$. Practical details of the apparatus used to obtain the isotherms are given in Appendix III. Appendix V contains the experimental results from which the isotherms were obtained.

The use of carbon dioxide as an adsorbate has recently been studied by a number of workers (131, 161, 167, 185, 186). Marsh and Wynne-Jones (186) have compared the adsorption of carbon dioxide at $195^{\circ}K$ and nitrogen at $77^{\circ}K$ on carbons. They concluded that the use of carbon dioxide was less likely to give erroneous results since it is sometimes found that nitrogen at $77^{\circ}K$ is unable to enter fine micropores in carbonaceous adsorbents because of a high activation energy of diffusion; this is sometimes known as the activated diffusion effect.

In using carbon dioxide at $195^{\circ}K$ as an adsorbate it is assumed that the adsorbate is in the form of a supercooled liquid; this assumption is based on the evidence of a number of workers (131, 161, 167, 185). Dubinin et al. (161) determined adsorption isotherms for carbon dioxide on silica gels in the temperature range 187° to $233^{\circ}K$. They concluded from an

analysis of these isotherms that if the adsorbate was in liquid form above the triple point, $216.6^{\circ}K$, then the adsorbate which was within the pores but not part of an initial monolayer, was in the form of a supercooled liquid down to a temperature of $187^{\circ}K$. Anderson et al. (167) concluded from comparison of surface areas of various solids determined from carbon dioxide and nitrogen isotherms that carbon dioxide was adsorbed in the form of a supercooled liquid at $195^{\circ}K$. Lamond and Marsh (131) showed that isotherms for carbon dioxide on carbons at $195^{\circ}K$ only fitted the characteristic curves determined at higher temperatures if the saturated vapour pressure of the supercooled liquid was employed to determine the relative pressure. From comparison of molecular areas obtained at 195° and $298^{\circ}K$ by the adsorption of carbon dioxide on coals Walker and Kini (185) suggested that the true state of the adsorbed carbon dioxide at $195^{\circ}K$ is intermediate between that of a perfect bulk liquid and a perfect bulk solid. However they do not make any suggestions for values of relevant properties of the adsorbate. Thus in the present work the properties of the adsorbate are obtained by extrapolations of data for liquid carbon dioxide. Such extrapolations yield values of 141.4cm.Hg. for the saturated vapour pressure (131, 187) and $1.23g.cm^{-3}$ for the density (161) of the supercooled liquid at $195^{\circ}K$.

Isotherms, measured at 195°K, for a series of carbons activated to 35 ($\pm$ 1)% burn-off at a number of temperatures between 400° and 726°C are given in Figure 5.1. Isotherms, measured at the same temperature for series of carbons activated to different extents at 456°C and 485°C are shown in Figs. 5.2. and 5.3. Isotherms measured at 273°K and 298°K for a number of carbons are given in Figs. 5.4. and 5.5. respectively.
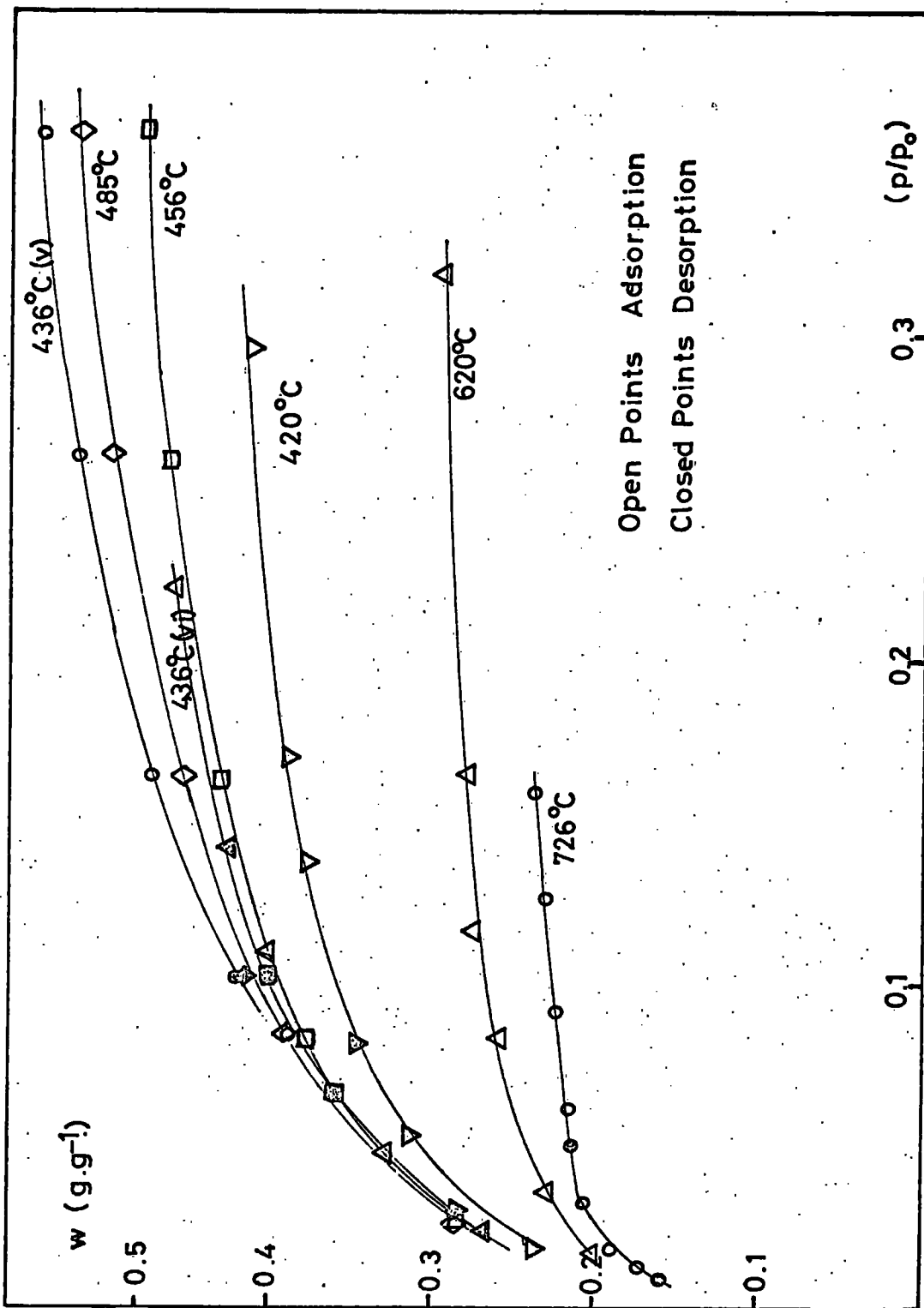
FIG.5.1.

Carbon Dioxide Isotherms at 195°K on Carbons Activated to ca.35 % Burn-off
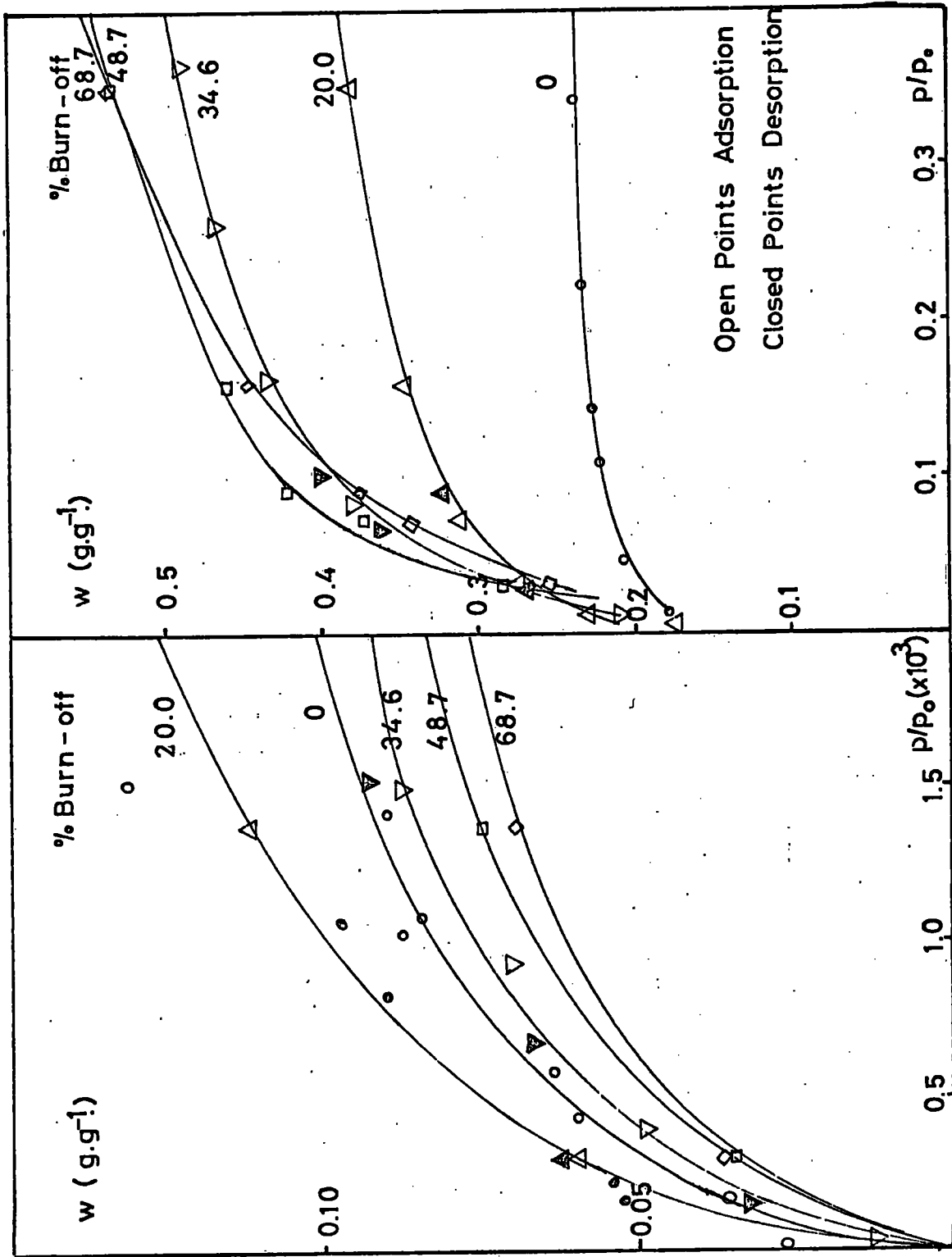
FIG.5.2.

Carbon Dioxide Isotherms at 195°K on Carbons Activated at 456°C
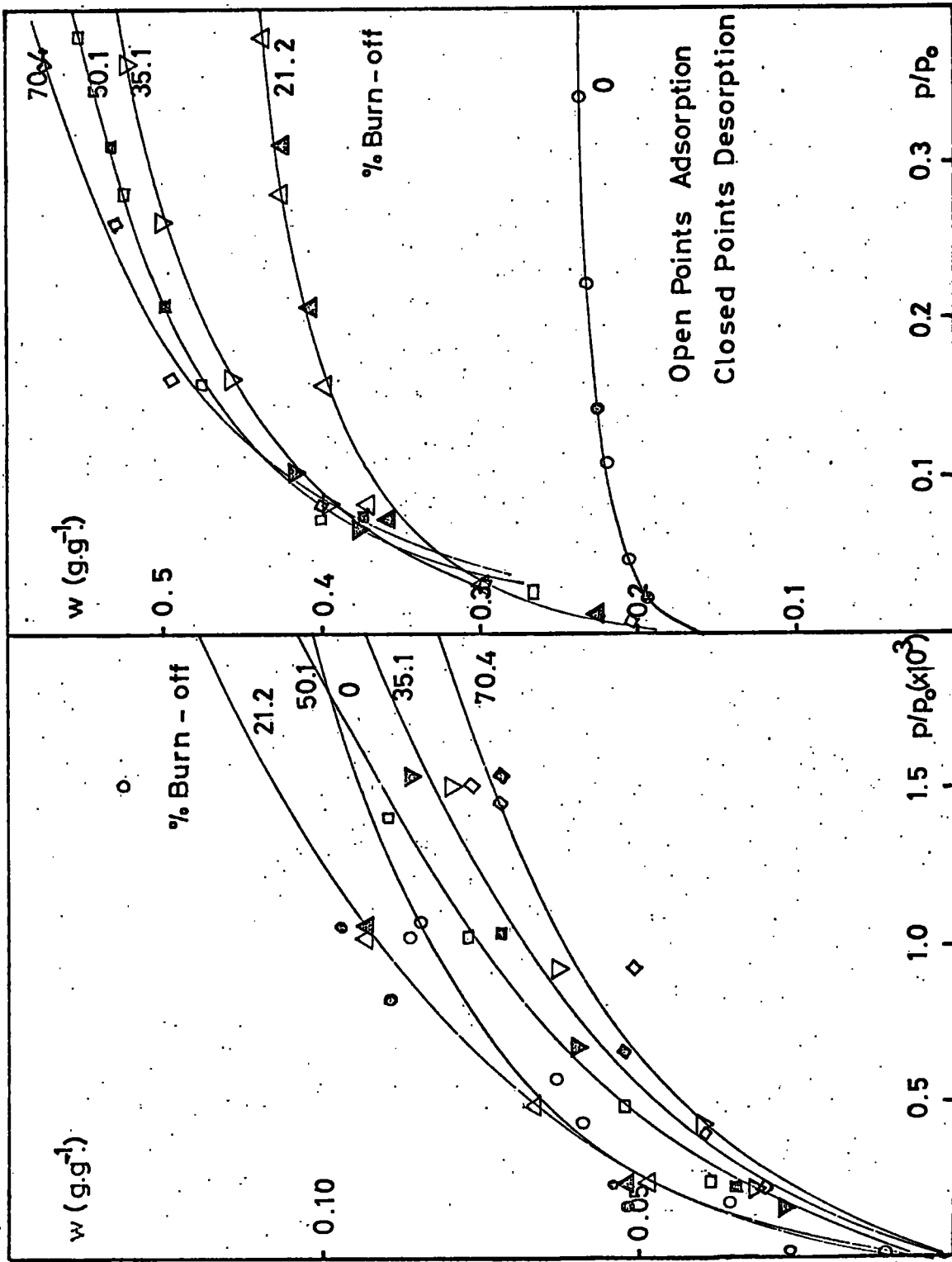
FIG. 5.3.

Carbon Dioxide Isotherms at 195°K on Carbons Activated at 485°C
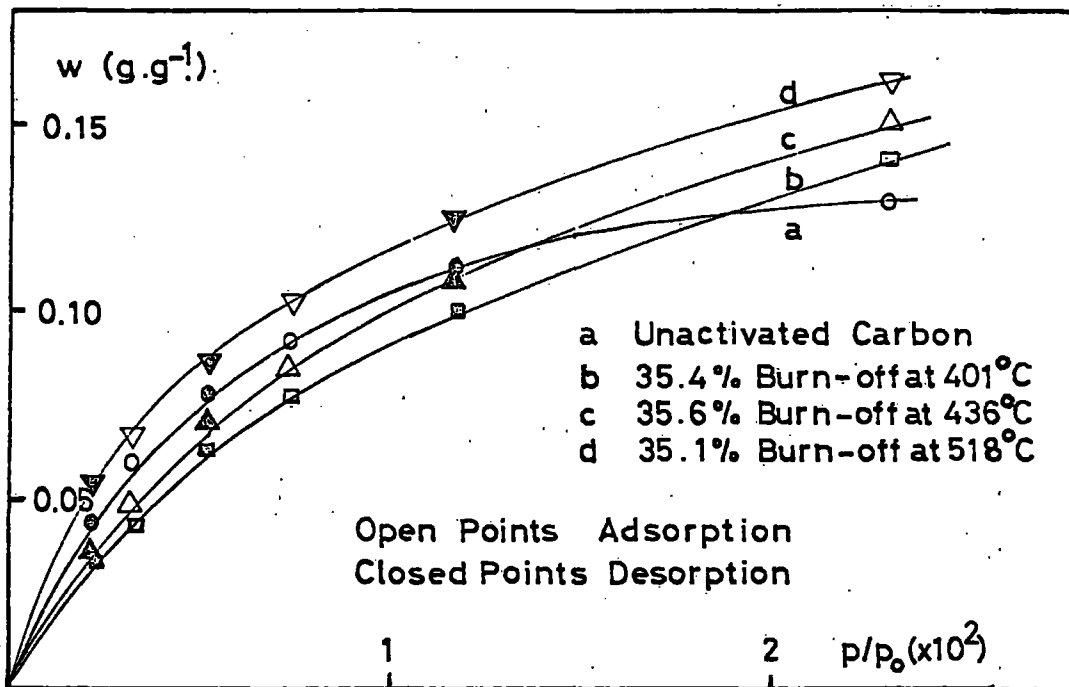
FIG. 5.4.

Carbon Dioxide Isotherms at 273°K
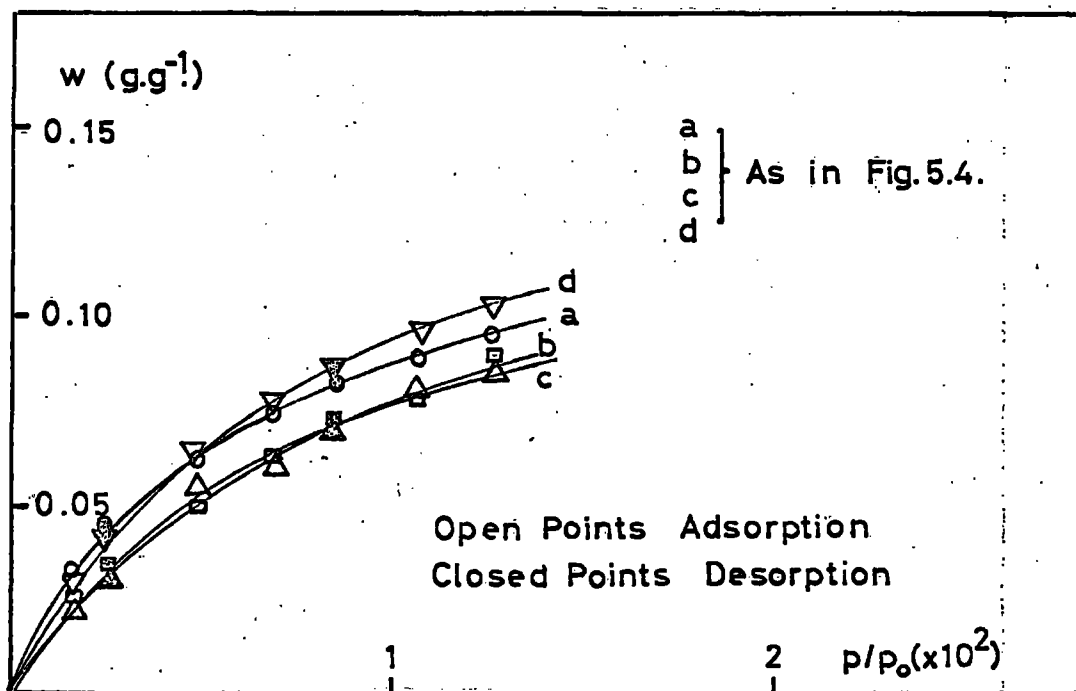
FIG. 5.5.

Carbon Dioxide Isotherms at 298°K

5.2. Discussion of Adsorption Measurements

5.2.1. Qualitative Interpretation of Adsorption Isotherms

For the purposes of applying the Dubinin Equation (Equation 3.15) it was only necessary to measure the isotherms in the present work over the relative pressure range 10^{-5} - 0.4 since when $p/p_o = 0.4$, $\log^2(p_o/p)$ is close to zero. Examination of this limited pressure range avoids the experimental difficulties of measuring isotherms at pressures greater than atmospheric and possible complications due to capillary condensation of the adsorbate in the pores of the carbons at higher relative pressures. However it is thus not possible to classify the adsorption isotherms in terms of the Brunauer classification (125) since this requires isotherms to be measured over a pressure range extending to near the saturated vapour pressure.

Before applying the Dubinin Equation to the isotherms a number of qualitative conclusions can be drawn by inspection of the isotherms. In order to investigate the influence of temperature of activation on the development of porosity a series of carbons activated at various temperatures to ca. 35% burn-off were examined. An inspection of the isotherms obtained (Fig. 5.1.) shows that the porosity development clearly depends on the temperature of activation. This is in contrast to the findings of Rowan (6) who concluded that the porosity developed by activation with carbon dioxide over the relatively narrow

temperature range 890° - $960^{\circ}C$ was independent of the temperature of activation.

The isotherms of the unactivated carbon and that of the carbon activated at $726^{\circ}C$ are almost identical, indicating that activation at this temperature does not develop the pore structure in any way. From the reactivity studies (See Section 4.2.1.) it was concluded that at $726^{\circ}C$ the reaction was in Zone III of the Hedden and Wicke classification in which the rate of reaction is controlled by the diffusion of reactant through an external layer of product gases. The adsorption measurements entirely confirm this view and show that the activation only burns away the external surface of the carbon. In the region of ca. 500° - $600^{\circ}C$ which was located at the lower end of Zone III on the basis of reactivity studies there is evidence from Fig. 5.1. that some pore structure is developed. This indicates that not all the reaction is occuring on the external surface of the carbon. This in turn suggests that the value of the activation energy may not always be a sensitive indication of temperature limits of the reaction zones.

At temperatures of activation lower than ca. $500^{\circ}C$ it was concluded from the reactivity studies that the reaction occurred in Zone II and therefore that the rate was controlled by diffusion within the pores of the carbon. This is consistent with the

adsorption studies since it is clear from Fig. 5.1. that substantial development of porosity occurs at these temperatures.

To enable the development of porosity in Zone II to be further examined and in order to compare the carbon-oxygen and carbon-carbon dioxide reactions, two temperatures 456° and $485^{\circ}C$, were chosen for the preparation of activated series of carbons. It can be seen (Figs. 5.2. and 5.3.) for both these activated series that the majority of adsorption takes place at relative pressures less than ca. 0.1 for all but the most highly activated carbons. This indicates that the major part of the adsorptive capacity of the carbons is due to very fine pores. The adsorption isotherms for the activated series follow the pattern found by Lamond and Marsh (131) (See Section 3.4) and by Rowan (6) for the adsorption of carbon dioxide at $195^{\circ}K$, on activated series of polyvinylidene chloride carbons and on activated series of cellulose and cellulose acetate carbons respectively. It can be seen that up to relative pressures of ca. 10^{-3} more adsorption takes place on unactivated carbon and carbons of up to ca. 20% burn-off than on more highly activated carbons. This indicates that activation widens the pores since the greater adsorption at low relative pressures found for the unactivated and slightly activated carbons is attributed to the stronger adsorption

forces in fine pores. At higher relative pressures adsorption takes place to a greater extent in more highly activated carbons. This is due to the increased adsorptive capacity of the highly activated carbons resulting from the widening of pores on activation.

A comparison of the adsorption isotherms for unactivated carbon and with those for slightly activated carbons shows that new pores are formed or closed pores are opened during the early stages of the activation. This can be deduced from the fact that at low relative pressures the amount of adsorption on the unactivated carbon is less than that on a carbon activated to ca. 20% burn-off. This initial opening of closed pores or formation of new pores has also been observed by Rowan (6) for activation of cellulose carbon by carbon dioxide. By an analysis of apparent density measurements McEnaney (4) (See Section 3.4) also came to the conclusion that in the initial stages of the activation of cellulose and coconut shell carbons the major process was the opening of restricted pores together with some creation of new pores. An alternative explanation in the present case is that activated diffusion of the carbon dioxide in the fine pores of the unactivated carbon may have resulted in the lack of equilibrium. There is some evidence for this view since although the majority of isotherms were completely reversible, some evidence of hysteresis was

found for the unactivated carbon at low relative pressures which might account for the effect.

In general agreement with previous work, the present results support the view that the major process occurring in the later stages of activation is the widening of existing pores.

5.2.2. The Thermodynamic Criterion for the Application of the Dubinin

It has been shown (Section 3.2.2.) that one of the basic postulates of the Dubinin Theory is that the characteristic curve $-\Delta G = f(V)$ should be independent of temperature, and that as a consequence the differential molar entropy change on adsorption measured relative to the entropy of the bulk liquid $\Delta S = -\left(\dfrac{\partial \Delta G}{\partial T} \right)_w$ must be negative. This condition has now to be expressed in a form more suitable for the analysis of experimental data before the application of the Dubinin Equation in the present work can be attempted.

The temperature dependence of the pressure of vapour (p) in equilibrium with a fixed amount (w) of adsorbate and of the saturated vapour pressure (p_o), can be plotted as functions of (1/T) and it is found that these plots usually approximate to straight lines. Bering and Serpinsky (157) therefore suggest that these lines can be expressed in the form

$$\ln p = -q_{st}/RT \pm C_w \qquad\qquad \text{Equation 5.1.}$$

and $\quad \ln p_0 = -\lambda_v/RT + C_s$ $\qquad$ Equation 5.2.

where q_{st} is the isosteric heat of adsorption, λ_v is the latent heat of vapourisation of the bulk liquid adsorbate and C_w and C_s are intercepts on the ordinate ($\ln p$) axis. If then $\Delta G = RT \ln (p/p_0)$ it follows that

$$\Delta G = (\lambda_v - q_{st}) - (C_s - C_w) RT \qquad \text{Equation 5.3.}$$

This equation can be compared with the Gibbs-Helmoltz Equation:-
$\Delta G = \Delta H - T\Delta S$ which in this case becomes

$$\Delta G = (\lambda_v - q_{st}) - T \Delta S \qquad \text{Equation 5.4.}$$

and thus $\Delta S = (C_s - C_w) R$ $\qquad$ Equation 5.5.

For ΔS to be negative, Bering and Serpinsky show that extrapolation of the adsorption isostere must cut the ordinate ($\ln p$) axis at a point C_w above the point C_s found by extrapolation of the vapour density data. Hence the isostere which on extrapolation intersects the ordinate axis at C_s determines the limiting value of adsorption below which the Dubinin theory is inapplicable. This method involves long extrapolations which therefore introduce errors in the values of the intercepts and so a more direct method of determining the limiting value of adsorption was developed in the present work.

The molar free energy change on adsorption has been defined in Section 3.2.2. as $\Delta G = \overline{G}^* - G_L^! = RT \ln p/p_0$. Similarly

the enthalpy change on adsorption can be defined as

$\Delta H = \overline{H}* - H'_L$ where $\overline{H}*$ is the partial molar enthalpy of the

adsorbate in the adsorbed state and H'_L is the molar enthalpy

of the bulk liquid at unit pressure. Thus in this case

$$\Delta H = -q_{st} + \lambda_v \qquad\qquad \text{Equation 5.6.}$$

where q_{st} is the isosteric heat of adsorption and λ_v is the

latent heat of vapourisation of the bulk liquid. Hence by

use of the Gibbs – Helmholtz Equation the entropy change on

adsorption, $\Delta S = - \left(\dfrac{\partial \Delta G}{\partial T} \right)_w$ is given by:-

$$\Delta S = \frac{\lambda_v}{T} - \frac{q_{st}}{T} - R \ln p/p_o \qquad\qquad \text{Equation 5.7.}$$

The isosteric heat of adsorption (q_{st}) is obtained from the

slope of the isosteres and the latent heat of vapourisation

(λ_v) is obtained from thermodynamic data for the bulk liquid

(187). Hence the limiting value of adsorption below which the

Dubinin theory is inapplicable can be obtained directly from

the slope of the isosteres, without the necessity for

extrapolations to determine intercepts.

The two methods for the determination of the limiting amount

of adsorption were compared for adsorption on a number of

carbons in the present work. To obtain the necessary isosteres,

isotherms (Figs. 5.4. and 5.5.) were measured at 273° and 298°K

---

* Denotes the adsorbed state,

in addition to those at 195°K. Isosteres were plotted for adsorption values of ca. 0.005 to ca. 0.14 $g.g^{-1}$. Some of the isosteres for adsorption on the unactivated carbon are shown in Fig. 5.6., which also includes the vapour pressure of liquid carbon dioxide plotted according to the Clausius-Clapeyron Equation. Although the assumption that q_{st} is constant is normally only considered valid over a smaller temperature range than used in the present work the isosteres obtained were straight lines (within the limits of experimental error). Plots of isosteric heats of adsorption obtained from the slopes of these curves against the amount of adsorption (w) were made. The plot obtained for the unactivated carbon is shown in Fig. 5.7; curves for the other carbons were very similar and details are included in Table 5.1.

It will be seen that as the amount of adsorption tends to zero the isosteric heat of adsorption increases. This has been observed for many adsorbate - adsorbent systems (188) and is attributed to the fact that the initial adsorption occurs at adsorption sites of highest energy. As the amount of adsorption, w, increases q_{st} tends to a constant value. In many systems q_{st} tends to the latent heat of vapourisation of the bulk liquid, λ_v, which has been attributed to the onset of multilayer formation. (188). However in the present case (Fig. 5.7., Table 5.1.) q_{st} tends to the latent heat of sublimation,

λ_s, (189). This observation therefore does not appear to support the conclusions of other workers that adsorbed carbon dioxide exists in the super-cooled liquid state at $195^{\circ}K$ (Section 5.1.). Unfortunately insufficient evidence has been obtained in the present work to draw firm conclusions, but this observation appears worthy of further study. A possible explanation might be that the limiting value of q_{st} is a function of the average pore size and that multilayer formation does not occur. The observation of Lamond and Marsh (131) that the limiting value of q_{st} decreases with activation and tends towards λ_v, could be interpreted in such terms.

Using the measured values of q_{st} and applying equation 5.7. values for the entropy of adsorption at $195^{\circ}K$ relative to the bulk liquid were obtained (See Table 5.1.). When the entropy values are plotted as a function of the amount adsorbed (Fig. 5.8.) it can be seen that the entropy change on adsorption is zero for $w = $ ca. 0.09 g.g^{-1}. and negative for larger adsorption values for the unactivated carbon. The limiting adsorption values, w_{lim}, and the corresponding values of (p/p_o) and $\log^2(p_o/p)$ for the other carbons were determined in a similar manner and are listed in Table 5.2.

The Bering and Serpinsky (159) method gives values for the entropy change on adsorption as a function of the amount adsorbed (See Table 5.3.) which are subject to errors due to difficulties in the extrapolation of the isosteres. Fig. 5.8.

is a plot which compares for the unactivated carbon the
entropy change on adsorption calculated by the two methods
as a function of the amount adsorbed. It will be seen that
the limiting adsorption value is approximately the same in
each case. This is to be expected since when $\triangle S = 0$ it
can be shown from Equations 5.3. and 5.7. that

$$RT \ln (p_o/p) = (\bar{q}_{st} - \lambda_v) \qquad\qquad \text{Equation 5.8.}$$

From Equation 5.8. it will be seen that the relative
pressure at which the limiting amount of adsorption occurs
depends on the isosteric heat of adsorption (See Fig. 5.9.).

For the carbons investigated in the present work limit-
ing values of adsorption occur in the regions of the isotherms
where q_{st} has reached limiting values (6.2. to 6.6. k.cals.mole^{-1}.)
corresponding to values of $\log^2(p_o/p)$ of 6 to 8.5. respectively.
Unfortunately it was not possible to determine isosteric heats
for a wider range of carbons, but on the basis of these results
it has been assumed that in general the limiting value of
p/p_o is not below 10^{-3} [$\log^2(p_o/p) = 9$] and hence that the
application of the Dubinin Equation at p/p_o values less than
10^{-3} need not be considered.

It is interesting to note that in the case of the unacti-
vated carbon only there is a second region of the isotherm
where $\triangle S < 0$ at low surface coverages, $w < 0.01$g.g^{-1}. (Fig. 5.8.,
Table 5.1.). However, as previously discussed the unactivated

carbon exhibits slight hysteresis at low surface coverages and hence the thermodynamic quantities determined in this region are of dubious value.

5.2.3. The Application of the Dubinin Equation

Dubinin plots for the isotherms shown in Fig. 5.1. (i.e. isotherms activated to ca. 35% at various temperatures in the range 400° - 726°C) were made and pore volumes and D-values were determined (Table 5.4.). Discussion of these and similar plots will follow later in this section. The micro-pore volumes and D-values are plotted as a function of temperature of activation in Figs. 5.10. and 5.11. These results in general support the conclusions drawn from a qualitative inspection of the isotherms (Section 5.2.1.). Fig. 5.10. shows clearly the effect on micro-pore volumes of the increasing amount of external attack on the carbon with increasing temperature in Zone III. This effect is corroborated by the variation in the value of D with increasing temperature of activation.

It can be seen that the development of micropore volume to ca. 35% burn-off in Zone II does not appear to be a reproducible process. The adsorptive capacity of the total amount obtained of each activated carbon was measured so there is no question of the samples being unrepresentative. The activated carbon pellets have an uneven appearance and some of them appear to have been activated preferentially. Although this

could be attributed to selective attack at impurity sites it
is more likely to be a function of the carbon-oxygen reaction.
The work of Rowan (6) using an almost identical cellulose
carbon found activation by carbon dioxide showed no evidence
of selective attack except at very high burn-off. Selective
attack may account in part for the reduced rate of develop-
ment of porosity in Zone II after the first ca. 20% burn-off
(see later) since it might be expected that in the later
stages of activation some of the carbon pellets might be
completely burnt away. It was in fact observed with some of
the more highly activated carbons that there was a decrease
in the number of pellets after activation.

It was hoped in the course of this work to determine
whether the presence of surface oxide had any influence on
the adsorption of carbon dioxide. However this has not proved
possible owing to the non-reproducible micro-porosity developed
in Zone II.

The isotherms (Figs. 5.2 and 5.3.) for activated series
of carbons prepared at 456° and 485°C are plotted according
to the Dubinin Equation in Figs. 5.12. and 5.13. However the
lines obtained are not generally straight as originally postu-
lated by Dubinin even over the relative pressure ranges where
the criterion $\Delta S < 0$ is almost certainly satisfied.

For carbons activated at 456° and 485°C the Dubinin plots

follow a similar pattern. For unactivated carbon the curve is concave to the $\log^2(p_o/p)$ axis, for slightly activated carbons the lines are nearly straight and for carbons of greater burn-off the lines become increasingly convex to the $\log^2(p_o/p)$ axis. Rowan (6) obtained similar curved plots for the adsorption of carbon dioxide at $195^{\circ}K$ on cellulose carbons activated by reaction with carbon dioxide. He considered these plots as two intersecting straight lines and used the parts of the curves in the low relative pressure range to determine surface areas using a method similar to that of Kaganer (190, 191) and Lamond and Marsh (129). Adsorption at low relative pressures was tentatively attributed to the formation of a monolayer on the surface of pores and at higher relative pressures to micropore filling. However in view of the dubious nature of the concept of surface area when applied to microporous materials (See Chapter 3) Rowan rejected this explanation.

The Dubinin plots are uncorrected for adsorption in transitional pores but this effect cannot account for the deviations from linearity. Dubinin has shown (133) that unless transitional porosity is especially developed as in de-colouris-ing charcoals, typical active carbons have transitional pores of about $50m^2.g^{-1}$ surface area. It was shown that in the case of an active carbon of micropore volume of $0.40cm^3.g^{-1}$ such a transitional porosity would make about 4% contribution to the

total adsorption up to a relative pressure of 0.1. The
deviations from linearity found in the present work are in
excess of this amount e.g. for the carbon activated to 34.6%
burn-off at $456^{\circ}C$ (micropore volume = $0.42 cm^3.g^{-1}.$) a deviation
of about 10% at p/p_o = 0.10 is observed. Also Dubinin and
co-workers (156, 192, 193) have recently found similar
curves for the adsorption of benzene on carbons at $20^{\circ}C$ which
have been corrected for adsorption in transitional pores.
These curves were interpreted in terms of two micro-porous
structures by a modification of Equation 3.12.,

$$V = V_{o_1} \ e^{-k_1(-\Delta G)^2/\beta^2} + V_{o_2} \ e^{-k_2(-\Delta G)^2/\beta^2}$$

Equation 5.9.

This approach was applied (Fig. 5.14 and Table 5.5.) to one of
the more highly active carbons obtained in the present work
and it can be seen that analysis gives two straight lines of
the forms

$$V_1 = V_{o_1} \ e^{-k_1(-\Delta G)^2/\beta^2} \text{ and } V_2 = V_{o_2} \ e^{-k_2(-\Delta G)^2/\beta^2}$$

where the total micropore volume is the sum of the two volumes
V_{o_1} and V_{o_2}. While this method clearly capable of interpret-
ing Dubinin plots it must be said that there is little other
evidence for the bimodal micropore size distribution implied by
Equation 5.9. It may well be that the success of this equation

in interpreting curved Dubinin plots is simply due to the increase from two to four in the number of adjustable parameters.

The application of the Dubinin Equation (3.15) to the isotherms gives the values of micropore volumes shown in Tables 5.6. and 5.7. which also include the slopes D of the plots at high relative pressures, which can be used as a semi-quantitative measure of the micro-pore size distribution (See Equation 3.12.). The values of V_o and D are plotted as a function of the degree of burn-off in Figs. 5.1.5. and 5.1.6. These results provide quantitative confirmation of the conclusions drawn from an inspection of the isotherms (Section 5.2.1.) showing that the porosity increases steadily with activation until 20 - 30% burn-off, the rate of development of porosity decreasing thereafter. A general widening of the pore size distribution with activation is shown by the steady increase in the value of D with increasing burn-off.

The isotherms at $273°$ and $298°K$ (Figs. 5.4. and 5.5.) were also plotted in terms of the Dubinin Equation (Figs. 5.1. and 5.18.) and the micro-pore volumes and D-values found by inspection of the plots are shown in Tables 5.8. and 5.9. The adsorbate density at these temperatures was determined by the method of Nikolaev and Dubinin (160). It will be seen that the micropore volumes are not in very good agreement with those found from the isotherms at $195°K$. This is possibly due to the

fact that longer extrapolations had to be made in the Dubinin plots at higher temperatures to obtain micropore volumes as the relative pressures obtained were much lower. It might also be assumed that curved Dubinin plots similar to those observed at $195^{o}K$ would also be found at higher temperatures and hence extrapolations from low relative pressures would not give accurate values for the micro-pore volumes.

5.3. Comparison of Porosity developed in a Cellulose Carbon by

Reaction with Carbon Dioxide and Oxygen

A comparison of the porosity developed in a 1000° cellulose carbon by activation with oxygen and carbon dioxide can be made by comparing the present work with that of Rowan (6).

It has been shown in Chapter 4 that the carbon-oxygen and carbon-carbon dioxide reactions occur in different temperature ranges and therefore comparison of porosity development by the two reactions must relate to the same zone of rate control in each case. Rowan found that porosity development was independent of the temperature of activation over the relatively narrow temperature range $890^{o} - 960^{o}C$ which he concluded was in Zones I and II of the carbon-carbon dioxide reaction. In the present work the temperature range ca. $400^{o} - 480^{o}C$ was assigned to Zone II.

Comparison of the porosity developed by the two reactions in Zone II has been made in Figs. 5.19. and 5.20. where the

micro-pore volume/g. carbon and micropore volume/g. unactivated carbon respectively are plotted as a function of the degree of burn-off for carbons activated by carbon dioxide at $935^{o}C$ and oxygen at $456^{o}C$. It will be seen from Fig. 5.19. that in the initial stages of activation the development of porosity is very similar for both reactions. After 20 - 30% burn-off the porosity developed on activation with oxygen becomes less than that produced by the carbon dioxide reaction. This effect is also shown in Fig. 5.20. where it will be seen that porosity development by carbon dioxide is a maximum ca. 40% burn-off; in the case of the carbon-oxygen reaction the maximum porosity is developed at ca. 30% burn-off. The figure for carbon dioxide compares well with that found by Wicke (60) for the development of surface area ($m^2.g^{-1}$. unactivated carbon) in an electrode carbon by reaction with carbon dioxide and that for the maximum porosity developed by activation of an anthracite with carbon dioxide (194). The relative inefficiency of oxygen as an activating agent has been attributed (Section 5.2.2.) to selective attack resulting in the complete combustion of previously activated carbon pellets in the later stages of activation.

TABLE 5.1. (i)

Values of Isosteric Heat and Entropy of Adsorption at 195°K

w $(g \cdot g^{-1} \cdot)$	Unactivated Carbon		35.4% burn-off at 401°C	
	q_{st} $(k.cal.mole^{-1} \cdot)$	$\overline{S}^*-S_L^!$ (e.u.)	q_{st} $(k.cal.mole^{-1} \cdot)$	$\overline{S}^*-S_L^!$ (e.u.)
$0.005^{\mathcal{I}}$	10.6 ($\pm$ 1.0)	-10 ($\pm$ 4.)	9.3 ($\pm$ 1.0)	+ 4 ($\pm$ 2)
$0.008^{\mathcal{I}}$	7.1 ($\pm$ 0.6)	+ 6 ($\pm$ 3)	7.3 ($\pm$ 0.5)	+ 8 ($\pm$ 3)
0.01	6.9 ($\pm$ 0.6)	+ 5 ($\pm$ 2)	6.9 ($\pm$ 0.3)	+ 4.6 ($\pm$ 1.0)
0.02	6.7 ($\pm$ 0.3)	+ 5.6 ($\pm$ 0.6)	6.9 ($\pm$ 0.3)	+ 3.0 ($\pm$ 0.6)
0.04	6.8 ($\pm$ 0.3)	+ 2.3 ($\pm$ 0.6)	6.9 ($\pm$ 0.3)	+ 0.9 ($\pm$ 0.6)
0.06	6.7 ($\pm$ 0.3)	+ 1.6 ($\pm$ 0.6)	6.7 ($\pm$ 0.3)	+ 0.3 ($\pm$ 0.6)
0.08	6.5 ($\pm$ 0.3)	+10.7 ($\pm$ 0.6)	6.3 ($\pm$ 0.3)	+ 1.0 ($\pm$ 0.6)
0.10	6.4 ($\pm$ 0.4)	- 0.1 ($\pm$ 0.6)	6.3 ($\pm$ 0.3)	+ 0.1 ($\pm$ 0.6)
0.12	6.4 ($\pm$ 0.4)	- 1.2 ($\pm$ 0.6)	6.3 ($\pm$ 0.3)	- 0.7 ($\pm$ 0.6)
0.14	6.4 ($\pm$ 0.4)	- 2.2 ($\pm$ 0.6)	6.3 ($\pm$ 0.3)	- 2.3 ($\pm$ 0.6)

$\mathcal{I}$
Values of q_{st} and $\overline{S}^*-S_L^!$ for these values of w were calculated
using data from Isotherms at 273° and 298°K. Entropy values
in this region were very inaccurate as the isotherms could not
be measured accurately in the lower relative pressure range.

TABLE 5.1. (ii)

Values of Isosteric Heat and Entropy of Adsorption at 195°K. (Cont.)

w (g.g^{-1}.)	35.6% burn-off at 436°C		35.1% burn-off at 518°C	
	q_{st} (k.cal.mole^{-1}.)	$\bar{S}*-S_L'$ (e.u.)	q_{st} (k.cal.mole^{-1}.)	$\bar{S}*-S_L'$ (e.u.)
0.005$^{\pm}$	7.5 ($\pm$ 0.5)	+ 1.8 ($\pm$ 2.0)	7.0 ($\pm$ 1.0)	+ 5.8 ($\pm$ 2.0)
0.008$^{\pm}$	6.9 ($\pm$ 0.3)	+10.5 ($\pm$ 1.5)	6.6 ($\pm$ 0.5)	+ 6.8 ($\pm$ 1.5)
0.01	6.8 ($\pm$ 0.3)	+ 5.4 ($\pm$ 1.0)	6.6 ($\pm$ 0.3)	+ 6.8 ($\pm$ 1.0)
0.02	6.9 ($\pm$ 0.3)	+ 3.2 ($\pm$ 1.0)	6.6 ($\pm$ 0.3)	+ 5.1 ($\pm$ 1.0)
0.04	6.8 ($\pm$ 0.3)	+ 1.6 ($\pm$ 1.0)	6.5 ($\pm$ 0.3)	+ 4.0 ($\pm$ 1.0)
0.06	6.6 ($\pm$ 0.3)	+ 1.0 ($\pm$ 1.0)	6.4 ($\pm$ 0.3)	+ 2.2 ($\pm$ 1.0)
0.08	6.5 ($\pm$ 0.3)	+ 0.2 ($\pm$ 1.0)	6.5 ($\pm$ 0.3)	+ 1.2 ($\pm$ 1.0)
0.10	6.5 ($\pm$ 0.3)	- 0.3 ($\pm$ 1.0)	6.5 ($\pm$ 0.3)	+ 0.2 ($\pm$ 1.0)
0.12	6.2 ($\pm$ 0.3)	0 ($\pm$ 1.0)	6.5 ($\pm$ 0.3)	- 0.7 ($\pm$ 1.0)
0.15	6.2 ($\pm$ 0.3)	- 1.1 ($\pm$ 1.0)	6.6 ($\pm$ 0.3)	- 2.2 ($\pm$ 1.0)

$\pm$
Values of q_{st} and $\bar{S}* -S_L'$ for these values of w were calculated using data from Isotherms at 273° and 298°K. Entropy values in this region were very inaccurate as the isotherms could not be measured accurately in the lower relative pressure range.

TABLE 5.2.

Limiting Adsorption Values

Carbon	Limiting Adsorption w_{lim} $(g.g^{-1}.)$
Unactivated	0.09 ($\pm$ 0.01)
35.4% burn-off at 401°C	0.10 ($\pm$ 0.01)
35.6% burn-off at 436°C	0.10 ($\pm$ 0.01)
35.1% burn-off at 518°C	0.10 ($\pm$ 0.01)

TABLE 5.3.

Entropy change on Adsorption on Unactivated Carbon

calculated by method of Bering and Serpinsky (157)

Amount Adsorbed w (g.g.$^{-1}$)	$\Delta S = (C_s - C_w)R$ (e.u.)
0.005	-3 ($\pm$ 2)
0.008	+2.5 ($\pm$ 0.5)
0.01	+2.8 ($\pm$ 0.3)
0.02	+2.2 ($\pm$ 0.3)
0.04	+1.4 ($\pm$ 0.3)
0.06	+0.7 ($\pm$ 0.3)
0.08	+0.1 ($\pm$ 0.3)
0.10	-0.3 ($\pm$ 0.3)
0.12	-0.6 ($\pm$ 0.3)

TABLE 5.4.

Micropore Volumes and D-values for Carbons Activated

to ca. 35% burn-off at 401° - $726^{o}C$ obtained

from Dubinin Plots

Isotherm	Temperature of Activation	% burn-off	Micropore^{I} Volume $(cm.^3g.^{-1})$ ($\pm$ 0.01)	D x 10^{2*}
(i) (ii)	-	0	0.20	4.2 ($\pm$ 0.2)
(iii)	401	35.4	0.43	14.5 ($\pm$ 1.0)
(iv)	420	34.5	0.35	8.4 ($\pm$ 0.5)
(v)	436	35.0	0.48	14 ($\pm$ 1)
(vi)	436	35.6	0.44	14 ($\pm$ 1)
(ix)	456	34.6	0.42	10.4 ($\pm$ 0.6)
(xiii)	485	35.1	0.44	11.5 ($\pm$ 1.0)
(xvii)	518	35.1	0.35	9.2 ($\pm$ 0.5)
(xviii)	572	35.3	0.32	7.0 ($\pm$ 0.3)
(xix)	620	36.3	0.25	6.0 ($\pm$ 0.3)
(xx)	726	32.1	0.20	4.2 ($\pm$ 0.2)

* D represents slope of the Dubinin Plot at high relative

pressures.

^{I} Adsorbate Density taken as 1.23 g.cm^{-3} for calculation of

micropore volume.

TABLE 5.5.

Analysis of Dubinin Plot for Carbon Activated to 68.5% burn-off at 456°C. (See also Fig. 5.14.)

	Micropore Volume $(cm^3.gm^{-1})$ (± 0.01)	D-value $(x\ 10^2)$
w_o	0.48	18
w_{o_1}	0.25	7.0
w_{o_2}	0.22	35.7

TABLE 5.6.

**Micro-pore Volumes and D-values for Carbons Activated at 456°C
Obtained from Dubinin Plots**

Isotherm	% burn-off	Micropore volume[I] $(cm^3.g^{-1}.)$ (± 0.01)	$D \times 10^{2*}$
(i) (ii)	0	0.20	4.2 ($\pm$ 0.2)
(viii)	20.0	0.32	6.5 ($\pm$ 0.2)
(ix)	34.6	0.42	10.4 ($\pm$ 0.6)
(x)	48.6	0.47	13 ($\pm$ 1)
(xi)	68.6	0.48	18 ($\pm$ 1)

TABLE 5.7.

**Micro-pore Volumes and D-values for Carbons Activated at 485°C
Obtained from Dubinin Plots**

Isotherm	% burn-off	Micropore volume[I] $(cm^3.g^{-1}.)$ (± 0.01)	$D \times 10^{2*}$
(i) (ii)	0	0.20	4.2 ($\pm$ 0.2)
(xii)	21.2	0.38	8.5 ($\pm$ 0.5)
(xiii)	35.1	0.44	11.5 ($\pm$ 1.0)
(xiv)	50.1	0.48	13.5 ($\pm$ 1.0)
(xv)	70.4	0.51	18 ($\pm$ 1)

*D represents the slope of the Dubinin Plot at high relative pressures.

[I]Adsorbate Density taken as 1.23 g.cm^{-3}. for calculation of micropore volume.

TABLE 5.8.

Micro-pore Volumes and D-values for a number of Carbons Obtained from Dubinin Plots derived from isotherms at 273°K.

Isotherm	Carbon	Micropore volume‡ $(cm^3.g^{-1}.)$ $(\pm\ 0.02)$	D x 10^{2*}
(xxi)	Unactivated	0.25	9.4 ($\pm$ 0.5)
(xxii)	35.4% burn-off at 401°C	0.32	12.4 ($\pm$ 0.6)
(xxiii)	35.6% burn-off at 436°C	0.36	13 ($\pm$ 1)
(xxiv)	35.1% burn-off at 518°C	0.36	11.4 ($\pm$ 0.5)

‡Adsorbate Density taken as 0.93 g.cm^{-3}. for calculation of micropore volume.

TABLE 5.9.

Micro-pore Volumes and D-values for a number of Carbons Obtained from Dubinin Plots derived from Isotherms at 298°K

Isotherm	Carbon	Micropore volume‡ $(cm^3.g^{-1}.)$	D x 10^{2*}
(xxv)	Unactivated	0.24 ($\pm$ 0.02)	10.6 ($\pm$ 0.5)
(xxvi)	35.4% burn-off at 401°C	0.35 ($\pm$ 0.02)	13.0 ($\pm$ 0.6)
(xxvii)	35.6% burn-off at 436°C	0.38 ($\pm$ 0.03)	14 ($\pm$ 1)
(xxviii)	35.1% burn-off at 518°C	0.38 ($\pm$ 0.03)	11.5 ($\pm$ 0.5)

‡Adsorbate density taken at 0.71 g.cm^{-3}. for calculation of micropore volume.

*D represents the slope of the Dubinin Plot at the relative pressures measured.
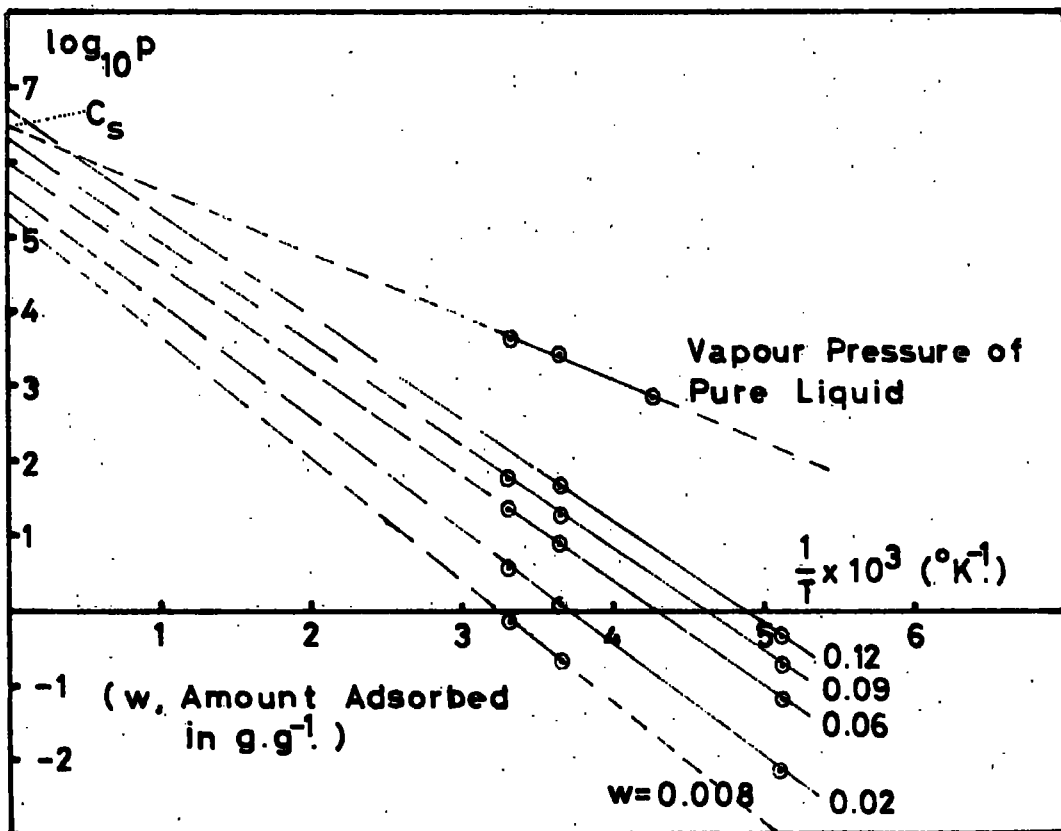
FIG. 5.6.

Isosteres for Unactivated Carbon
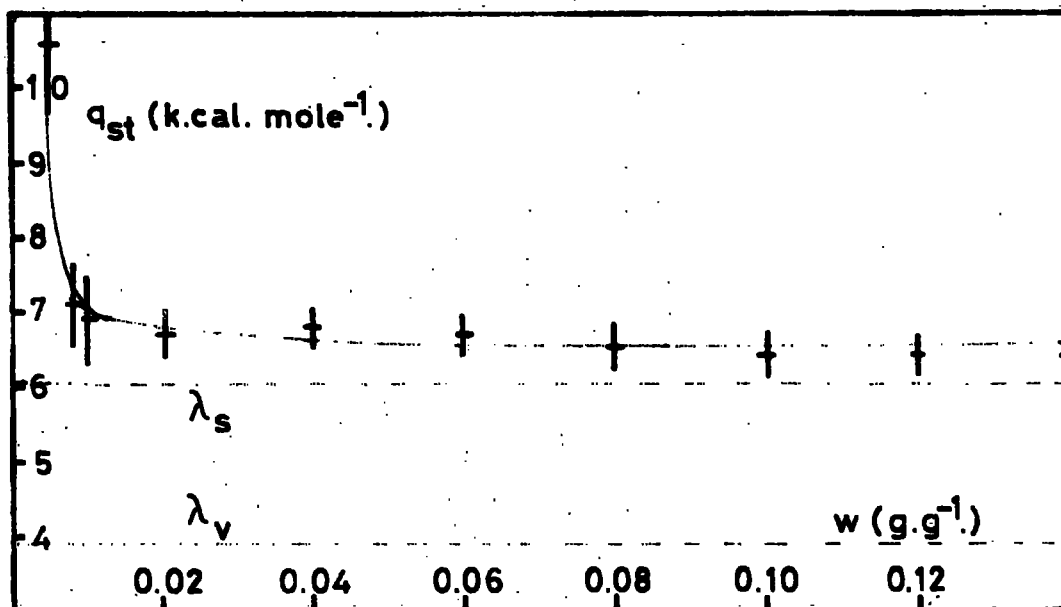
FIG. 5.7.

Isosteric Heat of Adsorption for Unactivated Carbon
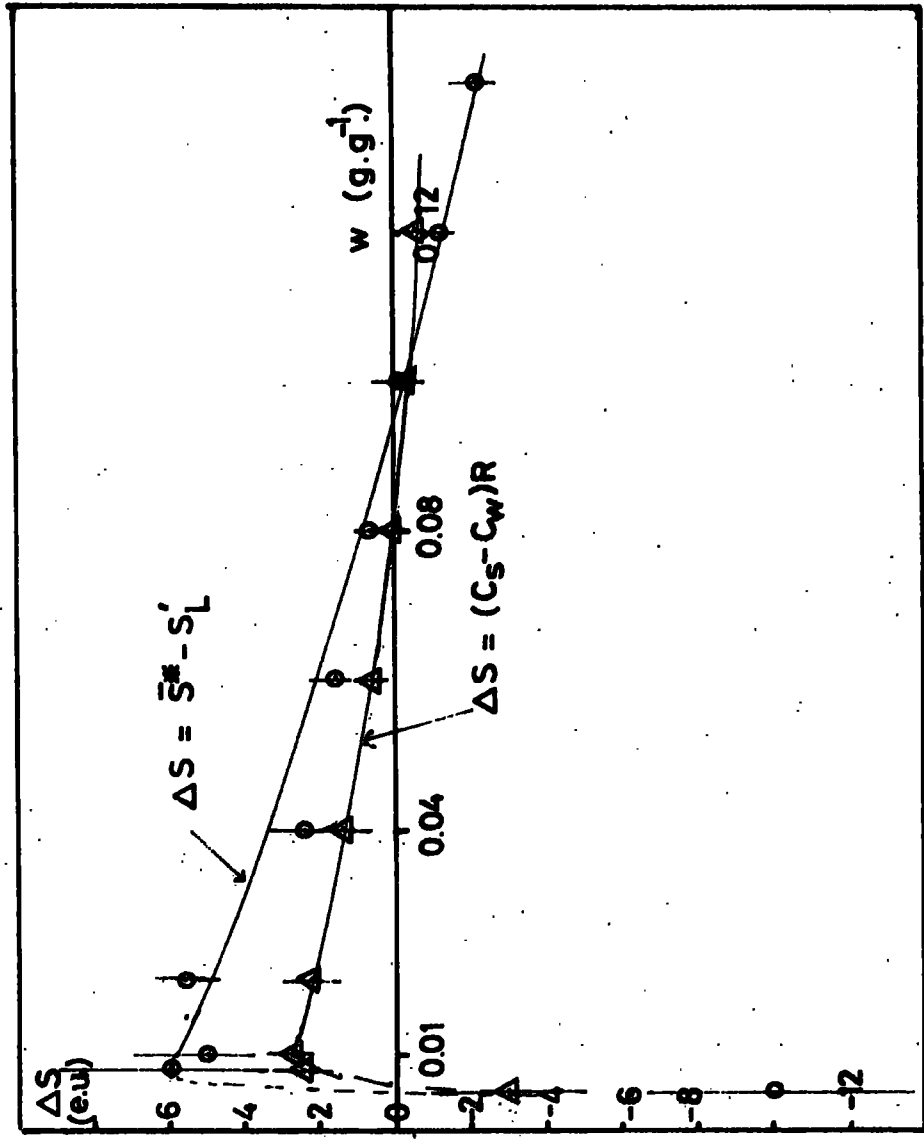
FIG. 5.8.

Differential Entropy Changes for Unactivated Carbon
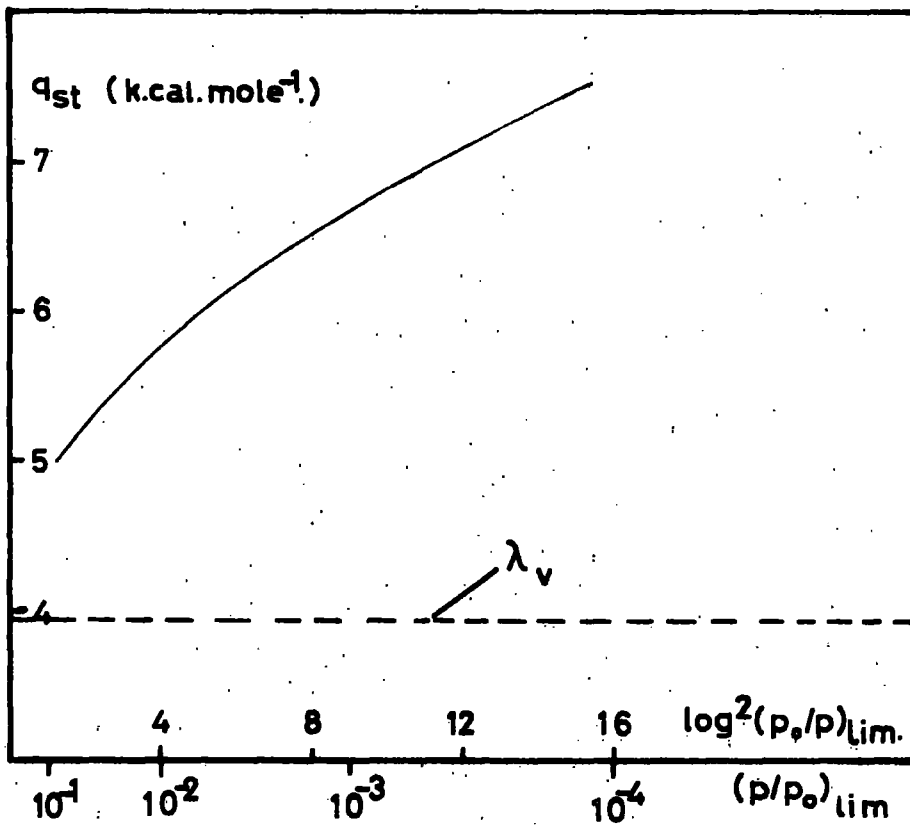
FIG. 5.9.

Variation of Limiting Values of $\log^2(p_o/p)$ and (p/p_o) with Isosteric Heat of Adsorption at $195°K$
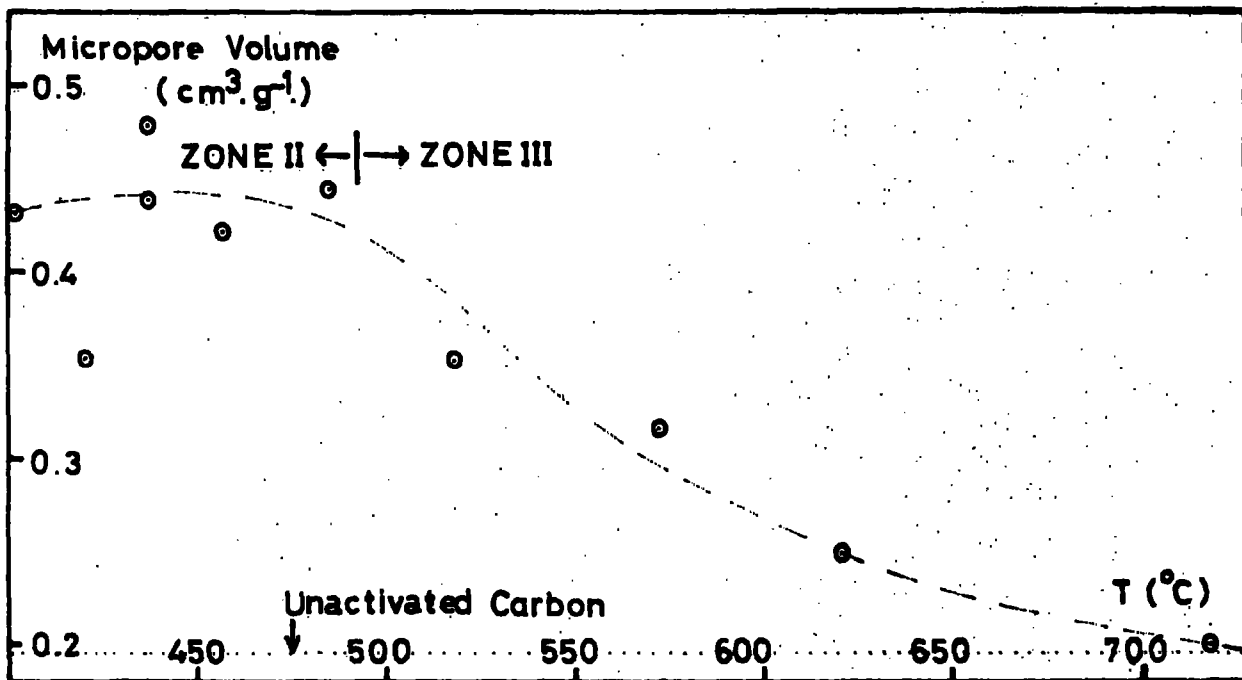
FIG. 5.10.

Variation of Micropore Volume with Temperature
of Activation for Carbons of ca. 35% Burn-off
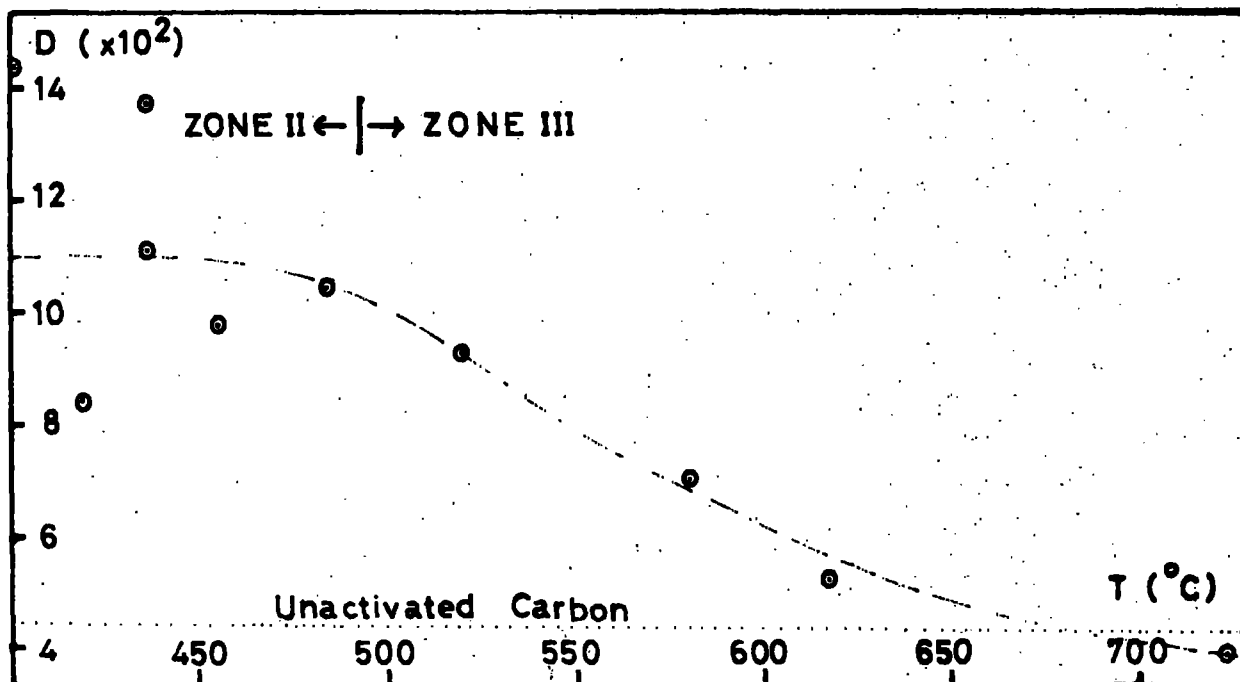
FIG. 5.11.

Variation of D with Temperature of Activation
for Carbons of ca. 35% Burn-off
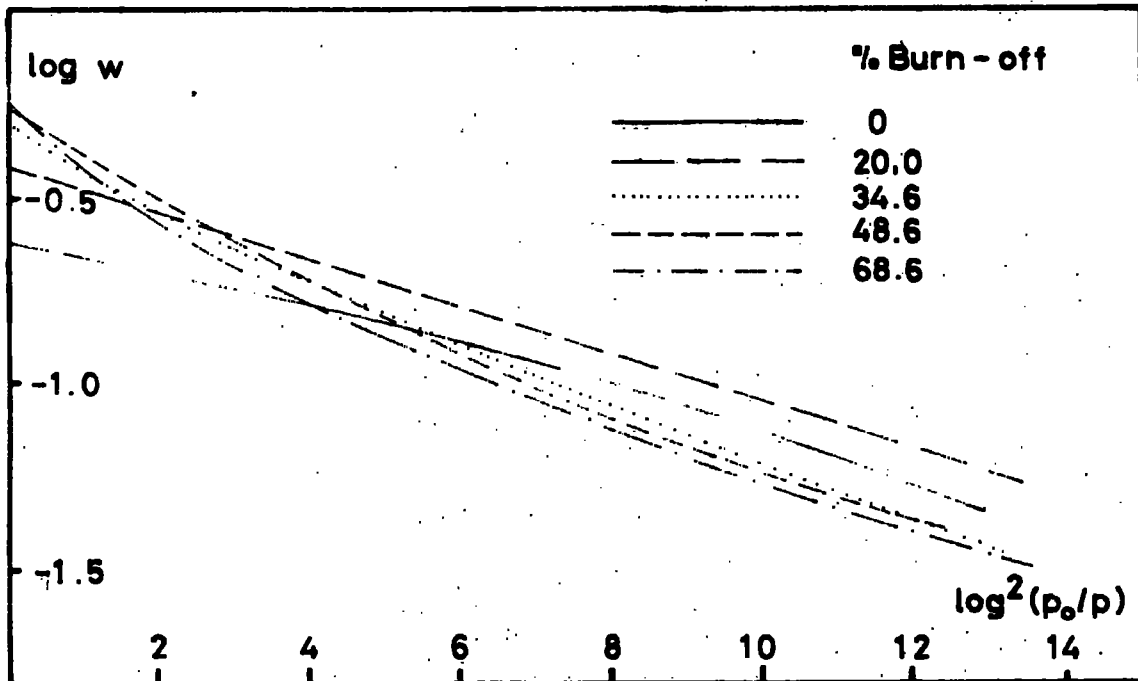
FIG.5.12.

Dubinin Plots of Isotherms at 195°K
for Carbons Activated at 456°C.
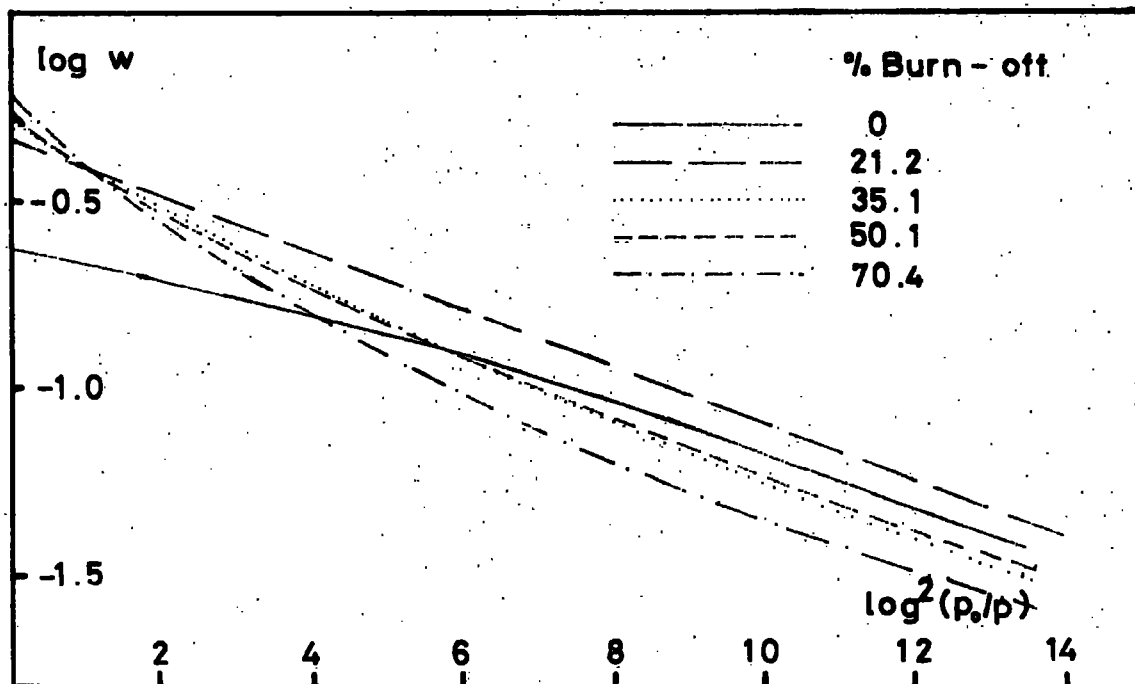
FIG.5.13.

Dubinin Plots of Isotherms at 195°K
for Carbons Activated at 485°C
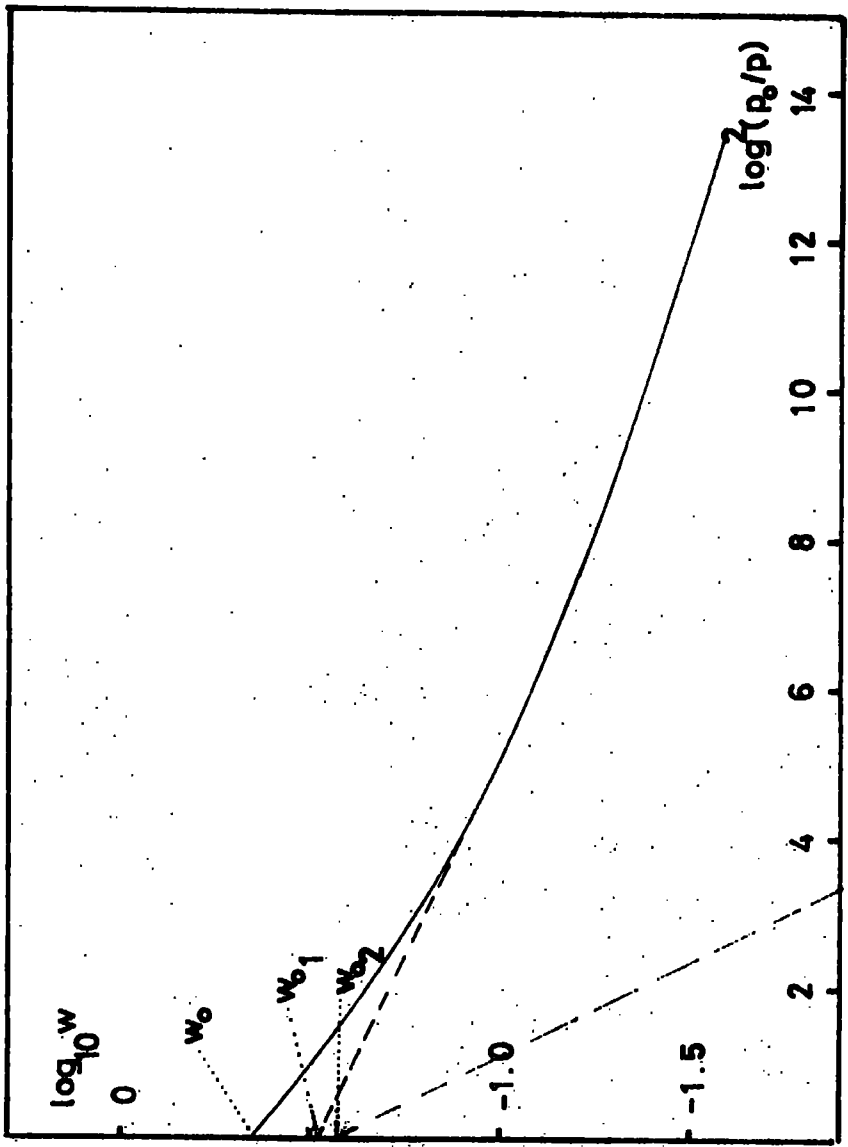
FIG. 5.14.

Dubinin Plot for an Activated Carbon (68.5% Burn-off at 456 °C)

according to Equation 5.9.
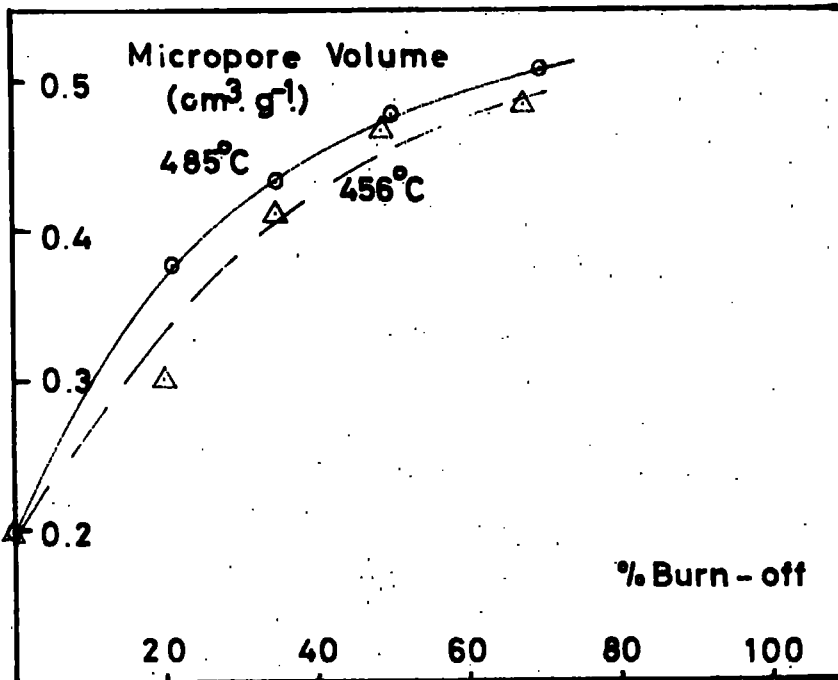
FIG. 5.15.

Micropore Volume as a Function of
Burn - off at 456° and 485°C
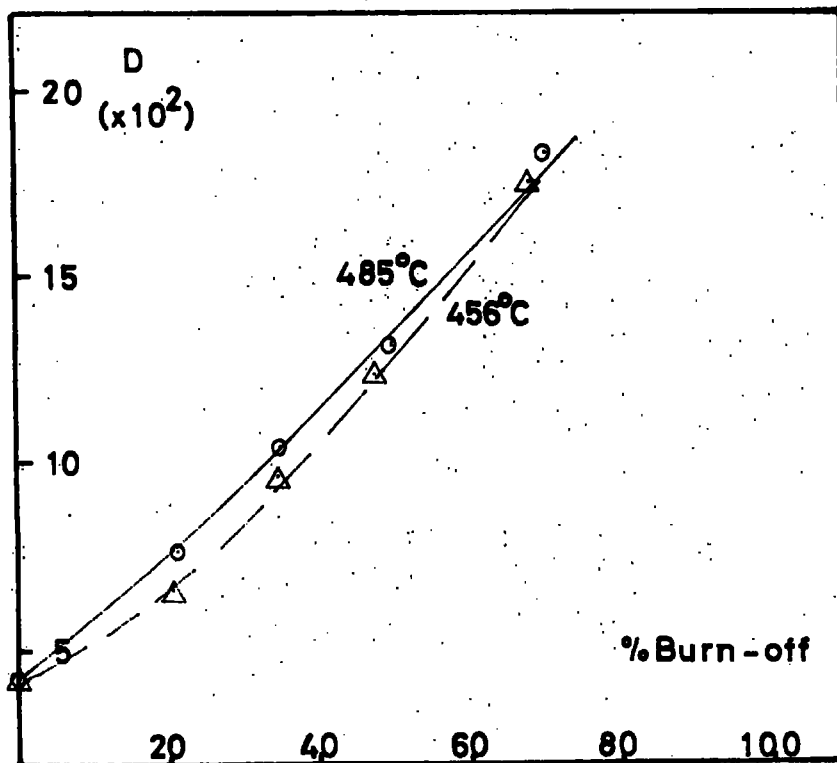
FIG. 5.16.

D-values as a Function of
Burn-off at 456° and 485°C
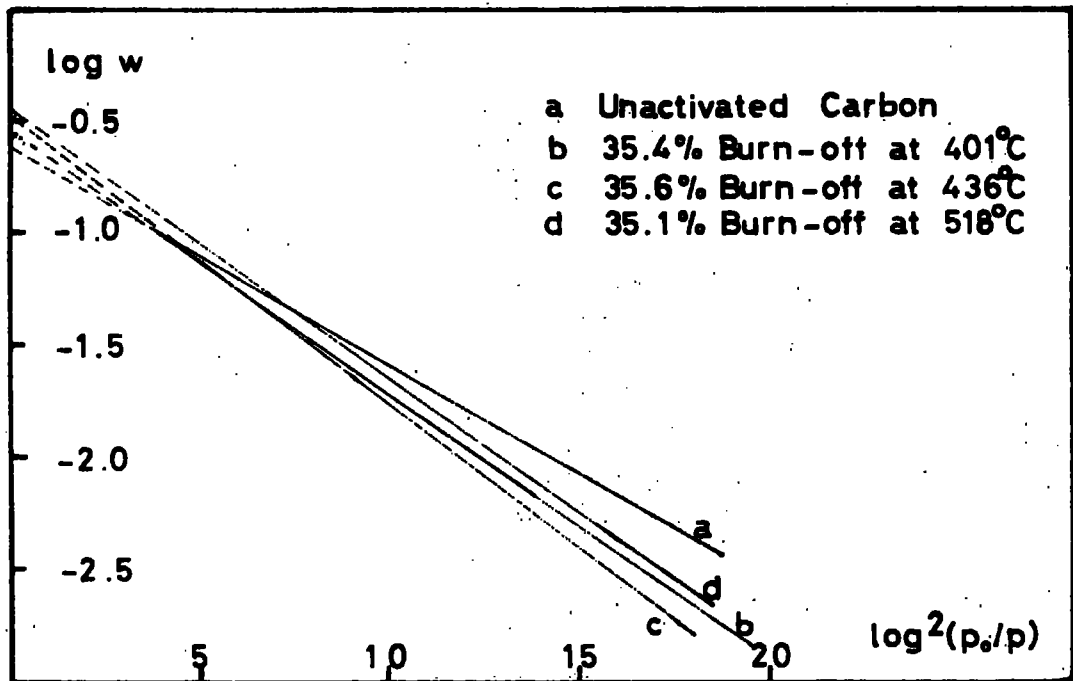
FIG. 5. 17.

Dubinin Plots of Carbon Dioxide Isotherms at 273°K
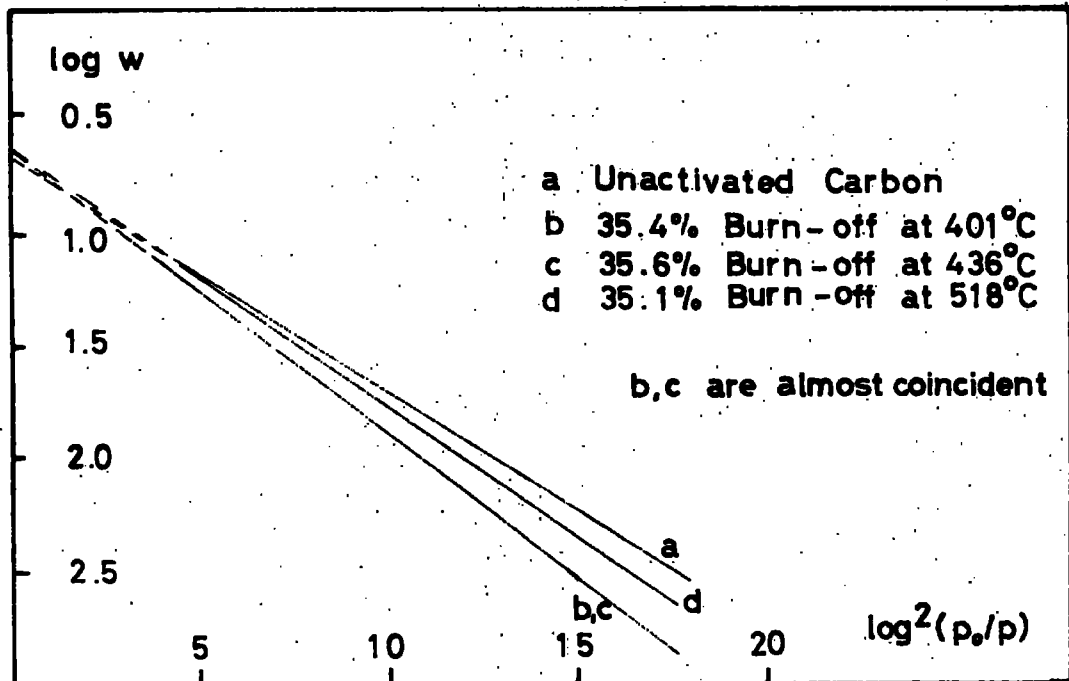
FIG. 5. 18.

Dubinin Plots of Carbon Dioxide Isotherms at 298°K.
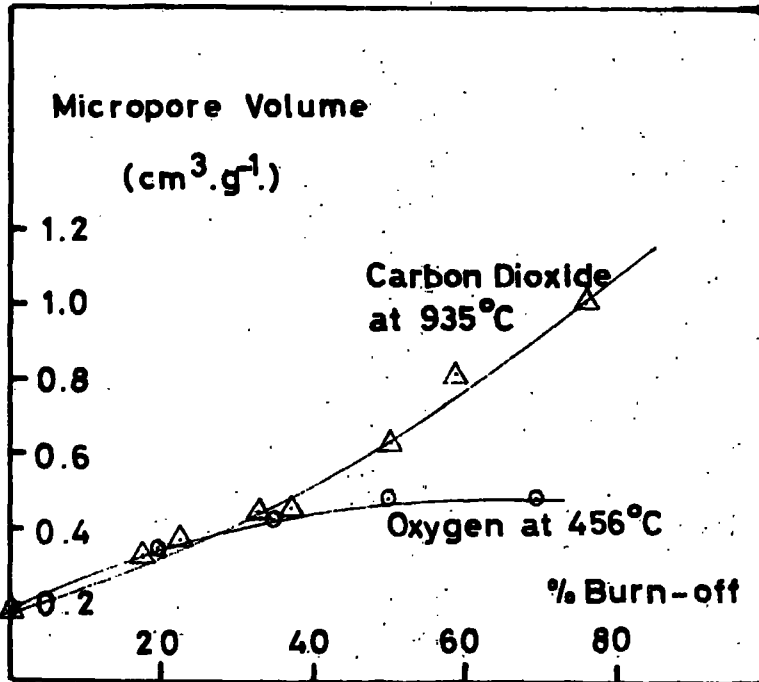
FIG. 5.19.

Comparison of Activation of Cellulose Carbon
by Carbon Dioxide and Oxygen in Zone II
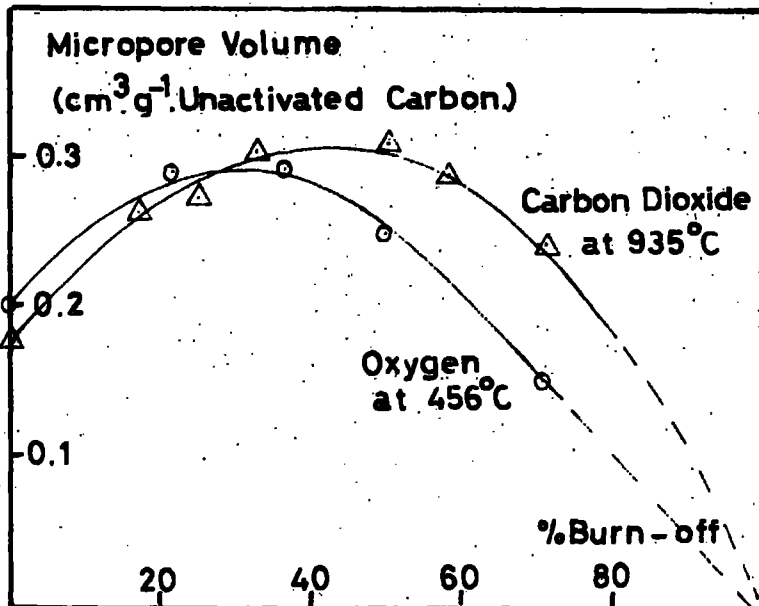
FIG. 5. 20.

Comparison of Activation of Cellulose Carbon
by Carbon Dioxide and Oxygen in Zone II

CHAPTER 6.

Summary and Conclusions

6.1.   Introduction

This chapter contains a summary of the results and con-
clusions of the work presented in the thesis. Firstly the
work will be reviewed in the light of the aims stated in
Chapter 1 and then other findings not directly related to
these aims will be outlined. The chapter concludes with a
number of comments and suggestions for extensions of the work.

6.2.   Summary of Main Findings

The first aim of the work reported in this thesis (Section
1.6.) was to investigate the rate of reaction of a porous
cellulose carbon with oxygen over a temperature range extend-
ing over Zones II and III of the classification of Hedden and
Wicke (40). It has been shown for the carbon-oxygen reaction
that under the conditions employed in the present work the
temperature range $400^{\circ} - 726^{\circ}C$ extends over Zones II and III.
From the kinetic studies (Chapter 4) an activation energy of
25.2 ($\pm$ 2.5) k.cal.mole^{-1} was found for the temperature range
$400^{\circ} - 460^{\circ}C$. indicating Zone II conditions and an activation
energy of 2.5 ($\pm$ 0.5) k.cal.mole^{-1} was found for the tempera-
ture range $480^{\circ} - 726^{\circ}C$ indicating Zone III conditions. It can
be seen from Chapters 2 and 4 that these values are similar to
those found by a number of other workers. The designations of

zones were confirmed by investigation of the influence of
partial pressure of oxygen, sample weight and crucible
geometry on the rate of reaction.

The second aim of the work was to attempt to relate the
development of porosity to the rate and extent of the activa-
tion process; in particular to investigate the influence of
diffusion control of reaction rate on the development of poro-
sity. Analysis of the adsorption isotherms and Dubinin plots
obtained in the present work (Chapter 5) showed that the devel-
opment of porosity clearly depends on the temperature of
activation. This is in contrast to the findings of Rowan who
concluded that the porosity developed by activation with carbon
dioxide in Zone II and on the Zone I and II borders was indepen-
dent of the temperature of activation. At $726^{o}C$ there is no
development of porosity on activation of the carbon with oxygen;
this is consistent with the view that in Zone III the reaction
occurs entirely on the external surface of the carbon. However
in the range 500° - $600^{o}C$ which is at the lower end of Zone III
as determined by the reactivity studies there is evidence that
some porosity is developed. As noted in Chapter 5, this suggests
that the value of the activation energy may not always be a
particularly sensitive indication of the temperature limits
of the reaction zone.

For carbons activated at 400° - $480^{o}C$ in Zone II and on the

Zone II - Zone III border where the rate of reaction is controlled by diffusion within the pores of the carbon, it was shown that substantial development of porosity occurs. However the variation in micropore volume with temperature of activation at ca. 35% burn-off as deduced from the application of the Dubinin Equation was found to be unreproducible and no clear indication of its variation with temperature within Zone II could be obtained.

Studies on activated series of carbons prepared at temperatures within Zone II showed in agreement with other workers (4, 6) that activation in the initial stages opens closed pores or forms new ones and that subsequently the major part of the activation process widens existing pores.

It is to be noted that this work has been the first systematic investigation of the influence of the temperature of activation on the development of porosity by activation of a carbon with oxygen.

The third aim of the thesis was to compare the properties of oxygen and carbon dioxide as activating gases by comparison with Rowan's work (6). To date no such comparison has been made. It was noted in Chapter 4 that if comparisons are made between two gas-carbon reactions it is necessary to ensure that the reactions are in the same zone of rate control. Thus in the present case it was only possible to compare the carbon-

oxygen and carbon-carbon dioxide reactions in Zone II. Under Zone II conditions i.e. 925° - $950^{\circ}C$ for the carbon-carbon dioxide reaction and 400° - $460^{\circ}C$ for the carbon-oxygen reaction, it was found that in the initial stages of activation porosity development is very similar. However after ca. 20 - 30% burn-off the porosity developed on activation with oxygen becomes less than that produced by the carbon dioxide reaction. The relative inefficiency of oxygen as an activating agent was attributed to selective attack resulting in the complete combustion of previously activated material in the later stages of activation.

6.3.   Summary of Other Findings.

On the assumption that the weight loss curves obtained on activation of the carbon (Chapter 4) are the net result of both weight loss due to loss of gaseous products and weight gain due to surface oxide formation it was deduced that the carbon forms most surface oxide on reaction with oxygen between temperatures of 450° and $500^{\circ}C$, in agreement with the findings of other workers (82, 102) (Chapter 2). An attempt to find kinetic parameters for the formation of surface oxide was unsuccessful possibly because the preheating programme did not remove all the surface oxide present.

A method for the determination of the thermodynamic criterion, entropy change on adsorption $\Delta S < 0$, for the

applicability of the Dubinin Theory was developed and compared with that used by Bering and Serpinsky (157) in Chapter 5. For the carbons examined the limiting adsorption values were found to depend on the limiting value of the isosteric heat of adsorption.

Application of the Dubinin Equation to the regions of the isotherms where the thermodynamic criterion was shown to apply gave lines that were not generally straight as originally postulated by Dubinin. However analysis of the results in terms of the Dubinin Equation in general confirmed the effects of temperature of activation and degree of burn-off on the development of porosity.

6.4. <u>Suggestions for Further Developments of the Work</u>

The investigation undertaken has to a large extent achieved the aims set out in Chapter 1 and produced a number of other observations pertinent to the study of microporous carbons. A number of suggestions can now be made for extension of the work undertaken.

An investigation of the reaction of a porous carbon with an activating gas over a temperature range encompassing the three reaction zones of Hedden and Wicke (40) would be a useful contribution to the study of activation processes. The elimination of the effects of mass transport necessary to attain Zone I conditions might be obtained by use of an activating gas at

reduced pressure and by a different sample presentation than that used in this work. Activation by oxygen of a wider range of carbons could be used to confirm whether the selective attack observed in the present work is a function of the carbon-oxygen reaction or merely a function of the cellulose carbon used in this work.

The theoretical basis of the Dubinin theory, as its author admits (39), requires further attention. The present work has shown that for adsorption of carbon dioxide at $195^\circ K$ in microporous cellulose carbon in the region of temperature invariance of the characteristic curve ($\Delta S < 0$) the Dubinin Equation is not always obeyed. A more detailed examination of this problem than was possible in the present work appears worthwhile.

The assumption that carbon dioxide at $195^\circ K$ is adsorbed as a supercooled liquid also appears to require further evaluation. The evidence for this assumption (reviewed in Section 5.1.) is not entirely convincing and it would be of interest to measure carefully the adsorption of carbon dioxide at $195^\circ K$ on a wide range of adsorbents.

To conclude, this investigation has been a study of the development of porosity in a $1000^\circ C$ cellulose char by activation with oxygen. It has illustrated the effect of variation in temperature of activation and reaction zone on the development

of porosity showing clearly the influence of diffusion control. Comparison of the properties of carbon dioxide and oxygen as reacting gases was made and showed the relative efficiency of oxygen as an activating agent.

APPENDIX I

Preparation of Cellulose Carbon

Cellulose Pellet Preparation

Chromatrographic Grade Cellulose Powder (Whatman's Column Chromedia CF 11) was dampened and then worked through a BS 22 mesh sieve. It was then dried in an oven at 60°C overnight. The cellulose obtained in this way has suitable flow characteristics for preparation of pellets using a pharmaceutical pelleting machine. The pellet weight was kept as closely controlled as possible between 0.010 - 0.014g.

Apparatus Constructed for Carbonisation

The thermal balance and associated apparatus is essentially that described by Hodgson (195). It consists of a furnace heated by an Ether Transitrol programme controller (Type 994/2) giving a stepless power supply through a saturable reactor. The circuit is shown as a block diagram in Fig. A.1.

The heating programme is obtained by cutting a suitable cam to drive a control arm to give a linear rate of heating, in this instance 3.5 ($\pm$ 0.2) deg.C.min^{-1}. The desired control temperature is indicated on the controller scale by a pointer. The furnace temperature is measured with a Pt/Pt, 13% Rh thermocouple and indicated on the scale by a galvanometer pointer. The position of the two pointers thus indicates the relation between the desired control temperature and the measured temperature.

Attached to the control arm is an optical system consisting of a small filament lamp, lens and photocell. When the two pointers are coincident a small flag attached to the galvanometer pointer intercepts the light beam. As the control pointer moves upscale ahead of the galvanometer pointer, the light beam produces a current in the photocell circuit. This current is then amplified and supplied to the D. C. winding of the saturable reactor. The impedance of the A. C. winding of the reactor is proportional to the current in the D. C. winding. Thus the current drawn from the A. C. winding of the reactor is proportional to the lag of the measured temperature behind the desired control temperature. In this way a smooth heating programme is obtained without the 'hunting' associated with 'on-off' controllers.

A nichrome crucible containing the sample is suspended from an analytical balance by a nichrome wire and located within a mullite work-tube (diameter ca.$1\frac{1}{4}$") placed vertically in the furnace. A glass tube is placed around the suspension wire to reduce erratic movement of the balance due to draughts. The end pieces of the work tube are designed to allow:- (a) the sample to be freely suspended, (b) an additional thermocouple for measuring sample temperatures to be introduced (See Fig. A.2.), and (c) gases to flow through the tube.

The inert atmosphere required for carbonisation is provided

by passing oxygen-free nitrogen through the furnace tube.
The gas is fed from a cylinder through a two-stage reducing
valve and a diaphragm valve (made by Scientific Instrument
and Model Co.). It then passes through a drying tower contain-
ing silica-gel and through a flow meter. The capillary flow-
meters containing di-butyl phthalate as an indicating fluid
were calibrated using a soap-bubble flowmeter. Flow-rates
range from 500 ($\pm$ 10) mls.min^{-1} to 1500 ($\pm$ 10) mls.min^{-1} and
can be held constant to $\pm$ 10 mls.min^{-1} for long periods.

The gas extracted from the bottom of the tube is passed
through a trap to collect the tars formed during carbonisation.
It is then drawn through a flowmeter, an adjustable air-bleed
and a diaphragm valve by means of a rough vacuum pump.

The sample thermocouple was placed as near as possible to
the sample. A potentiometer recorded the temperature of the
sample to $\pm$ 2°C at 960°C which is within the linearity of the
5cm. hot zone of the furnace at that temperature. Although the
furnace heating element was non-inductively wound, inductive
effects (of the order of 0.1 millivolts) were observed in the
signal of the sample thermocouple. An earthed inconel foil shield
was therefore placed around the work-tube in the furnace to
eliminate the A.C. pick-up by the sample thermocouple. In
addition care was taken that the sample thermocouple did not
touch the work-tube since leakage to earth was noticed when this
occured.

Inertness of Furnace Atmosphere

A sample of a carbon black, Spheron 6 (2700°), was used to test the inertness of the furnace atmosphere. During these tests the temperature of the furnace and the gas flow were held constant in order to avoid buoyancy effects. Some slight oxidation (2 - 3 x 10^{-6}g.sec^{-1}.g^{-1}.) was noticed above 800°C so at that temperature extraction of gas from the base of the furnace was discontinued. This gave an effectively inert atmosphere with a maximum weight loss due to oxidation of 0.3 x 10^{-6}g.sec^{-1}.g^{-1}. at 960°C. As the sample (ca.1g.) was above 900°C for approximately 60 minutes the total burn-off due to oxidation was about 0.1%. This was considered to be negligible since all the carbons to be studied were activated to at least 10% burn-off.

Operation of Thermal Balance for Carbonisation

An input flow-rate of 1000 mls. min^{-1}. of nitrogen and extract flow-rate of 850 mls.min^{-1}. were adopted. The extract flow was discontinued above 800°C when the carbonisation was virtually complete. The sample was heated at a linear rate of 3.5 ($\pm$ 0.2) deg.C.min^{-1}. up to 940 ($\pm$ 10)^{o}C and kept at that temperature for 30 minutes. It was then allowed to cool in nitrogen to room temperature.

In a typical experiment 0.8985g. of carbon was obtained from 4.5816g. of cellulose representing a yield of 19.6%. A

total of 24 carbonisations were carried out which yielded
20.0g. of cellulose carbon; the carbon yield varied from
19.4 to 20.1%. This is in good agreement with the results
obtained by Rowan (6). After completion of the carbonisa-
tions the carbon was thoroughly mixed to give representative
samples for activation.

THERMOCOUPLE COLD JUNCTION.

COMPENSATED LEADS

FURNACE

SATURABLE REACTOR

PROGRAMME CONTROLLER

PILOT AMPLIFIER

CONSTANT VOLTAGE TRANSFORMER

240 V A.C.
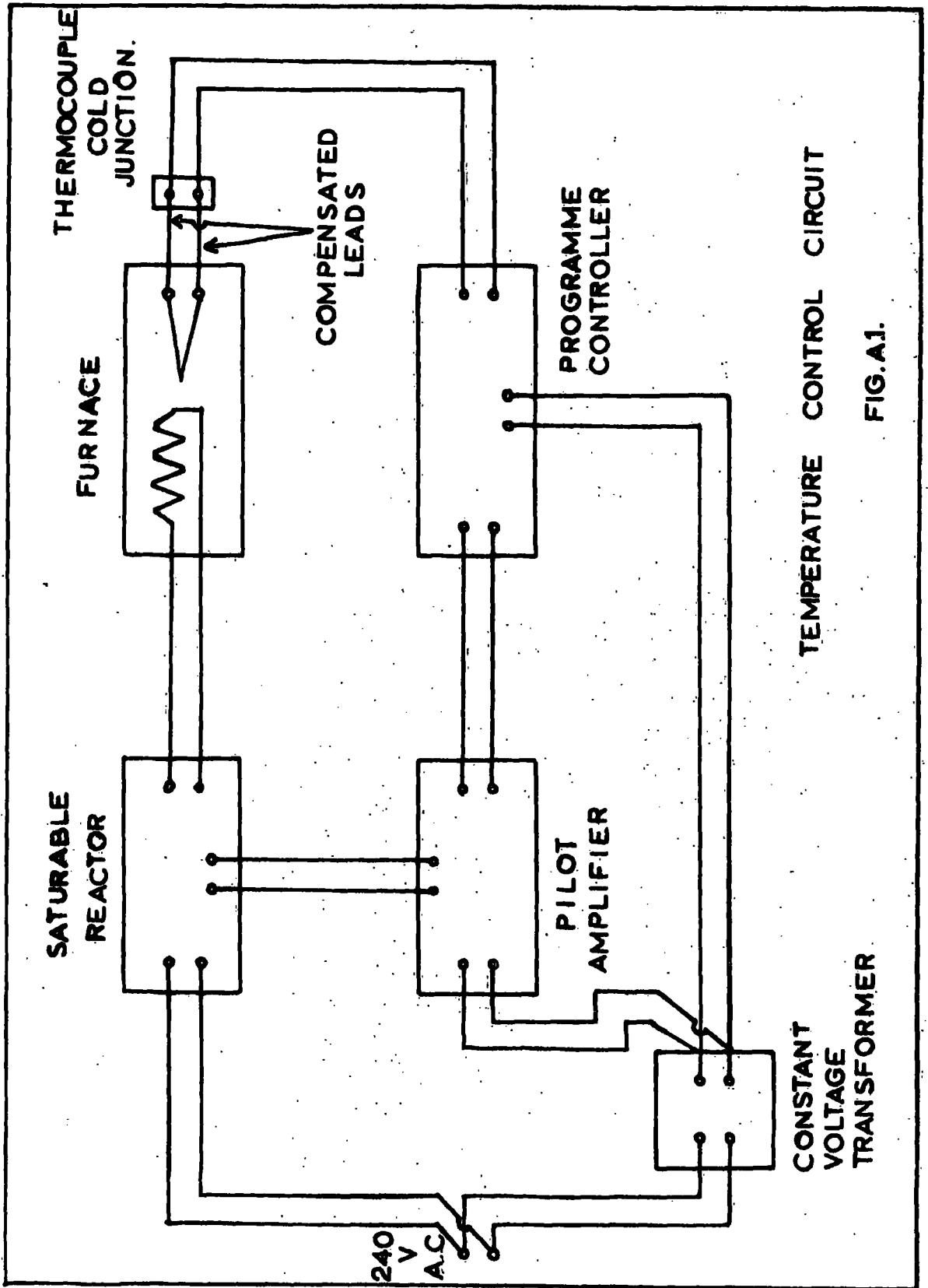
TEMPERATURE CONTROL CIRCUIT   FIG.A1.

APPARATUS USED FOR CARBONISATION

FIG. A.2.
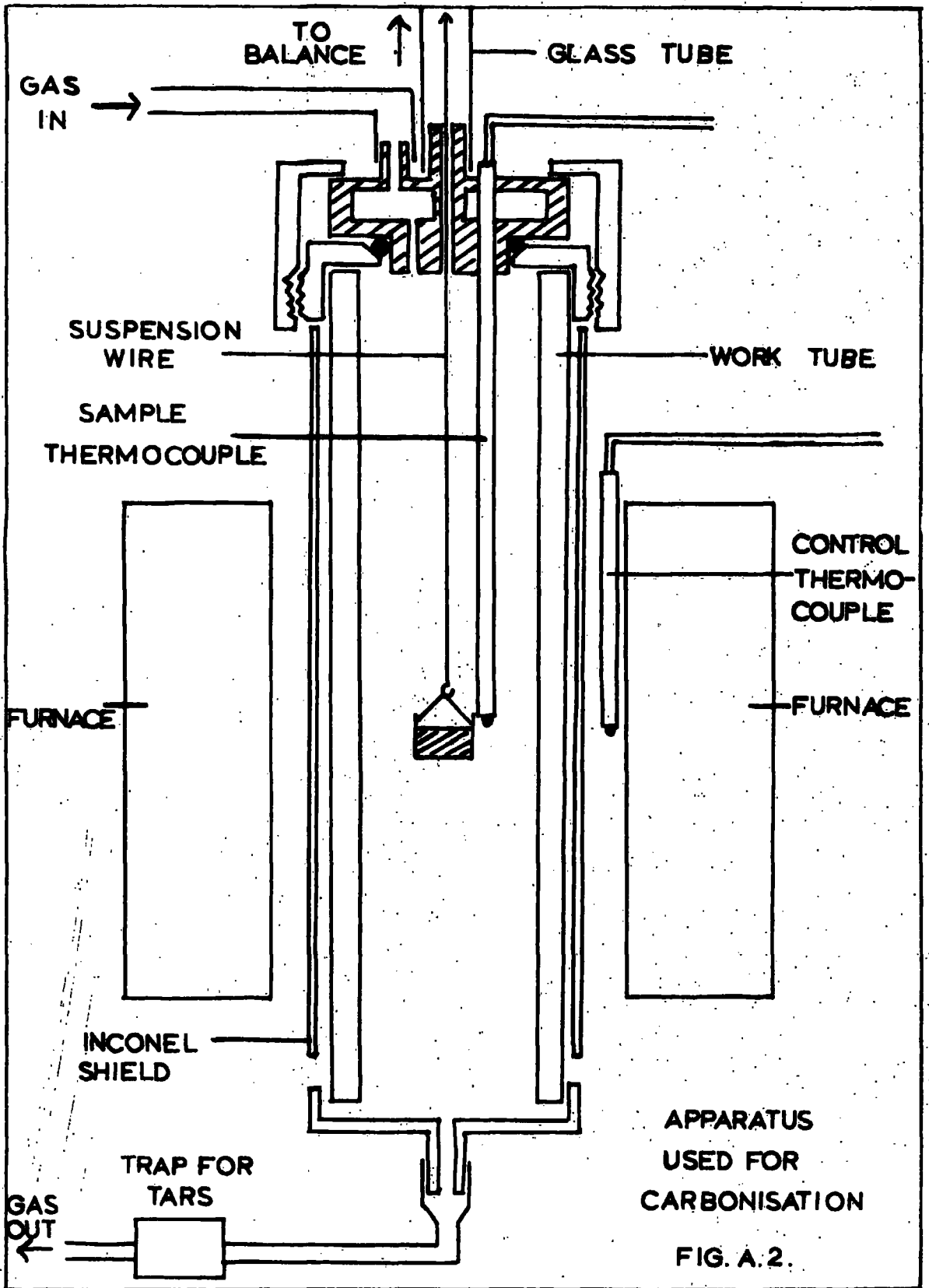
APPENDIX II

Activation

Experimental Procedure

The Stanton Thermal Balance, Model TR -01, modified (6, 196) to allow operation of the balance with gas flow over the sample was used for the activation work.

Oxygen and nitrogen were each fed from cylinders through a two stage reducing valve and a diaphragm valve (Scientific Instrument and Model Co.). They then each passed through a drying tower containing silica-gel, a flowmeter and finally through a mixing chamber before entering the furnace. The flowmeter system could be adjusted to give an inert nitrogen atmosphere or a partial pressure of oxygen ranging from 0.08 - 0.27 as required. The input flow rate is kept constant at 1000 ml.min^{-1}. and the lower extract at 600 ml.min^{-1}. Gas is not extracted from the top of the furnace and the remaining gas diffuses out through the balance case. The gases extracted from the bottom of the furnace tube are drawn through a flow-meter, an adjustable air-bleed and a diaphragm valve by means of a rough vacuum pump. A test of inertness was made by heating a sample of the carbon black Spheron 6 (2700°C) in the nitrogen stream. The maximum rate of weight loss when the temperature was 1000°C was 0.12 x 10^{-6}g.sec^{-1}. (0.3 x 10^{-6}g.sec.g^{-1}.). At the temperatures used for activation (400° - 700°C) the weight

loss was shown to be negligible.

The standardised procedure adopted for activation was to heat the carbon sample to 960°C at a rate of 8 deg.C.min^{-1}. in an atmosphere of nitrogen. A loss in weight was observed in the preliminary heating programme which is attributed to loss of water and chemisorbed oxygen. The temperature was held at 960°C for 30 minutes and then lowered to the temperature required for activation. When the temperature became constant, the nitrogen was exchanged for an oxygen-nitrogen mixture. After the required amount of oxidation had occured the oxygen-nitrogen mixture was replaced by nitrogen. When the weight of the sample became constant it was cooled to room temperature in nitrogen. When cold the samples were collected and stored in stoppered tubes.

APPENDIX III

Measurement of Adsorption Isotherms

A. Measurement of Isotherms using Cahn Electrobalance

Several adsorption isotherms were measured using a Cahn RG Electrobalance. This balance has a maximum capacity of 2.5g. and an ultimate sensitivity of 0.1 μg. As it is capable of working at atmospheric pressure, high vacuum or with controlled atmospheres, it is very suitable for adsorption studies on small samples.

The Cahn RG Electrobalance (197) operates on the null-balance principle. When in its equilibrium position a small flag attached to the end of the balance beam partially intercepts a light beam between a small filament lamp and a photocell. Movement of the balance beam alters the intensity of the light falling on the photocell and therefore alters the current in the photocell. This current is amplified in a two stage servo-amplifier and applied to a coil attached to the beam. The coil is positioned within a magnetic field and the current through it therefore exerts a restoring moment on the beam. Thus the change in electromagnetic force is equal to the change in the sample weight. The extremely accurate voltage generated by the current across the coil and its series circuit is measured by subtracting an known voltage from it by means of an accurate potentiometer and applying the difference to a recorder.

The balance is placed within a vacuum tight bottle which is connected to the auxiliary apparatus illustrated in Fig.A.3. and adsorption isotherms are measured using the following procedure. The balance is calibrated and the weighed carbon sample is placed in a small glass bucket and suspended within a long tube attached to the balance bottle by a B.40 cone and socket joint. A counterweight is suspended in another removable limb attached to the bottle. After recording the weight of the sample, the system is evacuated by opening taps to the main vacuum manifold. A vacuum of 10^{-7} cm.Hg. is obtained using a silicone oil diffusion pump backed by a rotary pump. A liquid air trap is used to freeze out all vapours from the gas stream. During evacuation of the system the carbon sample is heated to ca. 250°C by means of a heating coil placed around the tube. At this temperature, adsorbed gases are removed and after out-gassing, usually overnight, a pressure of 10^{-6} - 10^{-7} cm.Hg. is reached and the sample weight remains constant.

The adsorbate carbon dioxide is prepared as follows. Solid carbon dioxide is placed in trap A, and is surrounded by a salt-ice bath to retain water and any other less volatile impurities. The carbon dioxide is then distilled under vacuum into trap B, which contains a quantity of Linde Molecular Sieve 3A. From trap B. the carbon dioxide is redistilled into the gas reservoir R; trap B is surrounded by a salt-ice bath in

this case.

After the initial outgassing the adsorption system is isolated from the main manifold. The heater is then replaced by a constant temperature bath. For isotherms at $195°K$, Dewar vessels containing solid carbon dioxide are used; for isotherms at $273°K$ and $298°K$, an ice-water bath and a thermo-statically controlled water bath respectively are used.

To commence the measurement of the isotherm a small dose of carbon dioxide is admitted to the adsorption system by careful manipulation of the taps, using the U manometer as a guide to the pressure. A pressure of ca. 10^{-3}cm.Hg. is first attained and the system allowed to equilibrate. After equilibrium is obtained, as seen from the Electrobalance recorder, the weight of sample is noted and the pressure is measured using one of two McLeod Gauges which cover the ranges ca. $10^{-6} - 10^{-2}$cm.Hg. and ca. $10^{-2} - 1$cm.Hg. respectively; pressures of greater than ca. 1cm.Hg. are measured on the mercury manometer using a cathetometer. The procedure is repeated at a series of pressures until the pressure is ca. 50cm. Hg. The desorption branches of the isotherms are measured by progressively lowering the pressure, using a liquid air bath around the trap beneath the reservoir R to condense the carbon dioxide.

There are a number of experimental factors which may affect

the determination of the isotherms. Normal buoyancy effects due for example to the asymmetry of the balance design are less than 10^{-3}g. These are negligible in the procedure used since the required accurancy of measurement is of the same order. Thermal transpiration due to differences in temperature can give spurious weight readings (198). However these have been shown to be of the order of a few µg. and thus can be neglected. The influence of thermal transpiration on the pressure has also been considered (6, 199 - 201) and shown to be negligible at pressures greater than ca. 10^{-3}cm.Hg. for a similar system (6).

This apparatus was not entirely satisfactory for the present work as it required a long time to obtain a good vacuum due to long and narrow pumping paths; an apparatus of improved design has since been developed (202). An additional disadvantage is that only one isotherm can be determined at a time. For these reasons the majority of the adsorption isotherms were determined using silica springs.

B. Measurement of Isotherms using Silica Springs

This method employs the principle of the McBain-Bakr spring balance (203). Helical silica springs were set up within four adsorption chambers and with ancillary apparatus (Fig. A.4.) used to measured adsorption isotherms.

An advantage of this apparatus is that adsorption isotherms

can be measured on four samples simultaneously. The tubes are connected by B34 cone and socket joints to the vacuum line. The carbon samples are placed in small glass buckets and hung on fine glass loops attached to the springs. The springs are suspended by glass hooks from bridges across the necks of the cones. Taps isolate the adsorption tubes from the line so that any number of isotherms from one to four can be done at the same time. The springs are calibrated using standard weights and the extensions produced measured with a cathetometer.

Isotherms were obtained using a similar procedure to that used with the Cahn Electrobalance. Errors due to buoyancy effects and thermal transpiration were very similar to those found with the Cahn Electrobalance and therefore considered to be negligible.
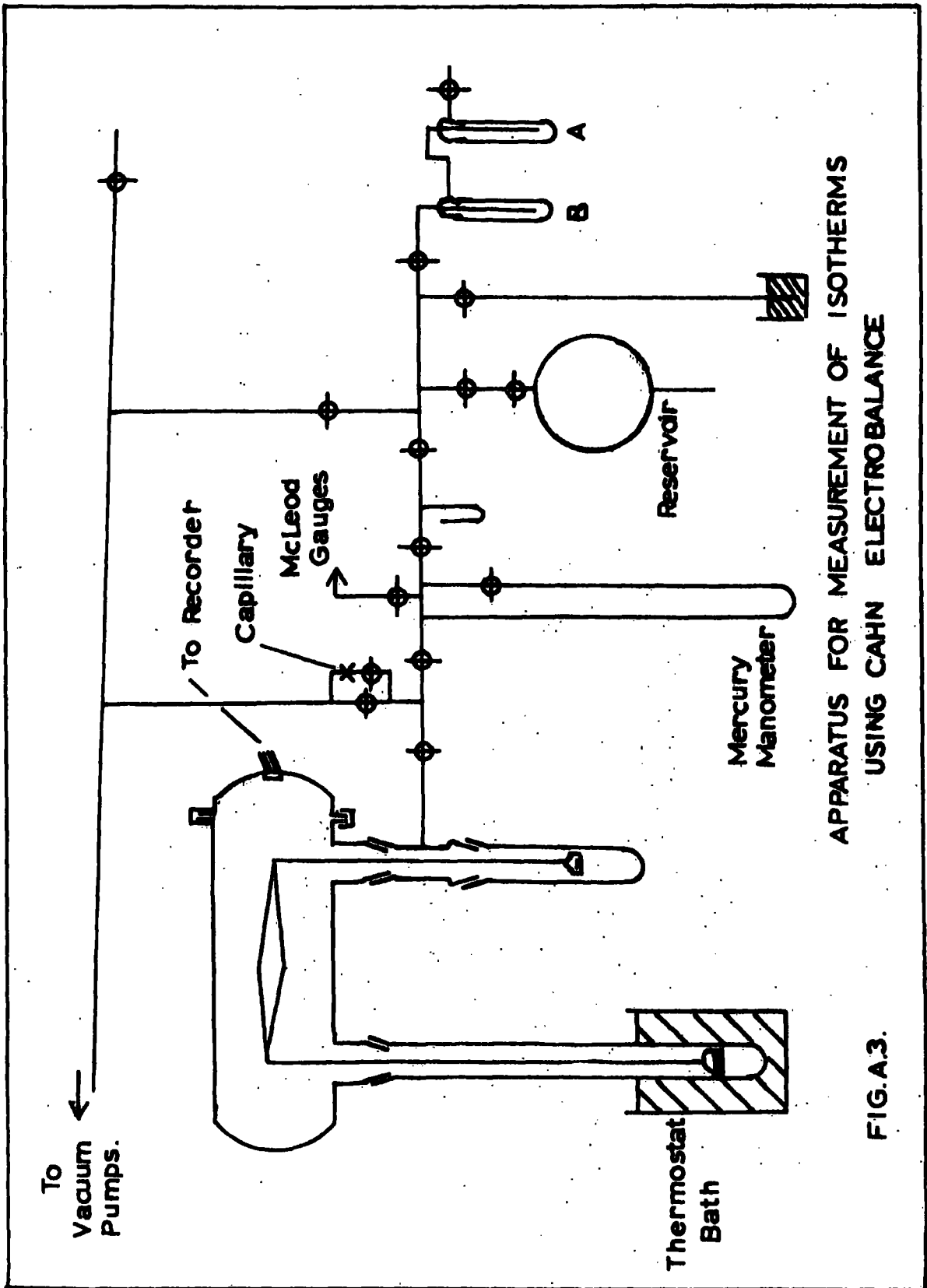
APPARATUS FOR MEASUREMENT OF ISOTHERMS USING CAHN ELECTROBALANCE

FIG. A.3.

To Vacuum Pumps

Mercury Manometer

McLeod Gauges

Reservoir
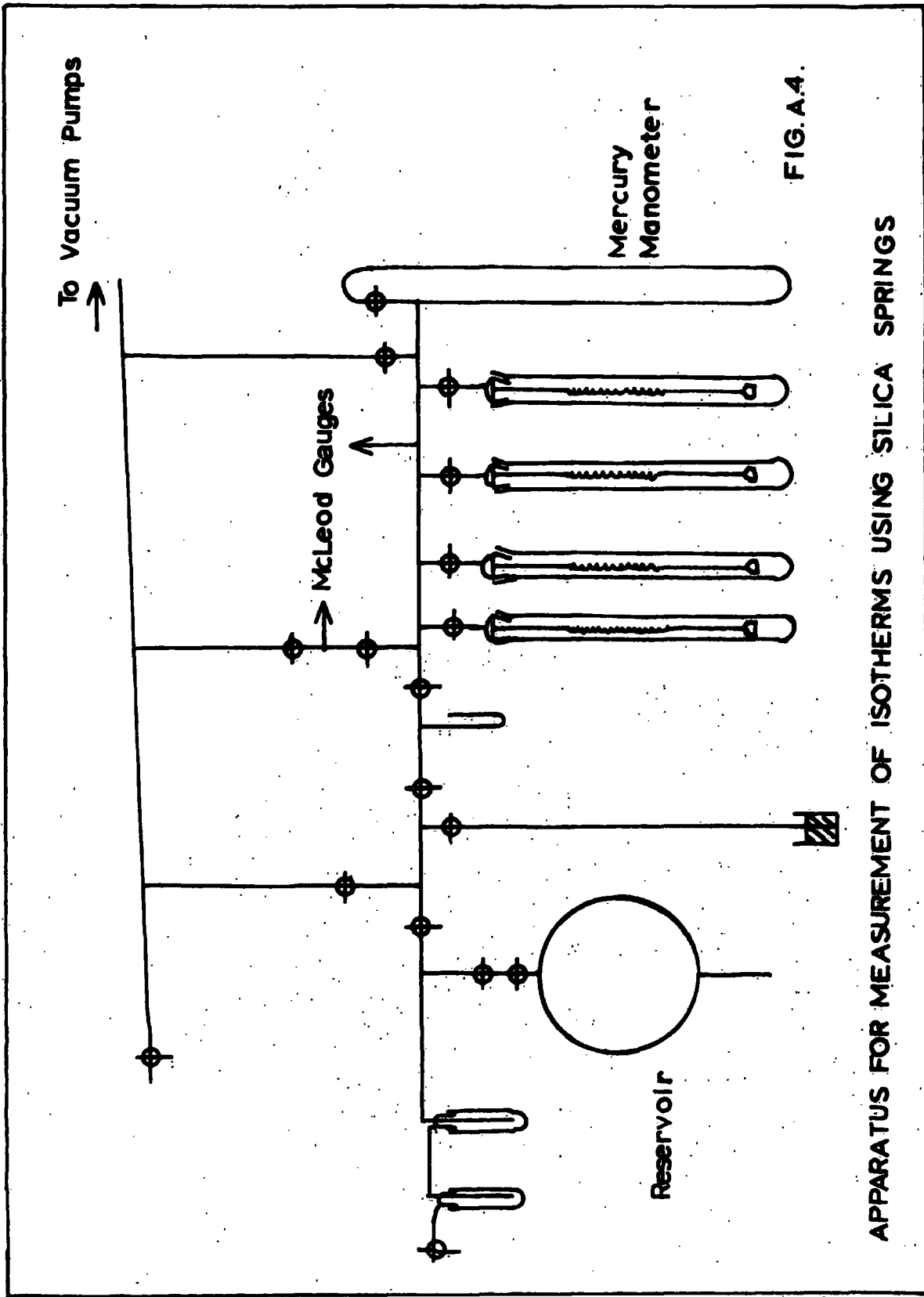
FIG. A.4.

APPARATUS FOR MEASUREMENT OF ISOTHERMS USING SILICA SPRINGS

APPENDIX IV

References

The abbreviations are those recommended by the Chemical Society.

1. de Saussure, Annals of Philosophy, 6, (1815), 241.

2. Long and Sykes, J. Chim. phys., 47, (1950), 361.

3. Gallagher and Harker, Carbon, 2, (1964), 163.

4. McEnaney, Ph.D. Thesis, Hull University, 1961.

5. Holmes and Emmett, J. Phys. Colloid Chem., 51, (1947), 1276.

6. Rowan, M.Sc. Thesis, Durham University, 1966.

7. Milner et al., J. Chem. Soc., (1943), 578.

8. Kipling, Sci. Progr., 37, (1949), 657.

9. Tang and Bacon, Carbon, 2, (1964), 211.

10. Davidson and Losty, 'Second Conference on Industrial Carbon and Graphite', Society for Chemical Industry, London, 1966, p. 20.

11. Bolton et al., J. Chem. Soc., (1942), 242.

12. Kipling and Wilson, 'Proceedings of Residential Conference on Science in the Use of Coal', (Sheffield, April, 1958), Institute of Fuel, London (1959), p.C6.

13. Wilson, M.Sc. Thesis, Hull University, 1960.

14. Bacon and Tang, Carbon, 2, (1964), 221.

15. Kipling and McEnaney, Fuel, 43, (1964), 367.

16. Debye and Scherrer, Phys. Z., 18, (1917), 291.

17. Riley, Quart. Rev., 1, (1947), 259.

18. Biscoe and Warren, J. Appl. Phys., 13, 364, (1942).

19. Hofmann and Wilm, Z. Elektrochem., 42, (1936), 504.

20. Franklin, Acta Cryst., 4, (1951), 253.

21. Franklin, Proc. Roy. Soc., 209A, (1951), 196.

22. Franklin, J. Chim. phys., 47, (1950), 573.

23. Steward and Davidson, 'Industrial Carbon and Graphite',
     Society for Chemical Industry, London, 1958, p.207.

24. Kuroda and Akamatu, Bull. Chem. Soc. Japan, 32, (1959),
     142.

25. Kipling et al. Carbon, 1, (1963), 315.

26. Kipling and Shooter, 'Second Conference on Industrial
     Carbon and Graphite', Society for Chemical Industry,
     London, 1966, p.15.

27. Brookes and Taylor, Carbon, 3, (1965), 185.

28. Blayden, Gas World, Coking Section, 140, (1954), 9.

29. Ingram et al., Nature, 174, (1954), 797.

30. Uerbersfeld et al., Nature, 174, (1954), 614.

31. Pope and Gregg, Brit. J. Appl. Phys., 10, (1959), 507.

32. Jackson and Wynne-Jones, Carbon, 2, (1964), 227.

33. Mrozowski, Phys. Rev., 86, (1952), 251.

34. Diamond and Hirsch, 'Industrial Carbon and Graphite',
     Society for Chemical Industry, London, 1958, p.197.

35. Gibson et al., J. Chem. Soc., (1946), 456.

36. Everett, 'The Structure and Properties of Porous
     Materials', Butterworths, 1958, p.47.

37. Dubinin, Quart. Rev., IX, (1955), 101.

38. Dubinin, 'Industrial Carbon and Graphite', Society for Chemical Industry, London, 1958, p.219.

39. Bering, Dubinin and Serpinsky, J. Colloid and Interface Sci., 21, (1966), 378.

40. Hedden and Wicke, 'Proceedings of the Third Conference on Carbon'., Pergamon Press, New York, 1959, p.249.

41. Walker et al., Adv. Catalysis, XI, (1959), 133.

42. Thomas, Chemistry and Physics of Carbon, Volume 1, Edward Arnold, 1965, p.121.

43. Smith, Quart. Rev., XIII., (1959), 287.

44. Tables of Selected Values of Chemical Thermodynamic Properties, National Bureau of Standards, Washington D.C, 1949.

45. Hougen and Watson, 'Chemical Process Principles', Part 1, Wiley, New York, (1950), p.254.

46. Langmuir, J. Amer. Chem. Soc., 37, (1915), 1139.

47. Eucken, Z. angew. Chem., 43, (1930), 986.

48. Meyer, Trans. Faraday Soc., 34, (1938), 1056.

49. Sihvonen, Trans. Faraday Soc., 34, (1938), 1052.

50. Strickland-Constable, Trans. Faraday Soc., 40, (1944), 333.

51. Duval, J. Chim. phys., 47, (1950), 339.

52. Rhead and Wheeler, J. Chem. Soc., 103, (1913), 461.

53. Grodozovskii and Chukhanov, Fuel, 15, (1936), 321.

54. Day et al., 'Industrial Carbon and Graphite', Society of Chemical Industry', London, 1958, p.348.

55. Day, Ph.D. Thesis, Pennsylvania State Univ., 1949.

56. Bridger, Nature, 157, (1946), 236.

57. Arthur, Nature, 157, (1946), 732.

58. Bridger and Appleton, J. Soc. Chem. Ind., 67, (1948), 445.

59. Arthur, Trans. Faraday Soc., 47, (1951), 164.

60. Wicke, '5th Symposium on Combustion', Reinhold, New York, 1955, p.245.

61. Arthur and Bowring, Ind. Eng. Chem., 43, (1951), 528.

62. Rossberg, Z. Elektrochem., 60, (1956), 164.

63. Lewis et al., Ind. Eng. Chem., 46, (1954), 1327.

64. Frey, Proc. Roy. Soc. (London), 228 A, (1955), 510.

65. Blyholder and Eyring, J. Phys. Chem., 61, (1957), 682.

66. Blyholder and Eyring, J. Phys. Chem., 63, (1959), 1004.

67. Sykes and Thomas, 'Proceedings of the Fourth Carbon Conference', Vol. 1., Pergamon Press, Oxford, 1963, p.29.

68. Laine et al., 'Proceedings of the Fifth Carbon Conference', Vol.2, Pergamon Press, Oxford, (1963), p.211.

69. Laine et al., J. Phys. Chem.,67, (1963), 2030.

70. Vastola et al., Carbon, 2, (1964), 65.

71. King, J. Chem. Soc., (1937), 1489; Chambers and King, ibid., (1938), 688; Bannister and King, ibid., (1938), 991.

72. Ong, Carbon, 2, (1964), 281.

73. Mayers, Trans. Amer. Inst. Min. Met. Engineers., 119, (1936), 304.

74. Sihvonen, Z. Elektrochem., 36, (1930), 806.

75. Chen et al., J. Phys. Chem., 59, (1955), 1146.

76. Duval, J. Chim. phys., 58, (1961), 3.

77. Gulbransen and Andrew, Ind. Eng. Chem., 44, (1952),
1034.

78. Klibanova and Frank-Kamenetskii, Acta Physiochim. U.R.S.S.,
18, (1943), 387.

79. Lambert, Trans. Faraday Soc., 32, (1936), 452.

80. Letort and Magrone, J. Chim. phys., 47, (1950), 576.

81. Earp and Hill, 'Industrial Carbon and Graphite', Society
of Chemical Industry, London, 1959, p.326.

82. Snow et al., 'Proceedings of the Third Conference on
Carbon', Pergamon Press, London, 1959, p.279.

83. Barradas et al., Can. J. Chem., 44, (1966), 165.

84. Marysin and Tesner, Doklady Akad. Nauk S.S.S.R., 163,
(1965), 1930.

85. Serpinet, Thesis, Nancy, 1956.

86. Bonnetain, Thesis, Nancy, 1958.

87. Heuchamps, Thesis, Nancy, 1960.

88. Gregg and Tyson, Carbon, 3, (1965), 39.

89. Tu et al., Ind. Eng. Chem., 26, (1934), 749.

90. Thiele, Ind. Eng. Chem., 31, (1939), 916.

91. Wheeler, Adv. Catalysis, 3, (1951), 249.

92. Weisz and Prater, Adv. Catalysis, 6, (1954), 143.

93. Grisdale, J. Appl. Phys., $\underline{24}$, (1956), 689.

94. Hennig, 'Proceedings of the Fifth Conference on Carbon', Vol. 1, Pergamon, New York, 1962, p. 143.

95. Smith and Polley, J. Phys. Chem., $\underline{60}$, (1956), 689.

96. Thomas and Hughes, Carbon, $\underline{1}$, (1964), 209.

97. Harker, 'Proceedings of the Fourth Carbon Conference', Pergamon Press, Oxford, 1963, p. 125.

98. Lambert, Trans. Faraday Soc., $\underline{34}$, (1938), 1080.

99. Strickland-Constable, 'La Combustion du Carbone', Colloques Internationaux, Nancy, 1949.

100. Shah, J. Chem. Soc., (1929), 2661, 2676.

101. Lowry and Hulett, J. Amer. Chem. Soc., $\underline{42}$, (1920), 1408.

102. Weller and Young, J. Amer. Chem. Soc., $\underline{70}$, (1948), 4155.

103. Puri and Bansal, Carbon, $\underline{1}$, (1964), 451.

104. Studebaker et al., Ind. Eng. Chem., $\underline{48}$, (1956), 162.

105. Blom et al., Fuel, $\underline{36}$, (1957), 135.

106. Bruns et al., Kolloid-Z., $\underline{63}$, (1933), 286.

107. Puri et al., Chem. and Ind., London, R 30 - 31½ (1956).

108. Puri et al., Ind. Eng. Chem., $\underline{50}$, (1958), 1071.

109. Beehm et al., Angew. Chem. Internat. Edit., $\underline{3}$, (1964), 699.

110. Garten and Weiss, Rev. Pure Appl. Chem., $\underline{7}$, (1957), 69.

111. Garten and Weiss, Austral. J. Chem., $\underline{10}$, (1957), 309.

112. Beebe and Young, J. Phys. Chem, $\underline{58}$., (1954), 93.

113. Boehm et al., Rev. gen. Caoutchouc Plastiques, 41, (1964), 461.

114. Kipling and McEnaney, 'Second Conference on Industrial Carbon and Graphite', Society for Chemical Industry, London, 1966, p.380.

115. Franklin, Trans. Faraday Soc., 45, (1949), 274.

116. Maggs et al., Nature, 186, (1960), 956.

117. Kipling et al., Carbon, 4, (1966), 5.

118. Ritter and Drake, Ind. Eng. Chem. Analyt., 17, (1945), 782.

119. Bond and Spencer, 'Industrial Carbon and Graphite', Society for Chemical Industry, London, 1958, p.231.

120. Bond and Spencer, 'Proceedings of the Third Conference on Carbon', Pergamon Press, New York, 1959, p. 357.

121. Wiggs, 'The Structure and Properties of Porous Solids', Butterworth, London, 1958, p.183.

122. Dubinin et al., Zhur. fiz. Khim., 34, (1960), 959.

123. Cochran and Cosgrove, J. Phys. Chem., 61, (1957), 1417.

124. Gurvitsch, Zhur. Russk. Fiz.-Khim. Obshch., Chast' Khim., 47, (1915), 805.

125. Brunauer et al., J. Amer. Chem. Soc., 62, (1940), 1723.

126. Brunauer, Emmett and Teller, J. Amer. Chem. Soc., 60, (1938), 309.

127. Hill, J. Phys. Chem., 17, (1949), 520.

128. Joyner et al., J. Amer. Chem. Soc., 67, (1945), 2182.

129. Lamond and Marsh, Carbon, 1, (1964), 281.

130. Culver and Heath, Trans. Faraday Soc., 51, (1955), 1569.

131. Lamond and Marsh, Carbon, 1, (1964), 293.

132. Spencer and Bond, American Conference on Coal Science, 1964, Pennsylvania State Univ., Adv. Chem. Ser., 55, (1966), 724.

133. Dubinin, 'Chemistry and Physics of Carbon', Vol. 2., Edward Arnold, London, 1967, p.51.

134. Alexandrov et al., Doklady Akad. Nauk S.S.S.R., 84, (1952), 301.

135. Dubinin and Zaverina, Izvest. Akad. Nauk S.S.S.R., Odtel. Khim. Nauk, (1952), 577.

136. Dubinin, Uspekhi Khim., 11, (1952), 513.

137. Radushkevich and Lukianovich, Zhur. fiz. Khim., 24, (1950), 21.

138. Barrett et al., J. Amer. Chem. Soc., 73, (1951), 373.

139. Pierce, J. Phys. Chem., 57, (1953), 149.

140. Spalaris, J. Phys. Chem., 60, (1956), 1480.

141. Harkins and Jura, J. Amer. Chem. Soc., 66, (1944), 1366.

142. Arnell and Barss, Can. J. Res., 26A, (1948), 236.

143. Dubinin et al., Carbon, 2, (1964), 261.

144. Polanyi, Verh. Deutsch. Phys. Ges., 16, (1914), 1012.

145. Polanyi, Trans. Faraday Soc., 28, (1932), 316.

146. Berenyi, Z. phys. Chem., 94, (1920), 628.

147. Titoff, Z. phys. Chem., 74, (1910) 641.

148. Bolanyi, Z. Elektrochem., 26, (1920), 371.

149. Berenyi, Z. phys. Chem., 105, (1923), 55.

150. Lindau, Kolloid-Z., 60, (1932), 253.

151. Vinogradov, Zhur. priklad. Khim., 21, (1948), 101.

152. Dubinin et al., Zhur. fiz. Khim., 21, (1947), 1351.

153. Dubinin and Zaverina, Zhur. fiz. Khim., 23, (1949), 1129.

154. Radushkevich, Zhur. fiz. Khim., 23, (1949), 1410.

155. Dubinin, Chem. Rev., 60, (1960), 235.

156. Dubinin, Zhur. fiz. Khim., 39, (1965), 1305.

157. Bering and Serpinskii, Doklady Akad. Nauk S.S.S.R., 148, (1963), 1331.

158. Dubinin and Timofeev, Zhur. fiz. Khim., 22, (1948), 101.

159. Dubinin and Zaverina, Doklady Akad. Nauk S.S.S.R., 72, (1950), 319.

160. Nikolaev and Dubinin, Izvest. Akad. Nauk S.S.S.R., Otd. Khim. Nauk, (1958), 1165.

161. Dubinin et al., 'Surface Phenomena in Chemistry and Biology', Pergamon Press, London, 1958, p.172.

162. Bering et al., Doklady Akad. Nauk S.S.S.R., 138, (1961), 1373.

163. Culver and Watts, Rev. Pure Appl. Chem., (Australia), <u>10</u>, (1960), 95.

164. Anderson and Emmett, J. Phys. Chem., <u>56</u>, (1952), 756.

165. Emmett and Anderson, J. Amer. Chem. Soc., <u>67</u>, (1945), 1492.

166. Dubinin <u>et al</u>., J. Chem. Soc., (1955), 1760.

167. Anderson <u>et al</u>., Fuel, <u>44</u>, (1965), 443.

168. Millard <u>et al</u>., J. Phys. Chem., <u>58</u>, (1954), 468.

169. Spencer <u>et al</u>., J. Phys. Chem., <u>62</u>, (1958), 719.

170. Dell and Beebe, J. Phys. Chem., <u>59</u>, (1955), 754.

171. Beebe and Dell, J. Phys. Chem., <u>59</u>, (1955), 746.

172. Holmes and Beebe, Can. J. Chem., <u>35</u>, (1957), 1542.

173. Nandi <u>et al</u>., Fuel, <u>35</u>, (1956), 133.

174. Allmand and Chaplin, Trans. Faraday Soc., <u>28</u>, (1932), 223.

175. Rius and Fuentes, Anales real. Soc. espan. Fis. Quim. (Madrid), <u>47B</u>, (1951), 555.

176. Puri <u>et al</u>., J. Phys. Chem., <u>62</u>, (1958), 756.

177. Pierce <u>et al</u>., J. Amer. Chem. Soc., <u>73</u>, (1951), 4551.

178. King and Lawson, Trans. Faraday Soc., <u>30</u>, (1934), 1094.

179. Emmett, Chem. Rev., <u>43</u>, (1948), 69.

180. McDermot and Arnell, J. Phys. Chem., <u>58</u>, (1954), 492.

181. Wilson and Bolam, J. Colloid Sci., <u>5</u>, (1950), 550.

182. Deitz <u>et al</u>., Carbon, <u>1</u>, (1964), 245.

183. McEnaney and Rowan, Chem. and Ind., (1965), 2032.

184. Armington, Ph.D. Thesis, Pennsylvania State University, 1960.

185. Walker and Kini, Fuel, $\underline{44}$, (1965), 453.

186. Marsh and Wynne-Jones, Carbon, $\underline{1}$, (1964), 269.

187. Bridgemann, J. Amer. Chem. Soc., $\underline{49}$, (1927), 1174.

188. Young and Crowell, 'Physical Adsorption of Gases', Butterworths, 1962.

189. Gianuque and Egan, J. Chem. Phys., $\underline{5}$, (1937), 45.

190. Kaganer, Zhur. fiz. Khim., $\underline{33}$, (1959), 2202.

191. Kaganer, Dokl, Akad, Nauk., $\underline{138}$, (1961), 405.

192. Dubinin and Polstyanov, Izvest. Akad. Nauk S.S.S.R., Ser. Khim., (1966) No. 9.

193. Izotova and Dubinin, Zhur. fiz. Khim., $\underline{39}$, (1965), 2796.

194. Kawahata and Walker, 'Proceedings of the Fifth Conference on Carbon', Pergamon Press, New York, Vol. 2, 1963, p.251.

195. Hodgson, J. Sci. Instr., $\underline{40}$, (1963), 61.

196. See Reference 183.

197. Cahn and Schultz, 'Vacuum Microbalance Techniques', Vol. 3., Plenum Press, New York, 1963, p.29.

198. Thomas and Williams, Quart. Rev., $\underline{19}$, (1965), 231.

199. Liang, J. Appl. Phys, $\underline{22}$, (1951), 148.

200. Bennett and Tompkins, Trans. Faraday Soc., $\underline{53}$, (1957), 185.

201. Katz and Gulbransen, 'Vacuum Microbalance Techniques', Vol. 1., Plenum Press, New York, 1961, p.211.

202. Dovaston, Unpublished work.

203. McBain and Bakr, J. Amer. Chem. Soc., <u>48</u>, (1926), 690.

APPENDIX V

Primary Data for Isotherms

Isotherms at $195^{\circ}K$ p_o = 141.4 cm. Hg.

(i) Unactivated Carbon (Electrobalance)				(ii) Unactivated Carbon (Springs)			
Adsorption		Desorption		Adsorption		Desorption	
p/p_o ($\times 10^3$)	w ($g.g^{-1}.$)	p/p_o ($\times 10^3$)	w ($g.g^{-1}.$)	p/p_o ($\times 10^3$)	w ($g.g^{-1}.$)	p/p_o ($\times 10^3$)	w ($g.g^{-1}.$)
0.191	0.0366	113	0.214	0.0262	0.0019	144	0.226
0.580	0.0634			0.177	0.0358	23.7	0.196
1.51	0.132			0.435	0.0596	3.61	0.1392
1.42	0.090			1.08	0.0849	0.821	0.0900
4.20	0.116			1.05	0.0862	0.165	0.0528
4.81	0.136			2.31	0.103	0.9205	0.0458
6.01	0.146			5.16	0.150		
20.8	0.185			13.1	0.179		
50.2	0.205			46.0	0.208		
198.	0.228			109	0.222		
				223	0.234		
				343	0.238		

Isotherms at $195^{\circ}K$　　　　　　　　p_o = 141.4 cm. Hg.

(iii) 35.4% burn-off at $401^{\circ}C$				(iv) 34.5% burn-off at $420^{\circ}C$			
Adsorption		Desorption		Adsorption		Desorption	
p/p_o ($\times 10^3$)	w ($g.g^{-1}.$)	p/p_o ($\times 10^3$)	w ($g.g^{-1}.$)	p/p_o ($\times 10^3$)	w ($g.g^{-1}.$)	p/p_o ($\times 10^3$)	w ($g.g^{-1}.$)
0.0262	0.0022	143.3	0.419	0.00368	0.0104	297	0.415
0.177	0.0269	144.3	0.417	0.113	0.0232	81.4	0.346
0.435	0.0481	23.7	0.257	0.396	0.0541	29.7	0.285
1.08	0.0716	3.61	0.123	1.19	0.0938	13.1	0.222
1.05	0.0709	0.821	0.0639	3.47	0.122	13.4	0.220
2.31	0.103	0.166	0.0330	4.95	0.187	6.72	0.184
5.16	0.148	0.205	0.0340	17.3	0.236	5.43	0.154
13.1	0.207			50.9	0.313	3.40	0.138
46.0	0.315			138	0.375	3.54	0.137
109.3	0.394			138	0.378	2.19	0.118
223.5	0.463			170	0.392	1.03	0.0812
343.4	0.496			297	0.415	0.438	0.0638
						0.290	0.0476
						0.170	0.0387

Isotherms at 195°K p_o = 141.4 cm. Hg

(v) 35.0% burn-off at 436°C				(vi) 35.6% burn-off at 436°C			
Adsorption		Desorption		Adsorption		Desorption	
p/p_o (x 10^3)	w (g.g^{-1})	p/p_o (x 10^3)	w (g.g^{-1})	p/p_o (x 10^3)	w (g.g^{-1})	p/p_o (x 10^3)	w (g.g^{-1})
0.0396	0.0130	363	0.541	0.0262	0.0227	143	0.433
0.219	0.0326	102	0.417	0.177	0.0285	23.7	0.266
0.396	0.0419	65.8	0.369	0.435	0.0512	3.61	0.127
0.920	0.0610	12.0	0.207	1.03	0.0761	0.821	0.0669
1.45	0.0748	4.24	0.136	1.05	0.0736	0.166	0.0319
1.51	0.0774	1.54	0.0835	2.31	0.108	0.205	0.0363
3.47	0.118	0.665	0.0625	5.16	0.152		
11.0	0.196	0.152	0.0333	13.1	0.214		
27.2	0.273			46.0	0.328		
82.1	0.387			109	0.407		
162	0.466			222	0.471		
262	0.517						
363	0.549						

Isotherms at 195°K p_o = 141.4 cm. Hg.

(vii) 63.9% burn-off at 436°C				(viii) 20% burn-off at 456°C			
Adsorption		Desorption		Adsorption		Desorption	
p/p_o ($\times 10^3$)	w ($g.g^{-1}$)	p/p_o ($\times 10^3$)	w ($g.g^{-1}$)	p/p_o ($\times 10^3$)	w ($g.g^{-1}$)	p/p_o ($\times 10^3$)	w ($g.g^{-1}$)
0.0199	0.0103	350	0.548	0.0199	0.0114	350	0.382
0.301	0.0335	89.1	0.383	0.301	0.0592	89.1	0.324
1.37	0.0745	25.5	0.246	1.37	0.113	25.5	0.271
3.03	0.0986	9.55	0.173	3.03	0.150	9.55	0.218
4.95	0.123	2.29	0.101	4.95	0.176	2.29	0.136
4.81	0.124	0.290	0.042	4.81	0.175	0.290	0.0623
12.0	0.187			12.0	0.230		
30.4	0.264			30.4	0.276		
73.2	0.350			73.2	0.313		
159	0.452			159	0.347		
350	0.539			350	0.381		

Isotherms at $195^{\circ}K$ $\qquad$ p_o = 141.4 cm. Hg.

(ix) 34.6% burn-off at $456^{\circ}C$				(x) 48.7% burn-off at $456^{\circ}C$			
Adsorption		Desorption		Adsorption		Desorption	
p/p_o (x 10^3)	w $(g.g^{-1})$	p/p_o (x 10^3)	w $(g.g^{-1})$	p/p_o (x 10^3)	w $(g.g^{-1})$	p/p_o (x 10^3)	w $(g.g^{-1})$
0.0396	0.0138	363	0.489	0.0199	0.0050	350	0.537
0.219	0.0358	102	0.401	0.301	0.0341	89.1	0.423
0.396	0.0485	65.8	0.364	1.37	0.0745	25.5	0.271
0.920	0.0695	12.0	0.223	3.03	0.105	9.55	0.183
1.5	0.0872	4.24	0.148	4.95	0.131	2.29	0.101
1.45	0.0856	1.54	0.0936	4.81	0.132	0.290	0.035
3.47	0.127	0.665	0.0673	12.0	0.196		
11.0	0.211	0.152	0.0355	30.4	0.282		
27.2	0.285			73.2	0.373		
82.1	0.379			159	0.458		
162	0.434			350	0.536		
262	0.468						
363	0.491						

Isotherms at 195°K p_o = 141.4 cm. Hg.

(xi) 68.6% burn-off at 456°C				(xii) 21.2% burn-off at 485°C			
Adsorption		Desorption		Adsorption		Desorption	
p/p_o ($\times 10^3$)	w ($g.g^{-1}$)	p/p_o ($\times 10^3$)	w ($g.g^{-1}$)	p/p_o ($\times 10^3$)	w ($g.g^{-1}$)	p/p_o ($\times 10^3$)	w ($g.g^{-1}$)
0.0199	0.0058	350	0.537	0.0177	0.0090	312	0.424
0.301	0.0360	89.1	0.377	0.238	0.0487	209	0.406
1.37	0.0697	25.5	0.240	0.481	0.0665	75.0	0.358
3.03	0.0970	9.55	0.166	1.03	0.0930	12.0	0.245
4.95	0.122	2.29	0.0941	2.29	0.132	5.20	0.183
4.81	0.121	0.290	0.0385	2.31	0.126	2.55	0.118
12.0	0.180			4.74	0.165	1.06	0.0927
30.4	0.255			10.3	0.215	0.221	0.0519
73.2	0.341			9.55	0.201		
159	0.444			27.9	0.299		
350	0.533			75.3	0.358		
				158	0.398		
				281	0.425		
				382	0.438		

Isotherms at 195°K $\qquad$ p_o = 141.4 cm. Hg.

(xiii) 35.1% burn-off at 485°C				(xiv) 50.1% burn-off at 485°C			
Adsorption		Desorption		Adsorption		Desorption	
p/p_o ($\times 10^3$)	w ($g.g^{-1}$)	p/p_o ($\times 10^3$)	w ($g.g^{-1}$)	p/p_o ($\times 10^3$)	w ($g.g^{-1}$)	p/p_o ($\times 10^3$)	w ($g.g^{-1}$)
0.0396	0.0093	363	0.521	0.0177	0.0101	312	0.532
0.219	0.0321	102	0.416	0.238	0.0387	209	0.499
0.396	0.0430	65.8	0.375	0.481	0.0521	75.0	0.372
0.920	0.0624	12.0	0.214	1.03	0.0711	12.0	0.214
1.51	0.0791	4.24	0.139	2.29	0.0976	5.20	0.141
1.45	0.0833	1.54	0.0858	2.31	0.104	2.55	0.114
3.47	0.124	0.665	0.0595	4.74	0.143	1.06	0.0713
11.0	0.207	0.152	0.0269	10.3	0.198	0.221	0.0345
27.2	0.287			9.55	0.195		
82.1	0.395			27.9	0.267		
162	0.456			75.3	0.403		
262	0.496			158	0.476		
363	0.521			281	0.525		
				382	0.553		

Isotherms at 195°K p_o = 141.4 cm. Hg.

(xv) 70.4% burn-off at 485°C				(xvi) 20.4% burn-off at 518°C			
Adsorption		Desorption		Adsorption		Desorption	
p/p_o (x 10^3)	w ($g.g^{-1}$)	p/p_o (x 10^3)	w ($g.g^{-1}$)	p/p_o (x 10^3)	w ($g.g^{-1}$)	p/p_o (x 10^3)	w ($g.g^{-1}$)
0.0396	0.0130	363	0.571	0.152	0.0423		
0.219	0.0314	102	0.400	0.545	0.0785		
0.396	0.0401	65.8	0.342	0.516	0.0779		
0.920	0.0512	12.0	0.178	0.969	0.100		
1.51	0.0673	4.24	0.117	1.51	0.111		
1.45	0.0723	1.54	0.0715	2.97	0.150		
3.47	0.107	0.665	0.0554	7.78	0.199		
11.0	0.209	0.152	0.0334	15.6	0.231		
27.2	0.285			35.7	0.272		
82.1	0.364			62.3	0.283		
162	0.495			97.6	0.301		
262	0.529			165	0.316		
363	0.577			319	0.343		

Isotherms at 195°K $\qquad$ p_o = 141.4 cm. Hg.

(xvii) 35.1% burn-off at 518°C				(xviii) 35.3% burn-off at 572°C			
Adsorption		Desorption		Adsorption		Desorption	
p/p_o ($\times 10^3$)	w ($g.g^{-1}.$)	p/p_o ($\times 10^3$)	w ($g.g^{-1}.$)	p/p_o ($\times 10^3$)	w ($g.g^{-1}.$)	p/p_o ($\times 10^3$)	w ($g.g^{-1}.$)
0.0262	0.0039	143	0.358	0.0177	0.0126	312	0.387
0.177	0.0363	23.7	0.264	0.238	0.0492	209	0.354
0.435	0.0598	3.61	0.154	0.481	0.0678	75.0	0.304
1.08	0.0888	0.821	0.0865	1.03	0.0908	12.0	0.224
1.05	0.0922	0.166	0.0452	2.29	0.124	5.20	0.172
2.31	0.132	0.205	0.0447	2.31	0.121	1.06	0.100
5.16	0.186			4.74	0.161	0.221	0.0479
13.1	0.238			10.3	0.199		
46.0	0.304			9.55	0.202		
109	0.346			27.9	0.265		
222	0.386			75.3	0.319		
343	0.407			158	0.362		
				281	0.385		
				382	0.394		

Isotherms at 195°K p_o = 141.4 cm. Hg.

(xix) 36.3% burn-off at 620°C				(xx) 32.1% burn-off at 726°C			
Adsorption		Desorption		Adsorption		Desorption	
p/p_o $(\times 10^3)$	w $(g.g^{-1}.)$	p/p_o $(\times 10^3)$	w $(g.g^{-1}.)$	p/p_o $(\times 10^3)$	w $(g.g^{-1}.)$	p/p_o $(\times 10^3)$	w $(g.g^{-1}.)$
0.152	0.0340			0.007	0.0049	159	0.240
0.545	0.0644			1.84	0.101	50.2	0.213
0.516	0.0666			1.73	0.102	8.49	0.164
0.967	0.0859			4.24	0.135	2.69	0.128
1.51	0.103			4.10	0.135	1.01	0.0901
2.97	0.128			6.37	0.150	0.778	0.0703
7.78	0.171			8.49	0.164	0.545	0.0657
15.5	0.203			12.0	0.173	0.382	0.0555
35.7	0.231			19.1	0.190	0.294	0.0494
62.2	0.250			19.4	0.192	0.244	0.0342
97.6	0.265			32.5	0.205		
165	0.281			61.2	0.217		
319	0.304			90.2	0.226		
				128	0.231		
				160	0.237		

Isotherms at 273°K p_o = 2614 cm. Hg.

(xxi) Unactivated Carbon				(xxii) 35.4% burn-off at 401°C			
Adsorption		Desorption		Adsorption		Desorption	
p/p_o ($\times 10^3$)	w ($g.g^{-1}.$)	p/p_o ($\times 10^3$)	w ($g.g^{-1}.$)	p/p_o ($\times 10^3$)	w ($g.g^{-1}.$)	p/p_o ($\times 10^3$)	w ($g.g^{-1}.$)
0.0509	0.0040	11.7	0.109	0.0509	0.0035	11.7	0.101
0.124	0.0067	5.18	0.0794	0.124	0.0074	5.18	0.0540
0.275	0.0134	2.14	0.0521	0.275	0.0079	2.19	0.0383
0.279	0.0144	2.14	0.0545	0.279	0.0087	2.14	0.0377
0.765	0.0292	0.459	0.0228	0.765	0.0190	0.459	0.0150
1.45	0.0414	0.199	0.0141	1.45	0.0296	0.199	0.0740
3.23	01627	0.0819	0.0057	3.23	0.0442	0.0819	0.0420
7.36	0.0907			7.36	0.0772		
23.0	0.131			23.0	0.141		

Isotherms at 273°K $\qquad\qquad$ p_o = 2614 cm. Hg.

(xxiii) 35.6% burn-off at 436°C				(xxiv) 35.1% burn-off at 518°C			
Adsorption		Desorption		Adsorption		Desorption	
p/p_o (x 10^3)	w (g.g^{-1}.)	p/p_o (x 10^3)	w (g.g^{-1}.)	p/p_o (x 10^3)	w (g.g^{-1}.)	p/p_o (x 10^3)	w (g.g^{-1}.)
0.0509	0.0017	11.7	0.108	0.0509	0.0023	11.7	0.125
0.124	0.0038	5.18	0.0718	0.124	0.0049	5.18	0.0873
0.275	0.0081	2.14	0.0440	0.275	0.0102	2.14	0.0553
0.279	0.0081	2.14	0.0362	0.279	0.0113	2.14	0.0486
0.765	0.0187	0.459	0.0116	0.765	0.0248	0.459	0.0170
1.45	0.0291	0.199	0.0048	1.45	0.0379	0.199	0.0070
3.23	0.0477	0.0819	0.0016	3.23	0.0675	0.0819	0.0038
7.36	0.0852			7.36	0.103		
23.0	0.151			23.0	0.162		

Isotherms at 298°K p_o = 4825 cm. Hg

(xxv) Unactivated Carbon				(xxvi) 35.4% burn-off at 401°C			
Adsorption		Desorption		Adsorption		Desorption	
p/p_o (x 10^3)	w (g.g^{-1}.)	p/p_o (x 10^3)	w (g.g^{-1}.)	p/p_o (x 10^3)	w (g.g^{-1}.)	p/p_o (x 10^3)	w (g.g^{-1}.)
0.0564	0.0022	8.42	0.0830	0.0564	0.0013	8.42	0.0713
0.139	0.0045	4.74	0.0638	0.139	0.0025	4.74	0.0499
0.290	0.0099	2.45	0.0458	0.290	0.0064	2.45	0.0333
0.694	0.0194	1.03	0.0276	0.694	0.0109	1.03	0.0175
1.55	0.0336	0.373	0.0128	1.55	0.0230	0.373	0.0077
4.87	0.0614	0.207	0.0086	4.87	0.0487	0.207	0.0052
6.80	0.0745	0.085	0.00320	6.80	0.0600	0.0850	0.0029
10.6	0.0896			10.6	0.0793		
12.6	0.0958			12.6	0.0869		

Isotherms at $298^{\circ}K$ $\qquad\qquad$ p_0 = 4825 cm. Hg.

(xxvii) 35.6% burn-off at $436^{\circ}C$				(xxviii) 35.1% burn-off at $518^{\circ}C$			
Adsorption		Desorption		Adsorption		Desorption	
p/p_0 (x 10^3)	w (g.g^{-1}.)	p/p_0 (x 10^3)	w (g.g^{-1}.)	p/p_0 (x 10^3)	w (g.g^{-1}.)	p/p_0 (x 10^3)	w (g.g^{-1}.)
0.0564	0.0024	8.42	0.0718	0.0564	0.0019	8.42	0.0868
0.139	0.0038	4.74	0.0502	0.139	0.0045	4.74	0.0642
0.290	0.0072	2.45	0.0311	0.290	0.0089	2.45	0.0423
0.694	0.0127	1.03	0.0178	0.694	0.0172	1.03	0.0249
1.55	0.0238	0.373	0.0083	1.55	0.0303	0.373	0.0109
4.87	0.0504	0.207	0.0052	4.87	0.0527	0.207	0.0078
6.80	0.0619	0.0850	0.0019	6.80	0.0760	0.0850	0.0029
10.6	0.0777			10.6	0.0927		
12.6	0.0898			12.6	0.104		